IDENTIFICATION AND CHARACTERIZATION OF MOLECULAR TARGETS FOR DISEASE MANAGEMENT IN TREE FRUIT PATHOGENS

By

Jingyu Peng

A DISSERTATION

Submitted to
Michigan State University
in partial fulfillment of the requirements
for the degree of

Plant Pathology – Doctor of Philosophy

2020

ABSTRACT

IDENTIFICATION AND CHARACTERIZATION OF MOLECULAR TARGETS FOR DISEASE MANAGEMENT IN TREE FRUIT PATHOGENS

By

Jingyu Peng

Fire blight, caused by *Erwinia amylovora*, is a devastating bacterial disease threatening the worldwide production of pome fruit trees, including apple and pear. Within host xylem vessels, *E. amylovora* cells restrict water flow and cause wilting symptoms through formation of biofilms, that are matrix-enmeshed surface-attached microcolonies of bacterial cells. Biofilm matrix of *E. amylovora* is primarily composed of several exopolysaccharides (EPSs), including amylovora, levan, and, cellulose. The final step of biofilm development is dispersal, which allows dissemination of a subpopulation of biofilm cells to resume the planktonic mode of growth and consequentially cause systemic infection. In this work, we demonstrate that identified the Hfq-dependent small RNA (sRNA) RprA positively regulates amylovoran production, T3SS, and flagellar-dependent motility, and negatively affects levansucrase activity and cellulose production. We also identified the *in vitro* and *in vivo* conditions that activate RprA, and demonstrated that RprA activation leads to decreased formation of biofilms and promotes the dispersal movement of biofilm cells. This work supports the involvement of RprA in the systemic infection of *E. amylovora* during its pathogenesis.

Bacterial toxin-antitoxin (TA) systems are small genetic loci composed of a proteinaceous toxin and a counteracting antitoxin. In this work, we identified and characterized a chromosomally encoded *hok/sok*-like type I TA system in *Erwinia amylovora* Ea1189. Ectopic overexpression of *hok* caused massive cell death in *E. amylovora* and its toxicity can be partially reversed through co-overexpression of the cognate sRNA *sok*. Phenotypic and transcriptomic

examination of *E. amylovora* cells expressing *hok* at subtoxic levels demonstrated that *hok* causes membrane rupture and proton motive force dissipation, upregulates expression levels of ATP biosynthesis genes and consequently cellular ATP levels. Hok also positively affects phage shock protein genes to protect cells from further membrane damage. Taken together, the *hok/sok* TA system, besides being potentially self-toxic, appears to facilitate *E. amylovora* to manage various stress responses when the toxin gene is expressed in low levels.

The succinate dehydrogenase inhibitor (SDHI) is a broad-spectrum fungicide class that has been widely utilized in agricultural fields. *Blumeriella jaapii*, the causative agent of cherry leaf spot (CLS), is the most important limiting factor for tart cherry production in the Midwestern United States. In the last decade, reduced efficacy in using SDHIs, i.e. boscalid, fluopyram, and fluxapyroxad, for management of CLS has been observed in many research and commercial orchard sites. Through whole-genome sequencing of *B. jaapii* using both PacBio long-reads and Illumina short-reads, we identified mutations in *SdhB* or *SdhC* that are correlative to resistance of this fungus to boscalid, fluopyram, and/or fluxapyroxad. SdhB and SdhC are components of the succinate dehydrogenase complex that contributes fungal respiration. In view of the widely conserved sequences of the *SdhB* and *SdhC* genes in phytopathogenic Ascomycete fungi, we expressed the wild-type or mutated alleles of the *B. jaapii Sdh* gene in the soybean white mold pathogen *Sclerotinia sclerotiorum*. We successfully validated the functions of the mutations in *Sdh* genes of *B. jaapii* in conferring resistance to several SDHIs examined in this study. The *S. sclerotiorum* heterologous expression system was also validated to be highly effective in characterizing the functions of other *Sdh* mutations of *B. cinerea*, *C. homoeocarpa*, and *M. fructicola*. The approach developed in this study can potentially be widely applied to interrogate SDHI fungicide resistance mechanisms in other phytopathogenic ascomycetes.

ACKNOWLEDGEMENTS

I would like to thank my great wife, Xinxin Wang, who has always been by my side throughout the PhD training. Thank you for being always supportive and making me so motivated to be a good husband and, soon, a good dad.

I want to express my sincere appreciation to my PhD advisor, Dr. George W Sundin, who has truly exemplified how a great scientist should look like. I thank him for always thinking the best for myself and also other students. His unreserved support has allowed me to always think questions broadly and critically, and I will benefit from his training for the rest of my life.

I also would like to thank my committee members, Dr. Martin Chilvers, Dr. Lindsay R Triplett, and Dr. Timothy Miles for their great guidance on my research projects as well as being so kind to me. I particularly would like to thank Dr. Lindsay R Triplett, who has co-authored with me in two research articles. I have benefited hugely from her critical thinking and guidance in scientific writing.

Finally, I want to thank my parents for being such supportive in the last seven years, while I have been pursuing degrees oversee. Their love has made me strong and determined to achieve our family goals.

TABLE OF CONTENTS

LIST OF TABLES

LIST OF FIGURES

CHAPTER 1

Literature review

1.1 Molecular mechanism and triggering of biofilm dispersal

Biofilms are communities of bacterial cells that are enclosed in a self-produced extracellular matrix and surface-attached (Costerton et al. 1995). Formation of biofilm allows bacterial cells to exhibit a sessile mode of growth in response to antibiotics, nutrient scarcity, and host defense (Mah and O'Toole 2001; Singh et al. 2017). Compared with their planktonic counterparts, biofilm cells have been shown to be 10–1,000 times more resistant to antibiotics (Davies 2003), posing great challenge in medical and industrial settings. For phytopathogenic bacteria, formation of biofilms is a common strategy to invade plant tissues for full colonization and contributes significantly to their pathogenesis. Biofilms clog the sap flow of host xylem lumen and consequentially cause wilting symptoms. Though varies in different bacteria, the extracellular matrix of biofilms mostly contains exopolysaccharides (EPSs), nucleic acids (eDNA) and proteins (Flemming and Wingender 2010; Karatan and Watnick 2009).

Despite wide recognition of the importance of biofilm formation, its dispersal, the final step of biofilm development, has not caught much attention until recently. The dispersal of biofilm cells has been shown to be indispensable for pathogenic bacteria to leave the matrix-enmeshed macrostructure and migrate to new infection sites (Danhorn and Fuqua 2007; Kaplan 2010). Here, we review the well-characterized mechanisms of biofilm dispersal, and the known native and environmental cues that triggers this biological process in mammalian- or plant-pathogenic bacteria.

1.1.1 Molecular mechanisms of biofilm dispersal

Biofilm dispersion is the last stage of biofilm development, that allows cells to be detached from the biofilm macrostructure and return to the planktonic mode of growth. The second messenger cyclic di-GMP (c-di-GMP) is a ubiquitous bacterial signaling molecule that

modulates biofilm formation (Jenal and Malone 2006; Römling et al. 2005). Overall, high levels of c-di-GMP promote the sessile mode of bacterial growth whereas low levels of c-di-GMP favor the planktonic lifestyle (Hengge 2009; Jenal and Malone 2006; Römling et al. 2005). The c-di-GMP molecules are synthesized through diguanylate cyclases (DGCs) and degraded through phosphodiesterases (PDEs) (Hengge 2009). Therefore, biofilm dispersal is fostered by increased PDE activity and reduced levels of c-di-GMP, as observed in *Pseudomonas aeruginosa*, *Pseudomonas putida*, and *Shewanella oneidensis* (Gjermansen et al. 2005; Li et al. 2013; Morgan et al. 2006; Roy et al. 2012; Thormann et al. 2006).

Quorum sensing (QS) signaling, a population density-dependent modulatory machinery (Bassler 2001), has also been demonstrated to affect biofilm dispersal in certain bacteria. In *Xanthomonas campestris* pathovar *campestris*, the causative agent of black rot of crucifers, the QS signal *cis*-11-methyl-2-dodecenoic acid (DSF) at high cell density activates the PDE activity of RpfG and consequently leads to reduction of the intracellular c-di-GMP level. The DSF signal also upregulates the expression of the endo-β-1,4-mannanase gene *manA* to degrade the biofilm EPS matrix (Dow et al. 2003) and suppresses the expression of the XagABC system, which contributes to EPS production and consequently biofilm formation in this bacterium (Tao et al. 2010). Similarly, the exogenous supplement of *cis*-2 decenoic acid (*cis*-DA), naturally produced by *P. aeruginosa*, was shown to induce biofilm dispersal in the matrix-enmeshed microcolonies of *P. aeruginosa* and many other bacterial organisms, including *Bacillus subtilis*, *E. coli* and *Klebsiella pneumoniae* (Davies and Marques 2009b). Through transcriptomic analyses and phenotypic assays, exposure of *Francisella novicida* to *cis*-2-dodecenoic acid (BDSF), discovered in *Burkholderia cenocepacia*, rendered increased chitinase activity through higher expression of the *chiA* and *chiB* genes and upregulation of the (p)ppGpp synthase gene *relA*

(Dean et al. 2015). Both chitinase and (p)ppGpp negatively correlate with biofilm formation in *F. novicida* (Chung et al. 2014; Dean et al. 2009; Margolis et al. 2010). Besides DSF-family QS signals, an N-acyl-L-homoserine lactone family QS signal, N-3-oxo-hexanoyl homoserine lactone, was also shown to affect the dissemination of biofilm cells in *Pantoea stewartia* subspecies *stewartia* (Koutsoudis et al. 2006). Koutsoudis *et al.* showed that, in comparison to the spatially specified biofilm formed by the WT *P. stewartii* subspecies *stewartia* in corn xylem vessels, QS-defective mutants were diffusely distributed within the xylem lumens and lost adhesion capacity *in vitro* (Koutsoudis et al. 2006). These studies suggest evolutionarily deep-rooted involvement of QS in biofilm dispersal in various microorganisms.

Although involvement of sRNAs in biofilm formation has been described in various bacterial species, such as *E. coli*, *P. aeruginosa*, *Salmonella enterica*, *Vibrio cholerae* (Bak et al. 2015; Chambers and Sauer 2013; Fazli et al. 2014; Martínez and Vadyvaloo 2014), the evidence of direct involvement of sRNAs in biofilm dispersal is scarce. In *P. aeruginosa*, the sRNAs *rsmY* and *rsmZ* have been shown to promote biofilm formation through sequestering RsmA, a negative regulator of the polysaccharide synthesis locus (*psl*) (Chambers and Sauer 2013; Fazli et al. 2014). Expression levels of *rsmY* and *rsmZ* are significantly reduced in biofilm dispersed cells compared with their corresponding planktonic counterparts (Chua et al. 2014), suggesting their roles in facilitating biofilm dispersal in *P. aeruginosa*. Similarly, QS-regulated sRNAs Qrr1-4, transcriptionally activated at low cell-density and ceased at high cell-density, contribute to biofilm development in *V. cholerae* through repressing translation of the transcription factor gene *hapR*, which inhibits expression of the EPS biosynthetic *vps* gene clusters and at the same time downregulates cellular c-di-GMP levels (Bardill et al. 2011;

Hammer and Bassler 2009; Lenz et al. 2004; Martínez and Vadyvaloo 2014; Waters et al. 2008).

Besides mannanase and chitinase, several additional biofilm matrix degradation enzymes have been identified. In *Aggregatibacter actinomycetemcomitans, E. coli, Staphylococcus epidermidis*, production of dispersin B, a glycoside hydrolase, degrades the polymers of *N*-acetyl-D-glucosamines that comprise the biofilm matrix in these bacteria (Chaignon et al. 2007; Kaplan et al. 2003; Kaplan et al. 2004). Mutant of dispersin B in *A. actinomycetemcomitans* was shown to fail to be released from biofilms into the medium, suggesting its importance in biofilm dispersal (Kaplan et al. 2003). A recent study of *P. aeruginosa* showed that biofilm-dispersed cells exhibit increased expression of extracellular nucleases, i.e. EndA, EddA, and EddB, that enable the digestion of eDNA and therefore promote dispersal of biofilm cells (Cherny and Sauer 2019).

1.1.2 Triggeration of biofilm dispersal

The environmental stimuli for biofilm dispersal have been studied mostly in *P. aeruginosa* and a few clinically relevant pathogens. Dispersal of *P. aeruginosa* biofilm cells has shown to be activated by oxygen depletion (An et al. 2010), nitric oxide (NO) accumulation (Barraud et al. 2006; Barraud et al. 2009; Li et al. 2013), nutrient starvation (Schleheck et al. 2009). Evidence of the involvement of oxygen depletion in biofilm dispersal originated from the observation of biofilm dispersal after cession of flow (Gjermansen et al. 2005; Thormann et al. 2006). Recently, it was shown that biofilm cells of *P. aeruginosa* experiencing oxygen deprivation and electron-rich conditions undergoes biofilm dispersal (Goodwine et al. 2019). The environmental cues for biofilm dispersal appear to coincide with increased bacterial PDE activity and decreased c-di-GMP levels (An et al. 2010; Barraud et al. 2009; Schleheck et al. 2009). For

example, addition of NO causes transcriptional activation of *P. aeruginosa nbdA*, encoding a MHYT-GGDEF-EAL domain-containing protein with PDE activity, and results in decreased c-di-GMP levels in biofilms (Li et al. 2013). Similarly, biofilm dispersal triggered by oxygen depletion is dependent on PDE RbdA (An et al. 2010). It remains largely unknown what environmental cues activate biofilm dispersal for a vascular phytopathogen. Given the facts that xylem vessels are nutrient-limited and colonizing bacteria quickly deplete oxygen which also possibly cause NO accumulation during anaerobic denitrification, it is reasonable to ask whether these environmental cues, as observed in clinically relevant pathogens, also contribute to biofilm dispersal in vascular phytopathogens.

1.2 Toxin-antitoxin system and antibiotic persistence

1.2.1 Classification of toxin-antitoxin (TA) systems

TA systems are genetic loci typically composed of two components: a stable self-toxic protein that interferes with essential biological processes of bacteria and an unstable antitoxin that counteracts its cognate toxin through various modes of action (Page and Peti 2016). Type I and type II TA systems are the most intensively studied TA systems. For type I TA systems, the antitoxin is an antisense sRNA that inhibits the translation and affects the stability of the toxin mRNA (Harms et al. 2018; Thisted et al. 1994). Under normal conditions, the sRNA-mRNA duplex can be quickly degraded by RNase III, resulting in no growth arrest effect (Gerdes et al. 1992). Several type I toxins are short, hydrophobic, and membrane-associated, including Hok, HokB, and TisB, and cause collapse of membrane proton motive force during overexpression. Most of the currently identified TA systems belong to the type II TA system class. In contrast to a type I antitoxin, the antitoxin of a type II TA system is proteinaceous, which inhibits the function of its cognate toxin through direct binding (Harms et al. 2018). Besides counteracting

with the corresponding toxin, a type II antitoxin, such as MqsA, can also have global regulatory roles (Wang et al. 2011). In response to stresses, some antitoxins have been shown to be selectively degraded, leading to the left toxins free and consequentially their cellular effects (Page and Peti 2016). Type II toxins have been characterized to prohibit DNA replication or mRNA translation (Bernard et al. 1993; Castro-Roa et al. 2013; Christensen-Dalsgaard et al. 2010; Jiang et al. 2002). In type III TA systems, the antitoxin is a sRNA. Instead of forming a duplex with the toxin mRNA as in a type I TA system, a type III antitoxin directly binds to the cognate toxin protein through formation of pseudoknots. The best-characterized type III TA system is the ToxIN TA system (Fineran et al. 2009; Short et al. 2013). ToxN is a sequence-specific endoribonuclease which cleaves the preceded transcript of tandem repeat sequences into individual 36-nt units, called ToxI. ToxN and ToxI are assembled into an inhibitory trimeric complex (Short et al. 2013). The ToxIN TA system appears to contribute to the abortive infection system, an 'altruistic' cell death mechanism to limit viral replication (Fineran et al. 2009). Types IV–VI TA systems were discovered in recent years. The type IV antitoxin is a protein, which, though not directly interacts with the toxin, stabilizes the targets of the toxin (Brown and Shaw 2003). The thus far only known type V TA system is the GhoT/GhoS TA system. In normal conditions, the antitoxin GhoS functions as an RNase that cleaves the toxin mRNA, *ghoT*. However, the *ghoS* mRNA, under stressful conditions, can be cleaved by the previously mentioned type II toxin MqsR, which consequently promotes the translation of the GhoT toxin (Wang et al. 2012b). In a recently identified type VI TA system, the antitoxin SocA acts as a proteolytic adaptor that binds to the toxin SocB and promotes its degradation through the ClpXP protease (Aakre et al. 2013). For plant pathogenic bacteria, functionality of a TA system has been examined only in a few cases (Shidore and Triplett 2017). Recently, Shidore *et*

al. conducted a genome-wide survey of type II and IV TA systems in *E. amylovora* and confirmed the functionality of three TA systems including CbtA/CbeA, ParE/RHH and Doc/PhD (Shidore et al. 2019). To the best of our knowledge, a type I TA system in *E. amylovora* has not been previously identified or characterized.

1.2.2 Regulation of TA systems

As indicated from its definition, a TA system is self-regulated, meaning that the antitoxin directly or indirectly inhibits the action of the cognate toxin. This self-regulation has also been shown to be modulated by global stress regulators, particularly the stringent response and the SOS response. The stringent response is modulated by (p)ppGpp that is produced by various bacteria in response to nutrient limitation (Cashel and Gallant 1969). An increased amount of (p)ppGpp inhibits RNA biosynthesis and therefore decreases translation to enable cells to be metabolically adapted to a harsh environmental condition (Dalebroux et al. 2010; Hauryliuk et al. 2015). Supplementation of serine hydroxamate, a known inducer of (p)ppGpp, has been shown to cause elevated mRNA levels of the *hicAB* type II TA system (Jørgensen et al. 2009). During isoleucine starvation, another stressful condition that causes high levels of (p)ppGpp, the promoter activity of multiple type II TA systems were shown to be upregulated including *dinJ/yafQ*, *hicA/hicB*, *mazE/mazF*, *mqsR/mqsA*, *relB/relE* and *yafN/yafO* (Shan et al. 2017; Traxler et al. 2008). Although direct cross talk between (p)ppGpp and a type I TA system has not been shown, the GTPase Obg was recently shown to contribute to antibiotic persistence through transcriptional activation of the type I toxin *hokB*, and the crosstalk between *hokB* and Obg is (p)ppGpp-dependent (Verstraeten et al. 2015). Accumulation of (p)ppGpp also leads to activation of Lon protease, which selectively degrades type II antitoxins and therefore releases the action of the cognate toxin (Muthuramalingam et al. 2016). The SOS response, triggered by

DNA damage due to reactive oxygen species accumulation, UV irradiation or antibiotic exposure, triggers DNA repair machineries and also induces several type I (*dinQ/agrB*, *hokE/sokE*, *tisB/istR-1*, *symE*/*symR*) and type II TA systems (*dinJ/yafQ* and *yafN/yafO*) (Baharoglu and Mazel 2014; Berghoff and Wagner 2017; Dörr et al. 2010; Fernández De Henestrosa et al. 2000; Kawano et al. 2007; Prysak et al. 2009; Singletary et al. 2009; Vogel et al. 2004). These results together suggest the possible involvement of TA systems of different classes in bacterial stress response.

1.2.3 Implication of TA systems in bacterial persistence

Antibiotic persistence is a phenomenon in which a subpopulation of bacteria becomes temporarily tolerant to high levels of antibiotics without any inheritable mutations (Gefen and Balaban 2009). In contrast to antibiotic resistance, which can be indicated by the increased level of minimal inhibitory concentration (MIC), the MIC level is unchanged due to persistence (Brauner et al. 2016). Persistence can be further classified as triggered persistence and spontaneous persistence. Triggered persistence refers to the phenomenon that persister frequency increases in response to environmental cues, such as nutrient starvation, DNA damage, oxidative stress, and subinhibitory concentrations of drugs (Harms et al. 2016; Helaine et al. 2014).

Whether persisters are metabolically active or dormant is still under scientific debate. Several studies provide supportive evidence of the contribution of active cells to persistence. Through fluorescence-activated cell sorting (FACS), Orman and Brynildsen showed that rapid-growing and metabolically active cells gave rise to persisters whereas most of the dormant cells were not persistent (Orman and Brynildsen 2013). Pu *et al.* showed that several multi-drug efflux genes, including the essential component *tolC*, were expressed significantly higher in persisters (Pu et al. 2016). They demonstrated that, during β-lactam antibiotic treatment, persisters actively

pumping out the cytoplasmic drug through enhanced efflux activity (Pu et al. 2016). With an assay that induces persistence through nutrient shift, Radzikowski *et al.* showed that metabolism of persisters shifted to maximize ATP production through respiration, and the alternative sigma factor σ^{54}-mediated stress response was activated (Radzikowski et al. 2016). However, several other researchers support the view that persisters are dormant (Kim and Wood 2016; Kwan et al. 2013; Shah et al. 2006a). Wood and colleagues have questioned studies supporting the alternative hypothesis, arguing that the methods used may have introduced dormant persisters into the FACS assays and skewed the conclusions (Kim and Wood 2016).

The linkage between TA systems and persistence originated from a study screening for mutants exhibiting high levels of persistence (Moyed and Bertrand 1983). This study identified *hipA7*, the HipA toxin gene with a gain-of-function mutation (Moyed and Bertrand 1983). The antitoxin, HipB, was later identified (Black et al. 1991). It was shown that the kinase activity of HipA causes accumulation of ppGpp through inactivation of glutamyl t-RNA synthetase, which consequently leads to persistence (Bokinsky et al. 2013; Germain et al. 2013). Except HipA, the involvement of other type II in persistence seems to be still controversial. Several type II toxins, i.e. MazF, MqsR, RelE, and YafQ, are endoribonucleases that cleave mRNA to block translation. Although ectopic overexpression of an individual toxin gene increases persistence in *E. coli* (Christensen et al. 2001; Harrison et al. 2009; Kim and Wood 2010; Vázquez-Laslop et al. 2006), chromosomal deletion of a single endonuclease toxin gene or successive deletion of multiple toxin genes did not significantly affect persistence (Harms et al. 2017; Maisonneuve et al. 2011), suggesting these type II TA toxins may affect persistence only under inducing conditions.

Besides type II TA systems, other TA systems that contribute to persistence are mainly membrane-associated TA systems, including the type I toxins TisB and HokB, and the type V toxin GhoT. The involvement of TisB in persistence in *E. coli* was concluded from assays using both a deletion mutant and an overexpression strain (Dörr et al. 2010). It was concluded that these toxins provoke membrane potential dissipation, leakage of cellular ATP, and ultimately cell dormancy to enhance persistence (Cheng et al. 2014; Gurnev et al. 2012a; Wilmaerts et al. 2018). Interestingly, the MqsR toxin exhibits endoribonuclease activity to degrade the *ghoS* mRNA under stress and therefore activates the function of GhoT (Wang et al. 2013), suggesting that persistence may be primed during specific conditions through cross-talk between TA systems.

1.3 Resistance mechanisms of SDHI fungicides in phytopathogenic fungi

The succinate dehydrogenase inhibitor (SDHI) class belongs to FRAC group 7 that has been applied for agricultural uses since the late 1960s (Schmeling and Kulka 1966). The third generation SDHI fungicides have been introduced on the market since 2003 with the release of boscalid. SDHI is a fastest growing fungicide class regarding compound discovery and market launch in agriculture field. The SDHI class ubiquitously inhibits the complex II of the mitochondrial respiration through blocking the binding site for electron transfer from succinate to ubiquinone (Sierotzki and Scalliet 2013). SDHIs exhibit broad-spectrum antifungal activity that have been applied for management of both ascomycetes fungi, such as *Botrytis cinerea*, and basidiomycete fungi, such as *Ustilago maydis* (Avenot and Michailides 2010; Sierotzki and Scalliet 2013). SDHI is a class of site-specific fungicide and repeated usage of SDHI fungicides over years poses heightened risk of selecting fungicide resistance populations of the target

pathogens. Due to its unique mode of action, cross-resistance between SDHIs and other chemical classes is not expected (Avenot et al. 2008a; Zhang et al. 2007).

1.3.1 History and current status of SDHI fungicides

The succinate dehydrogenase inhibitor (SDHI) class exhibits broad-spectrum antifungal activity that has been widely applied in agricultural fields. Due to the increasingly reduced efficacy of DMI and QoI fungicides in managing fungal diseases in the fields, SDHI, exhibiting no known cross-resistance to the DMI and QoI classes, has been applied as an alternative fungicide class to manage DMI- and QoI-resistant fungal populations. The SDHI class was originally termed as carboxamide, and the first compound, carboxin, was marketed in 1966 (Schmeling and Kulka 1966). Carboxin, together with the later discovered flutolanil, were mainly used against basidiomycete pathogens, such as smut, rust and Rhizoctonia diseases, exhibiting limited efficacy for other diseases (Avenot and Michailides 2010; Motoba et al. 1988; Ulrich and Mathre 1972). The first broad-spectrum carboxamide was boscalid, that was launched in the market in 2003 and was shown to be highly effective against a diverse range of ascomycete fungi of fruits, vegetables, and crops (Glättli et al. 2011). Soon after that, multiple new fungicides that exhibit broad-spectrum succinate dehydrogenase (SDH)-inhibitory effects was introduced to the market, collectively called SDHIs since 2009 (Sierotzki and Scalliet 2013). Currently, a total of 23 SDHI compounds in 11 different chemical groups are listed in the Fungicide Resistance Action Committee, including benodanil, benzovindiflupyr, bixafen, boscalid, carboxin, fenfuram, fluopyram, fluindapyr, fluxapyroxad, flutolanil, furametpyr, inpyrfluxam, isofetamid, isoflucypram, isopyrazam, mepronil, oxycarboxin, penflufen, penthiopyrad, pydiflumetofen, pyraziflumid, thifluzamide, and sedaxane (Frac 2020). SDHIs with oomyceticidic activity is still lacking.

1.3.2 SDHI mode of action

Oxidative phosphorylation is the process of ATP generation through a chain of electron transfer that takes place within the inner membrane of mitochondria in eukaryotes. Succinate-Q oxidoreductase (complex II) is an essential enzyme for electron transport chain, which transfers succinate-originated electrons directly to ubiquinone. It is composed of four subunits including a flavoprotein (SdhA), an iron-sulfur protein (SdhB), and two membrane anchor subunits (SdhC and SdhD). SdhA catalyzes the oxidation reaction from succinate to fumarate, and SdhB contains three iron–sulfur clusters, where electrons are transferred (Ackrell 2000; Ōmura and Shiomi 2007). The ubiquinone binding pocket (Qp) is hold by SdhB, SdhC, and SdhD (Maklashina and Cecchini 2010). Current marketed SDHI fungicides specifically disturb the fungal mitochondrial respiration process through competitive binding to the Qp pocket and therefore blocking the succinate cycling and the electron transfer event (Horsefield et al. 2006; Huang et al. 2006). Three-dimensional protein structures of the Sdh complex have been characterized using X-ray crystallography for a limited number of species, such as *Escherichia coli* (Yankovskaya et al. 2003), *Gallus gallus* (chicken) (Huang et al. 2006) and *Sus scrofa* (pig) (Sun et al. 2005). Through co-crystallization analysis, Ruprecht *et al.* showed delicate rearrangements of the Qp site in response to different inhibitors (Ruprecht et al. 2009). Although crystal structures of Sdh proteins for phytopathogenic fungi have not been currently determined, measurement of ubiquinone reductase activities through 2,6-Dichlorophenolindophenol (DCPIP) indicated the importance of the Qp site for the antifungal activity of the SDHI class (Jones and Hirst 2013; Szeto et al. 2007). Despite overall relatively low sequence conservation for SdhC and SdhD, a few critical amino acid residues for the catalysis of the ubiquinone reduction reaction are highly conserved across species (Cecchini 2003). Using homology-based modeling approach, SDHI

docking models are available for several ascomycete phytopathogenic fungi, including *Botrytis cinerea* and *Mycosphaerella graminicola* (Fraaije et al. 2012; Glättli et al. 2009; Scalliet et al. 2012; Steinhauer et al. 2019). The amino acid residues that are directly involved in Qp binding in *M. graminicola* have been predicted, including Trp224 in SdhB, Ser83 in SDHC, and Tyr130 in SdhD (Sierotzki and Scalliet 2013). His267 in SDHB and Arg87 in SDHC are buried in the bottom of the pocket. Mutations of Trp224 in SdhB or Tyr130 in SdhD have not been identified in any natural fungal isolates or lab mutants, suggesting the fitness advantage in maintaining these residues (Sierotzki and Scalliet 2013).

1.3.3 Resistance mechanism of SDHI fungicides

SDHI resistance risk level is currently listed as medium to high (Frac 2020), and reduced efficacy of SDHIs has been described in more than 20 fungal species, including several economically-important plant pathogens: *Alternaria alternata*, *A. solani*, *B. cinerea*, *Blumeriella jaapii*, *Clarireedia homoeocarpa*, *Corynespora cassiicola*, *Sclerotinia sclerotiorum*, and *Zymoseptoria tritici* (Frac 2020). Overall, fungicide resistance in fungal populations can be achieved through four distinct mechanisms: alteration of fungicide target site, overproduction of the fungicide target, enhanced drug efflux transporter activity, and detoxification through fungal self-metabolism (Deising et al. 2008). For the SDHI class, alteration of the fungicide target site through mutation is, to date, the most frequently observed mechanism to gain resistance in a fungal population. The mechanism of SDHI fungicide resistance has been investigated mainly through two approaches: functional characterization of lab mutants and correlative analysis of the phenotypes and the genotypes of field isolates. Through site-directed mutagenesis and gene replacement, Lalève *et al.* (2014) showed that specific mutations of P225, N230, and H272 in *SdhB* confer different levels of resistance to several SDHI fungicides in *B. cinerea*, i.e. bixafen,

boscalid, carboxin, and fluopyram (Lalève et al. 2014). SDHI resistance mechanisms have also been functionally characterized in the *Zymoseptoria tritici*, the causal agent of septoria leaf blotch on wheat, through plasmid expression of Sdh alleles (Skinner *et al.*, 1998), bulked segregant analysis (Steinhauer *et al.*, 2019), chromosomal deletion mutation (Steinhauer *et al.*, 2019), and UV radiation-induced mutagenesis (Fraaije *et al.*, 2012; Scalliet *et al.*, 2012). Particularly, mutations that alter the H267 codon in SdhB (corresponding to H272 in *B. cinerea*) are shown to confer resistance to bixafen, boscalid, carboxin, fluopyram, and isopyrazam in *Z. tritici* (Fraaije *et al.*, 2012; Scalliet *et al.*, 2012; Skinner *et al.*, 1998). Similarly, for *C. homoeocarpa*, the H267Y and H267R mutations in SdhB and the G91R and G150R mutations in SdhC have been characterized to confer reduced efficacy to SDHI fungicides through expression of a mutated *SdhB* or *SdhC* allele in an SDHI-sensitive strain of *C. homoeocarpa* (Popko et al. 2018).

Although functions of Sdh mutations in conferring SDHI fungicide resistance have been genetically characterized in a few cases, most frequently, SDHI fungicide resistance mechanisms are inferred based on the identification of mutations that are overrepresented in the SDHI-resistant field isolates, without functional demonstration. For *B. cinerea*, besides the Sdh mutations that have been functionally characterized, field isolates carrying mutation(s) at codon G85, I93, M158, V168 of *SdhC*, and codon H132 of *SdhD* have been shown to correlate with reduced sensitivity to SDHIs (Amiri *et al.*, 2020; Fernández-Ortuño *et al.*, 2017; Leroux *et al.*, 2010). Sequence comparison between boscalid-resistant and boscalid-susceptible isolates of *Alternaria alternata*, the causative agent of Alternaria late blight of pistachio, revealed that the H277Y and H277R mutations in SdhB are predominating in the resistant isolates of this fungus (Avenot et al. 2008b). The corresponding mutations of SdhB (H278Y and H278R) in *Alternaria*

solani have also been shown to correlate with increased resistance to boscalid of this fungus (Mallik et al. 2014; Miles et al. 2014). The SdhD H133R mutation was also observed in multiple isolates of *A. solani* exhibiting moderate to high levels of boscalid resistance (Mallik et al. 2014).

1.3.4 SDHI cross resistance

The consequence of potential cross resistance due to a *Sdh* mutation varies among different species. Avenot *et al.* found that isolates of *Didymella bryoniae* that were boscalid-resistant and carried a H277Y mutation in SdhB were also highly resistant to penthiopyrad, suggesting a positive correlation of resistance between the two SDHIs (Avenot and Michailides 2010). The cross-resistance between boscalid and penthiopyrad was also observed in *A. alternata* strains carrying the SdhB H277Y, SdhC H134R, or SdhD H133R mutation (Avenot and Michailides 2010). However, none of these three mutations in *A. alternata* confers resistance to fluopyram (Avenot and Michailides 2010). For *Corynespora cassiicola*, though a specific mutation was not identified, penthiopyrad was shown to be still effective against strains exhibiting very high tolerance to boscalid (Ishii et al. 2011). For *B. cinerea*, the P225F substitution in SdhB was shown to confer resistance to all the SDHI fungicides included in a previous study, i.e. benodanil, bixafen, boscalid, carboxin, fenfuram, fluopyram, fluxapyroxad, isopyrazam (Veloukas et al. 2013). The N230I substitution in SdhB confers resistance to boscalid, fluopyram, carboxin, and bixafen (Lalève *et al.*, 2014). The *B. cinerea* with the H272L substitution in SdhB was shown to be highly resistant to boscalid but yet exhibit low to intermediate levels of resistance to the other SDHIs examined (Veloukas et al. 2013). In contrast, a different mutation at the same codon position, H272Y in SdhB, showed enhanced sensitivity to benodanil and fluopyram, and only moderate level of resistance to boscalid (Veloukas et al. 2013). These studies suggest that although all SDHIs consistently target the Qp site of the

complex II, the actual binding sites and binding affinity different drastically across different SDHIs in different fungi. Therefore, systemic investigations of *Sdh* mutations in conferring different SDHI fungicides for each fungus are necessary to provide robust recommendations for management of different fungal diseases.

CHAPTER 2

Orchestration of virulence factor expression and modulation of biofilm dispersal in *Erwinia amylovora* through activation of small RNA RprA

2.1 Abstract

Erwinia amylovora is the causative agent of the devastating disease fire blight of pome fruit trees. After infection of host plant leaves at apple shoot tips, *E. amylovora* cells form biofilms in xylem vessels, restrict water flow, and cause wilting symptoms. Although *E. amylovora* is well known to cause systemic infection, the means by which biofilm cells of *E. amylovora* transit from the sessile mode of growth in xylem to the planktonic mode of growth in cortical parenchyma remains unknown. Increasing evidence has suggested the important modulatory roles of small RNAs (sRNAs) in the pathogenesis of *E. amylovora.* Here, we demonstrate that sRNA RprA acts as a positive regulator of amylovoran production, the type III secretion system (T3SS), and flagellar-dependent motility, and as a negative regulator of levansucrase activity and cellulose production. We also show that RprA affects the promoter activity of multiple virulence factor genes and regulates *hrpS,* a critical T3SS regulator, at the posttranscriptional level. We determined that *rprA* expression can be activated by the Rcs phosphorelay, and that expression is active during T3SS-mediated host infection in an immature pear fruit infection model. We further showed that overexpression of *rprA* activated the *in vitro* dispersal of *E. amylovora* cells from biofilms. Thus, our investigation of the varied role of RprA in affecting *E. amylovora* virulence provides important insights into the functions of this sRNA in biofilm control and systemic infection.

2.2 Introduction

Fire blight, caused by *Erwinia amylovora,* is a devastating bacterial disease threatening the worldwide production of many rosaceous fruits, such as apple and pear (Malnoy et al. 2012). The primary infection of *E. amylovora* is manifested by several distinct stages: flower infection, infection of leaves at shoot tips, xylem colonization, and systemic infection. During flower infection, large populations of *E. amylovora* cells (ca. 10^{6-7} cfu/flower) are established on stigmas; these bacteria are then further disseminated down to the hypanthium, and ultimately initiate infection via natural openings in the flower nectaries (Thomson 2000; Vanneste 1995). Within host xylem vessels in leaves, *E. amylovora* cells block water transport and cause wilting symptoms by formation of biofilms, that are static microcolonies of bacterial cells enmeshed in a matrix of exopolysaccharides (EPSs) (Koczan et al. 2011; Koczan et al. 2009). *E. amylovora* can migrate further within the vascular tissue to cause systemic infection, but more commonly exit from xylem vessels and move further systemically through the host in cortical parenchyma tissue. The systemic spread of *E. amylovora* through host apple trees follows a downward path, ultimately ending at the crown:rootstock junction, where cankers can develop that girdle and kill the host (Norelli et al. 2003). Frequently, *E. amylovora* cells emerge from flower pedicel, leaf petiole, or stem tissues as ooze, which serves as the inoculum for secondary infection (Slack et al. 2017).

The pathogenesis of *E. amylovora* is mediated by several important virulence factors, including the T3SS (Oh et al. 2005; Zhao et al. 2009a), motility (Bayot and Ries 1986), and several EPSs including amylovoran (Goodman et al. 1974; Sjulin and Beer 1978), levan (Geier and Geider 1993), and cellulose (Castiblanco and Sundin 2018). The primary infection of *E. amylovora* through flowers requires the T3SS to defeat host defense mechanisms and initiate

pathogenesis, and motility to facilitate the migration of *E. amylovora* cells from stigmas to nectarthodes (Bayot and Ries 1986; Bogdanove et al. 1998; Kim et al. 1997; Oh et al. 2005). The *E. amylovora* T3SS has been well characterized to be regulated in a hierarchical manner. HrpL, an alternate sigma factor, activates transcription of the *hrp* genes, including the structural gene *hrpA* encoding the T3SS pilus, and the major effector gene *dspE*, through recognition of the "*hrp* box" motif (McNally et al. 2012; Triplett et al. 2009; Wei and Beer 1995). *hrpL* expression is tightly regulated by the enhancer-binding protein HrpS and the two-component system HrpX/HrpY (Lee et al. 2016; Wei et al. 2000). Amylovoran is an acidic exopolysaccharide composed of repeating units of galactose molecules and a glucuronic acid residue (Nimtz et al. 1996). Amylovoran biosynthesis is mediated by the 12-gene *ams* operon (Bugert and Geider 1995). Levan is a homopolymer of fructose molecules synthesized through hydrolysis of sucrose via the levansucrase enzyme, that is encoded by the *lsc* gene (Geier and Geider 1993; Gross et al. 1992). Amylovoran, levan, and cellulose together constitute the matrix of *E. amylovora* biofilms (Castiblanco and Sundin 2018; Koczan et al. 2009).

The chaperone protein Hfq and its dependent small RNAs (sRNAs) have been shown to be important in modulating virulence factors of *E. amylovora* (Zeng et al. 2013; Zeng and Sundin 2014). The Hfq-dependent sRNA ArcZ was shown to positively affect amylovoran, T3SS, levansucrase activity, and flagellar swimming motility, partially through posttranscriptional regulation of the leucine-responsive regulatory protein, Lrp (Schachterle and Sundin 2019; Zeng and Sundin 2014). However, the functions and regulatory mechanisms of most Hfq-dependent sRNAs identified in *E. amylovora* are still enigmatic. A deletion mutant of the Hfq-dependent sRNA *rprA* (Ea1189*ΔrprA*) was previously shown to cause decreased levels of virulence in an immature pear infection model, suggesting the positive involvement of this

sRNA in the pathogenesis of *E. amylovora* though unknown mechanisms (Zeng et al. 2013). RprA was initially identified in *Escherichia coli*, and was shown to stimulate the translation of the stationary-phase sigma factor RpoS in this bacterium (Majdalani et al. 2001). Through imperfect reverse complementarity with RprA, the inhibitory structure of the 5′ untranslated region (5′ UTR) of the *rpoS* mRNA is disengaged, and the translation of *rpoS* is consequently activated (Majdalani et al. 2001; McCullen et al. 2010; Urban and Vogel 2007). *E. coli* RprA has also been shown to downregulate *csgD*, encoding a stationary phase-induced biofilm regulator, and *ydaM*, encoding a diguanylate cyclase (Andreassen et al. 2018; Mika et al. 2012). Expression of *E. coli* RprA has been demonstrated to be induced by the RcsC/RcsB phosphorelay (Majdalani et al. 2002) and by the CpxA/CpxR two-component signal transduction systems (Vogt et al. 2014). RprA expression in *E. coli* or *Salmonella enterica* serovar Typhimurium can also be activated by high population density and by environmental stressors including osmolarity shock and low pH (Madhugiri et al. 2010; Srikumar et al. 2015).

We hypothesized that RprA affects virulence of *E. amylovora* through modulation of its virulence factor(s), and expression of *rprA* could be activated or deactivated in during *E. amylovora* pathogenesis upon perception of certain environmental or native cue(s). In this study, we demonstrate that RprA acts as a positive regulator of amylovoran, T3SS, and flagellar-dependent motility, and as a negative regulator of levansucrase activity and cellulose production. We also identified the *in vitro* and *in vivo* conditions that activate RprA and demonstrated that activation of RprA decreased biofilm formation and promoted biofilm dispersal. This study provides important evidence for the involvement of RprA in the systemic movement of *E. amylovora* during pathogenesis.

2.3 Results

2.3.1 RprA positively regulates amylovoran, T3SS, and motility, and negatively regulates levansucrase activity and cellulose production

RprA was previous identified as a 111-nt Hfq-dependent sRNA that contributed to the full virulence of *E. amylovora*, as the deletion mutant Ea1189*ΔrprA*, showed compromised virulence in an immature pear infection model (Mika et al. 2012). To validate the positive involvement of RprA in the virulence of *E. amylovora*, we first examined the virulence of *ΔrprA* (pJP-*rprA*), in which *rprA* was expressed *in trans.* We showed that *ΔrprA* (pJP-*rprA*) exhibited strong virulence on the inoculated immature pears that was comparable to the *E. amylovora* WT strain (Figure 2.1A), confirming the importance of RprA on the virulence of *E. amylovora*. Secondary structure modeling of RprA showed that RprA had four stem loops with a characteristic Rho-independent terminator in the 3' end (Figure 2.1B). Sequence alignment of the RprA homologs in Enterobacteriaceae suggested that nucleotide sequences of RprA are highly conserved towards the 3' end but much less conserved towards the 5' end (Figure 2.1C).

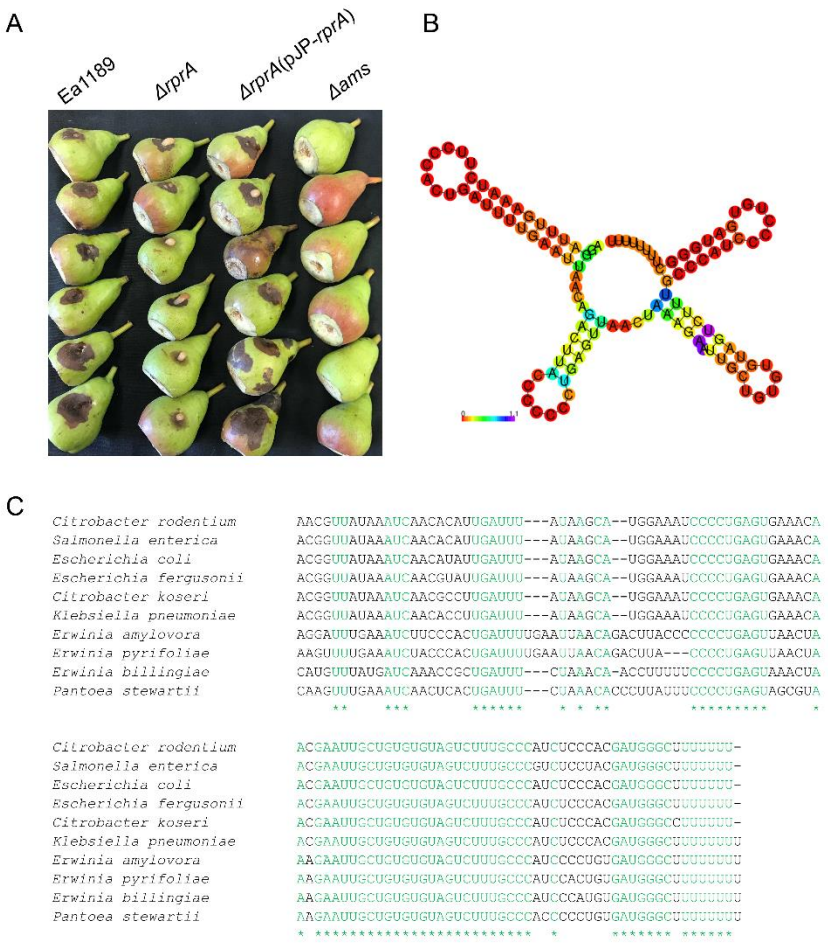

Figure 2.1. The effect of *RprA* on virulence of *E. amylovora* and sequence characteristics of RprA. (A) *E. amylovora* cultures at approximately 2×10^4 CFUs in 2 µl were stab-inoculated into immature pears. Images were captured 4 days post inoculation. The amylovoran-null mutant *Δams* was used as a negative control for the assays. (B) Secondary structure of RprA was predicted with the minimum free energy model of RNAfold (http://rna.tbi.univie.ac.at/cgi-bin/RNAWebSuite/RNAfold.cgi). The positional entropy of each nucleotide is color-coded. (C) Sequence alignment of RprA homologs in representative species of Enterobacteriaceae. Shared nucleotide sequences were highlighted in green color.

To understand the molecular mechanisms of RprA in affecting the full virulence of *E. amylovora*, we examined how mutagenesis or overexpression of *rprA* affected virulence factors of this bacterium including amylovoran production, hypersensitive response (HR), flagellar swimming motility, levansucrase activity, and cellulose production. We showed that amylovoran production was significantly reduced in the Ea1189*ΔrprA* mutant, and that production was

restored to the WT level in the complementation strain (Figure 2.2A). In contrast, overproduction of RprA rendered significantly increased level of amylovoran production in *E. amylovora* (Figure 2A). Our results therefore suggested that RprA is a positive regulator of amylovoran production. To investigate if RprA affected the function of T3SS, we examined whether *rprA* mutation or overproduction affected the ability of *E. amylovora* to elicit the HR. Compared with the other strains examined, the *ΔrprA* mutant exhibited minimal HR on *Nicotiana benthamiana* leaves, suggesting a positive effect of RprA on the function of T3SS (Figure 2.2B). The *rprA* mutation had a small effect on the swimming motility of *E. amylovora* (Figure 2.2C). In contrast, the *rprA* overexpression strain Ea1189(pOE-*rprA*) was hypermotile (Figure 2.2C). These results suggested that the basal level of RprA contributes little to the swimming motility of *E. amylovora*, but its effect on this phenotype was greater when *rprA* was overexpressed. Deletion mutation of *rprA* had negligible effects on the activity of levansucrase and the production of cellulose, but these EPSs were greatly compromised when *rprA* was overexpressed (Figure 2.2D and 2.2E). Therefore, a basal level of RprA had minimal effects on levansucrase activity and cellulose production; a high level of RprA, nevertheless, negatively correlated with the production of these extracellular polymeric substances. Taken together, RprA exhibited complex regulatory roles on the virulence factors of *E. amylovora*, and its impacts were overall greater when RprA was overproduced.

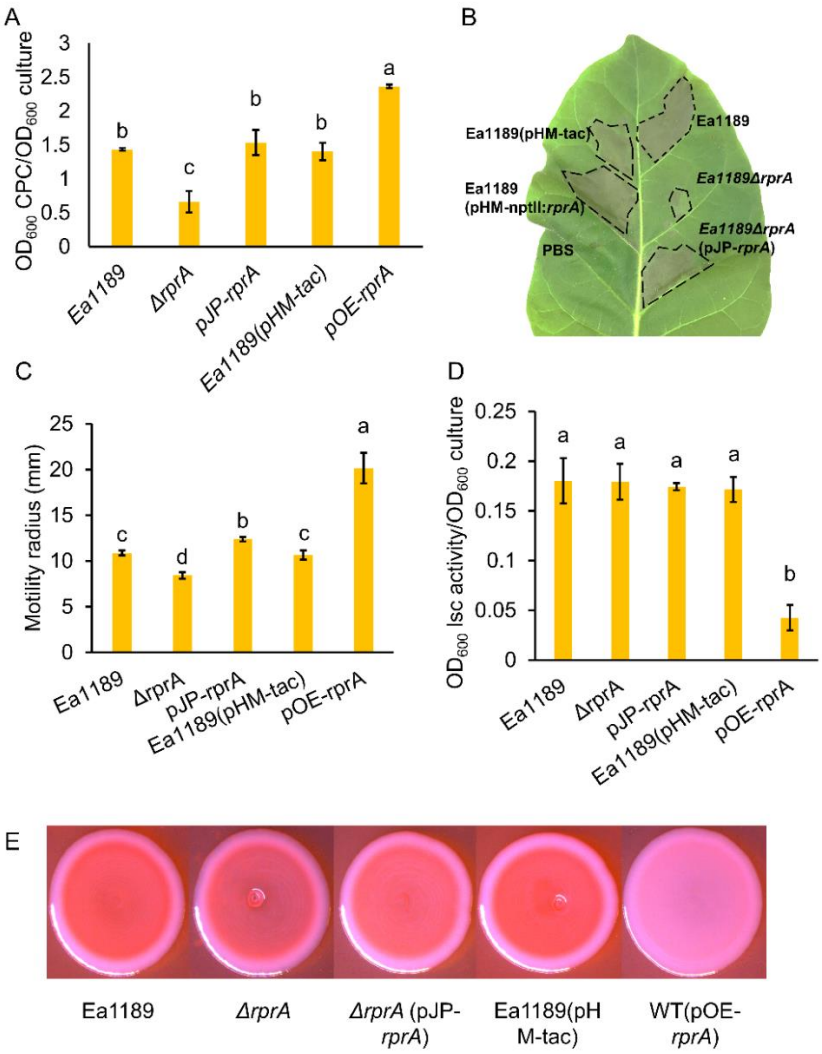

Figure 2.2. Multifaced regulatory roles of RprA on virulence factors of *E. amylovora*. (A) RprA positively regulates amylovoran production. Amylovoran was determined in cultures grown for 24 h in MBMA medium with 1% galactose through a cetylpyridinium chloride-binding assay. (B) Positive involvement of RprA on hypersensitive reaction. Approximately 100 µl cell suspension at OD_{600}=0.05 was infiltrated into *Nicotiana benthamiana* leaves of 10-week-old. The HR symptom was observed 16 h post inoculation. (C) RprA increases the swimming motility of *E. amylovora*. Overnight cultures in 2 µl were inoculated into 0.3% agar LB plates and the motility area in radius was determined 48 h after inoculation. (D) RprA inhibits levansucrase (lsc) activity of *E. amylovora* quantified as previous described (Schachterle and Sundin 2019). (E) RprA inhibits cellulose biosynthesis in *E. amylovora* determined through a Congo red-binding assay. Greater amount of Congo red absorbance into the colony indicates an increased amount of cellulose production. For all the *in vitro* assays, cultures were grown in the test media amended with 1 mM IPTG. Results represent the means of three biological replications and error bars represent the standard deviations. Different letters indicate significant differences ($P < 0.05$) using Tukey's HSD test. The assays were done at least three times with similar results.

2.3.2 RprA regulates the promoter activity of virulence factor genes

To examine how RprA affect the transcriptional activity of virulence factor genes, we generated green fluorescent protein (gfp) transcriptional fusion reporter constructs of *amsG*, the first gene of the amylovoran biosynthetic gene operon, *lsc*, the levansucrase gene, and representative T3SS genes, including *hrpL*, *hrpA*, and *dspE*. Comparing with the empty vector strain, the *rprA* overexpression strain exhibited significantly higher promoter activity of *amsG* and all the T3SS genes included (Figure 2.3). The promoter activity of *lsc* in the *rprA* overexpression strain was nevertheless significantly lower, that was consistent with observation of reduced levansucrase activity in this strain compared with the control (Figure 2.3).

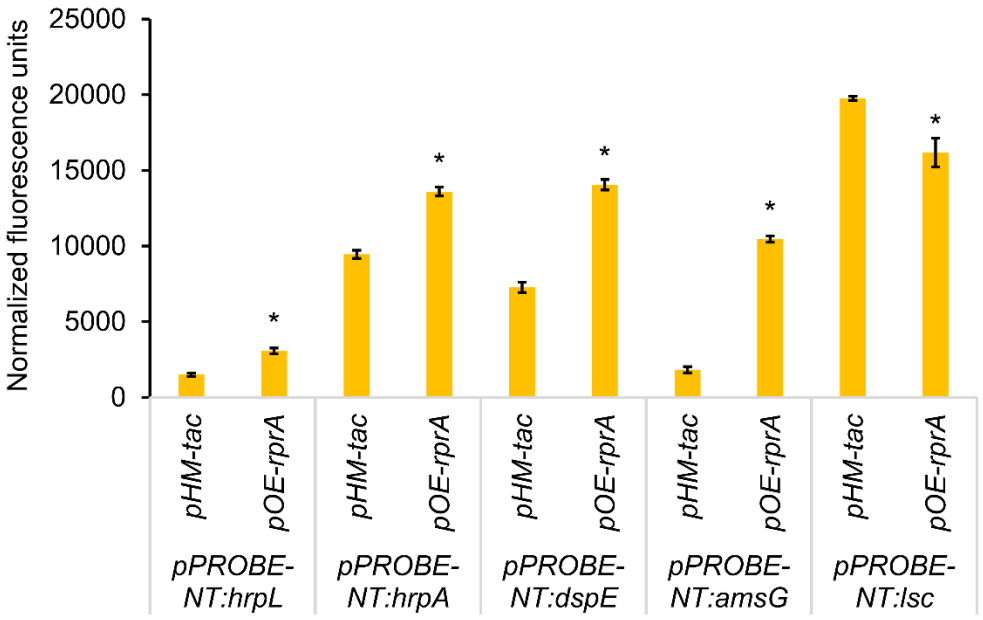

Figure 2.3. RprA regulates the promoter activity of virulence factor genes. Relative fluorescence units of the indicated transcriptional fusion construct in Ea1189(pHM-tac) and Ea1189(pOE-rprA) were measured using a Tecan spectrophotometer followed by normalization with the corresponding OD_{600} values. IPTG at 1 mM was amended into the media to induce *rprA* overexpression. Results represent the means of three biological replications and error bars represent the standard deviations. Asterisks indicate significant difference ($P < 0.05$). The assays were done three times with similar results.

2.3.3 RprA regulates *hrpS* at a post-transcriptional level

To identify possible direct targets of RprA, we conducted a genome-wide prediction of the targets of RprA using TargetRNA2 (Kery et al. 2014), which employs structural accessibility and sequence conservation for sRNA target screening. This yielded prediction of 31 putative targets of RprA. Of interest, the enhancer binding protein gene *hrpS* was predicted as a target of RprA in this analysis. RprA was predicted to interact with the region from -20 to -7 bp relative to the translational start site of *hrpS* (Figure 2.4A). Two transcriptional start sites of *hrpS* were previously identified at 129 and 227 nt upstream from its start codon, respectively (Lee and Zhao 2018). To determine whether RprA affected *hrpS* mRNA post-transcriptionally, we constructed pxg-20:*hrpS*129 and pxg-20:*hrpS*227, that fused the 5' untranslated region in 129 nt or 227 nt and the first 30 codons of *hrpS* in-frame with *gfp* in pXG-20. We found that overexpression of *rprA* resulted in significantly higher fluorescence in *E. amylovora* cells carrying pxg-20:*hrpS*129, but no significant difference was observed in cells carrying the pxg-20:*hrpS*227 construct (Figure 2.4B).

A

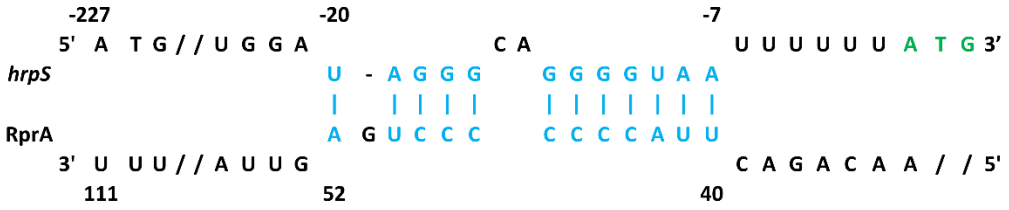

B

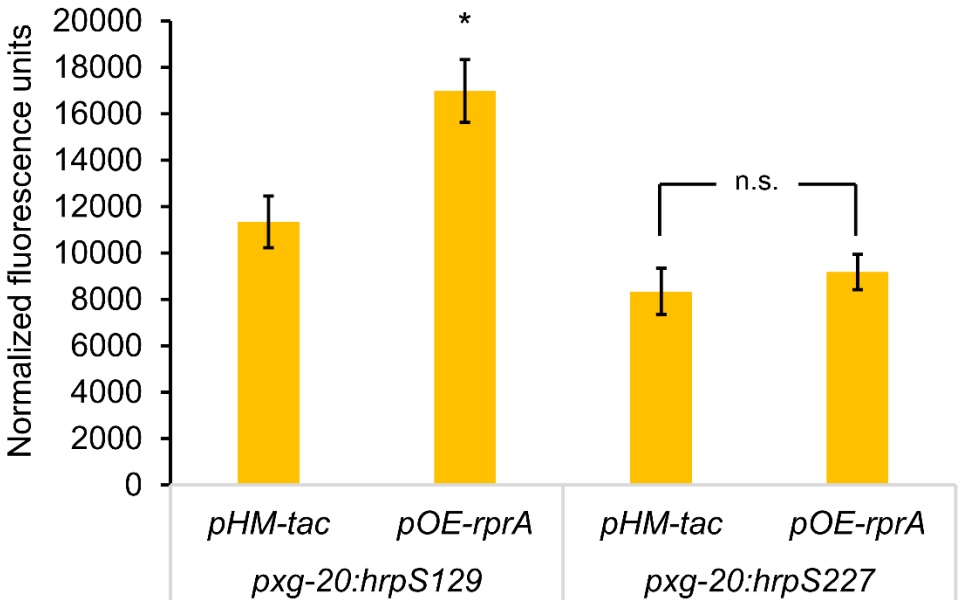

Figure 2.4. RprA regulates *hrpS* at the post-transcriptional level. (A) Proposed interaction region between RprA and *hrpS* mRNA. (B) Relative fluorescence units of the indicated translational fusion in Ea1189(pHM-tac) and Ea1189(pOE-rprA) were measured using a Tecan spectrophotometer followed by normalization of their corresponding OD_{600} values. Results represent the means of three biological replications and error bars represent the standard deviations. Asterisks indicate significant difference ($P < 0.05$) whereas "n.s." indicates no significant difference using Student's *t*-test using Student's *t*-test. The assays were done three times with similar results.

2.3.4 *rprA* expression is activated by native and environmental cues

A previous study in *E. coli* showed that *rprA* was transcriptionally regulated by the Rcs phosphorelay, that is composed of the histidine kinase RcsC and the response regulator RcsB (Majdalani et al. 2002). We identified an "Rcs box", the consensus binding site of RcsB, immediately upstream of the -35 region of the promoter of *rprA*, suggesting that *rprA* in *E. amylovora* may also be subject to the regulation by the Rcs phosphorelay. As expected, compared with that in the WT strain, the expression of *rprA* was reduced approximately two-fold in the *rcsB* deletion mutant, Ea1189*ΔrcsB* (Figure 2.5A). Introduction of the complementation construct pJP-*rcsB* completely restored the *rprA* expression defect in Ea1189*ΔrcsB*, which was four-fold lower compared with the WT strain (Figure 2.5A). We also measured expression of *rprA* in Ea1189*ΔrcsB*(p*rcsB*-D56E) and Ea1189*ΔrcsB*(p*rcsB*-K154Q), that encoded RcsB with a D56E (aspartate to glutamic acid) substitution or a K154Q (lysine to glutamine) substitution to mimic the constitutively phosphorylated or the acetylated state of RcsB, respectively (Ancona et al. 2015; Hu et al. 2013). We showed that *rprA* expression was elevated in Ea1189*ΔrcsB*(p*rcsB*-D56E) compared with Ea1189*ΔrcsB*(p*rcsB*), whereas its expression in Ea1189*ΔrcsB*(p*rcsB*-K154Q) was similar to that of Ea1189*ΔrcsB* (Figure 2.5A). Together, these results indicated that *rprA* expression is positively and negatively modulated by the phosphorylation and the acetylation of RcsB, respectively.

To examine whether expression of *rprA* could be affected by external stressors, *E. amylovora* Ea1189 WT cultures were grown in LB broth to exponential phase (OD_{600}=0.5) and then challenged with either low pH (pH=5) or osmotic shock (0.4 M NaCl), or immersed in HrpMM medium, a low pH and low nutrient medium that mimics the conditions of the plant apoplast (Huynh et al. 1989). We also examined how the population density of *E. amylovora*

(exponential phase versus stationary phase) may affect *rprA* expression. We did not observe any significant change of *rprA* expression in *E. amylovora* cells undergoing low pH stress or osmotic shock or in high population density (Figure 2.5B). However, *rprA* expression was significantly induced in *E. amylovora* cultures grown in HrpMM (Figure 2.5B), suggesting that *rprA* may be induced during host infection.

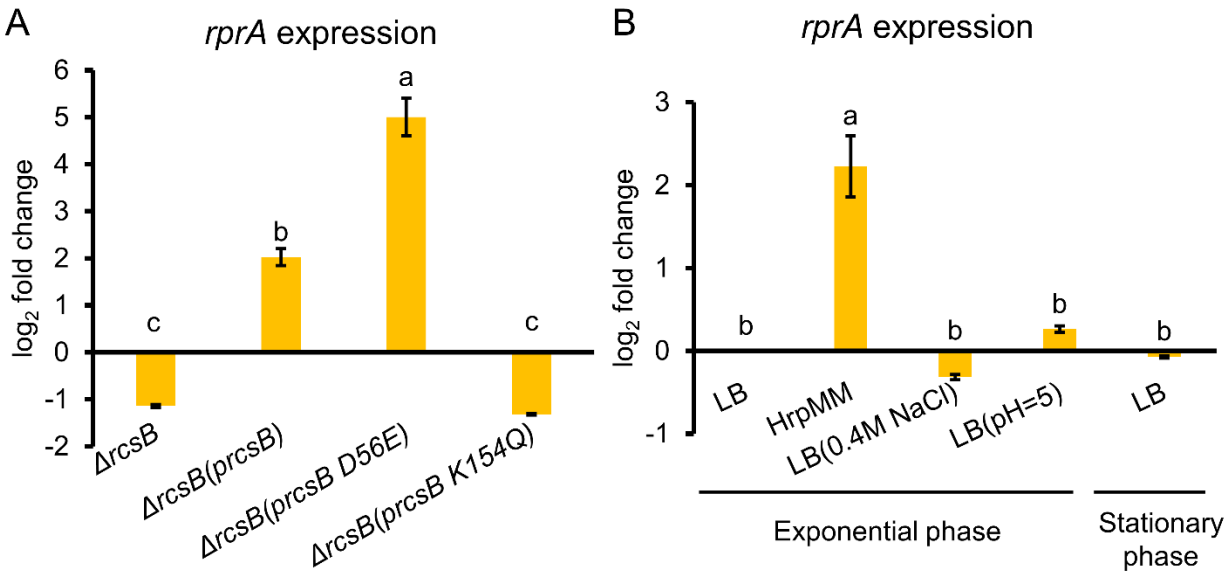

Figure 2.5. Activation of RprA by native and environmental cues. (A) Regulation of RprA expression by the Rcs phosphorelay system (B) Effect of environmental stressors on *rprA* expression. Expression levels of *rprA* were quantified through quantitative real-time PCR (qRT-PCR), and fold changes were calculated using the $2^{-\Delta\Delta C_T}$ formula. The housekeeping gene *recA* was used as an endogenous control. Error bars indicate standard variations. Different letters indicate significant differences ($P < 0.05$) using Tukey's HSD test.

To enable *in vivo* examination of *rprA* transcriptional activity, we generated the dual reporter construct p*NptII-gfp-rprA-mCherry*, that allowed cellular *gfp* expression in a constitutive manner and mCherry under the control of the native promoter of *rprA*. As observed using a confocal microscope, the transcriptional activity of *rprA* was very low in Ea1189(p*NptII-gfp-rprA-mCherry*) cultures grown in LB broth (Figure 2.6A), as indicated by the very dim fluorescence from mCherry. In immature pear flesh tissues that were inoculated with Ea1189(p*NptII-gfp-rprA-mCherry*) cultures, *E. amylovora* cells were shown to colonize the apoplast region of the flesh tissues (green fluorescence) and also exhibited strong levels of red fluorescence (Figure 2.6A). In pear ooze, that contained a large population of *E. amylovora* cells emerging from the infection site of the inoculated pears, *E. amylovora* cells also exhibited very high levels of red fluorescence compared with that in LB broth. Through qRT-PCR, we confirmed that *rprA* expression increased by ~30-fold in *E. amylovora* cells from pear ooze compared with that grown in LB broth (Figure 2.6B). We also showed upregulation of the T3SS genes and the amylovoran biosynthetic gene *amsG*, and downregulation of the levansucrase gene *lsc* of *E. amylovora* in pear ooze, that were consistent with the up- or down-regulation of these genes during RprA overproduction (Figure 2.6B). Taken together, our results showed that *rprA* expression was activated *in vitro* by condition mimicking the plant apoplast environment or *in vivo* during host infection.

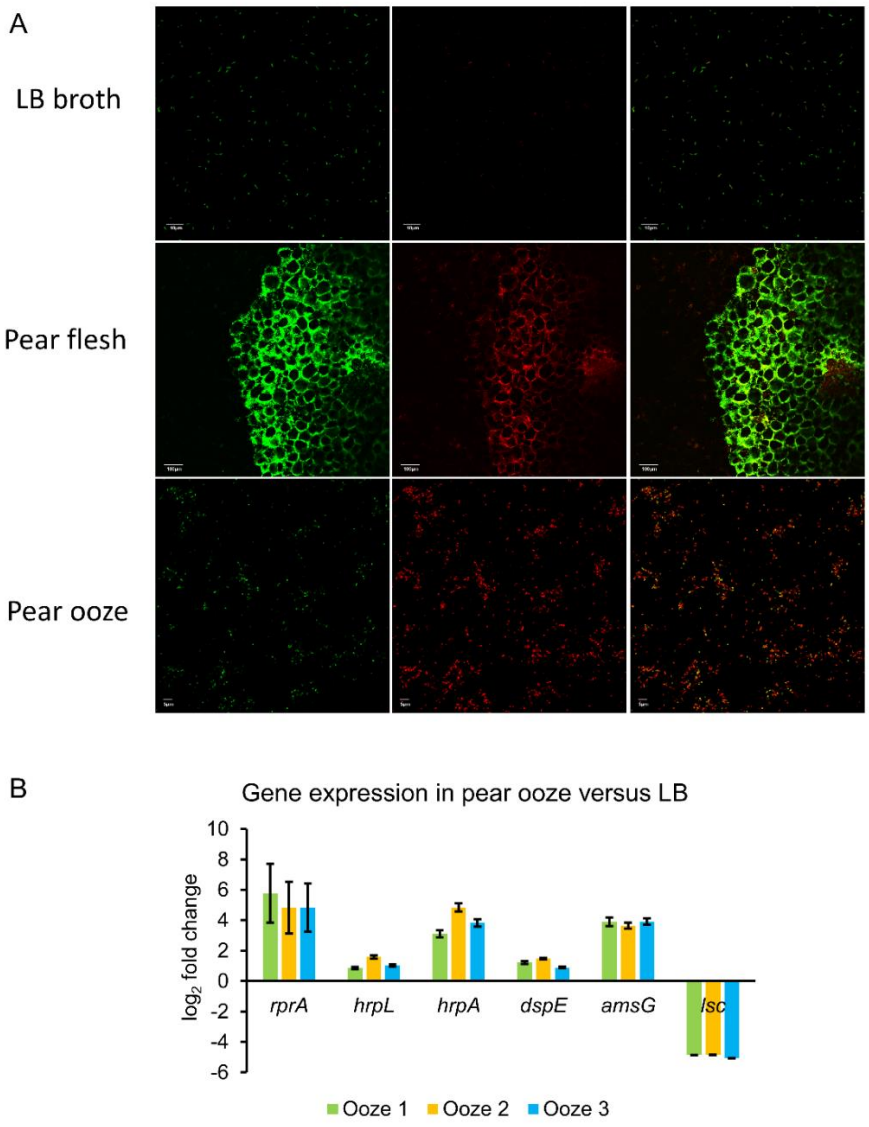

Figure 2.6. *In vivo* activation of RprA during host infection. (A) Confocal observation of *rprA* promoter activity in *E. amylovora* Ea1189(p*NptII-gfp-rprA-mCherry*) in LB medium and in flesh and ooze of inoculated immature pears. Gfp (ex/em=488nm/510nm) is expressed constitutively, whereas mCherry (ex/em=587nm/610nm) is expressed under the control of the promoter of *rprA* in Ea1189(p*NptII-gfp-rprA-mCherry*) cultures. Images were captured through sequential scanning using a FluoView 1000 (Olympus, Tokyo, Japan) laser scanning confocal microscope. (B) Expression of *rprA* and several virulence factor genes in *E. amylovora* Ea1189 cells emerged as oozes from the inoculated immature pears and that grown overnight in LB medium. To ensure representativity of gene expression levels in *E. amylovora* cells from pear oozes, oozes from every six of the 18 inoculated pears were pulled together as one biological replications (labelled as "Ooze 1", "Ooze 2", and "Ooze 3"). Gene expression levels were quantified through qRT-PCR, and fold changes were calculated using the $2^{-\Delta\Delta C_T}$ formula. The housekeeping gene *recA* was used as an endogenous control. Error bars indicate standard variations within each biological replication.

2.3.5 *rprA* inhibits biofilm formation and activates dispersal of biofilm cells

In view of the multifaced regulatory roles of RprA on the virulence factors of *E. amylovora*, we therefore wondered the total effects of RprA on formation of biofilm, that contains sessile surface-attached communities of *E. amylovora* cells encased in EPSs. To test this, we quantified biofilm formation in IPTG-supplemented cultures of Ea1189(pHM-*tac*) and Ea1189(pOE-*rprA*) through a microtiter plate assay. Compared with the empty vector control, Ea1189(pOE-*rprA*) cultures formed significantly less amount of biofilm (Figure 2.7A), suggesting an overall negative effect of RprA on biofilm formation. We then questioned how *rprA* induction affects biofilm dispersal? To investigate this, we first let strains of Ea1189(pHM-*tac*) or Ea1189(pOE-*rprA*) form biofilms on polystyrene beads without addition of any IPTG into the medium. Washed beads covered with biofilms were then transferred to fresh medium containing 1 mM IPTG. Cells that dispersed into the medium were periodically quantified through dilution plating. We showed that overexpression of *rprA* did not affect the number of dispersed cells in the first hour after induction (Figure 2.7B). However, significantly more cells of Ea1189(pOE-*rprA*) were dispersed in the IPTG induction condition compared with Ea1189(pHM-*tac*) from 2-5 hrs after IPTG addition, and the differences were greater as the experiments continued (Figure 2.7B). These results indicated that induction of *rprA* negatively impacts biofilm formation and positively impacts dispersal of *E. amylovora* cells from biofilms. A working model for the functions of RprA is proposed (Figure 2.8).

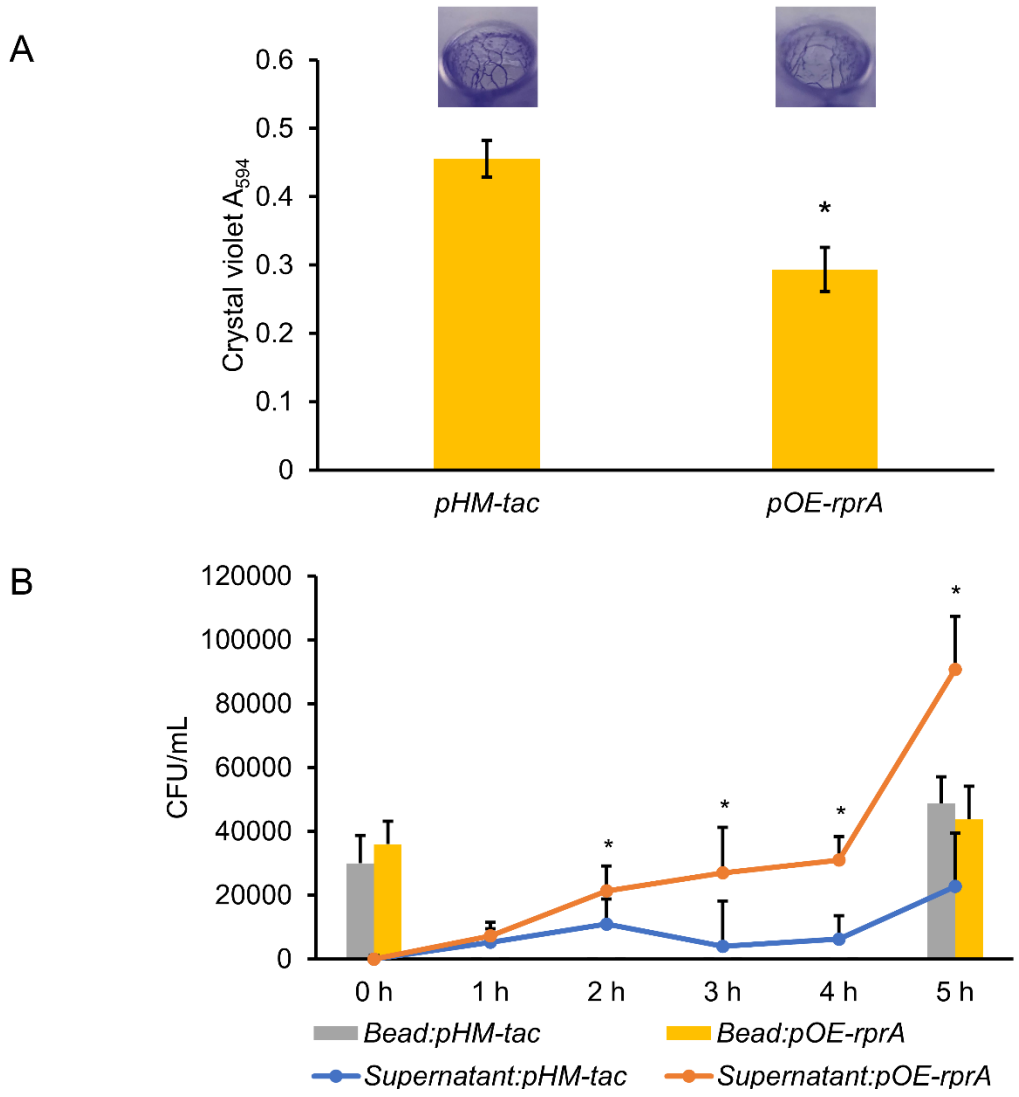

Figure 2.7. **RprA negatively affects biofilm formation and activates biofilm dispersal *in vitro*.** (A) Biofilm formation of *E. amylovora* Ea1189(pHM-*tac*) and Ea1189(pOE-*rprA*) cultures. Cultures at OD_{600}=1.0 were resuspended in ×0.5 LB containing 1 mM IPTG and were inoculated into acetone-etched microtiter plates for 48 h. Biofilms were quantified through a crystal violet (CV) staining assay at the absorbance of 594 nm (A_{594}). (B) Temporal dispersal of biofilm cells. Polystyrene beads (7 mm) were inoculated into *E. amylovora* cultures in 0.5× LB without any IPTG for 48 h. Beads covered by biofilm were washed and dipped into fresh 0.5× LB with 1 mM IPTG. Planktonic cultures were periodically withdrawn, and CFUs were calculated through dilution plating (line graph). To count the number of cells covered on the beads before and after dispersal, biofilm-covered beads were inoculated into 0.5× PBS buffer and were sonicated for 5 min to release the attached cells for cell count through dilution plating (bar graph). The assays were done three times with similar results.

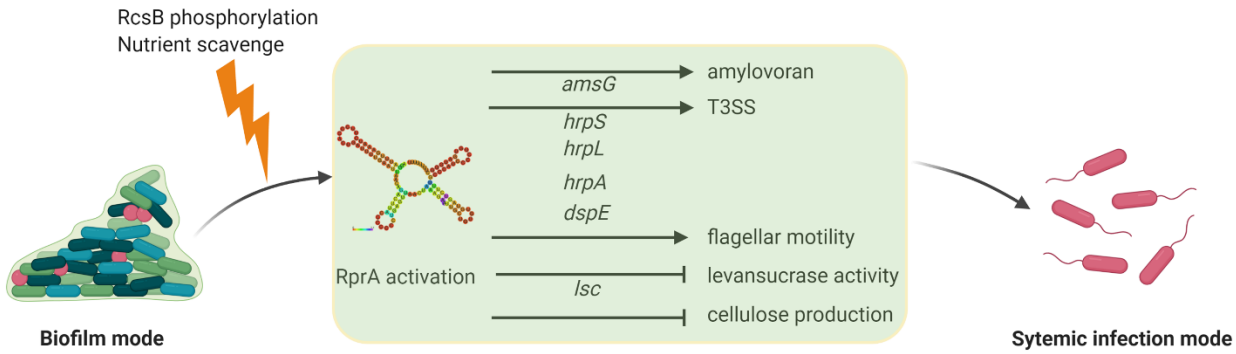

Figure 2.8. Proposed model of the functions of RprA in modulating virulence factors and systemic infection of *E. amylovora*.

2.4 Discussion

Our results demonstrate that the Hfq-dependent sRNA RprA regulates a varied group of virulence factors of *E. amylovora* that impact pathogenesis and systemic movement through the apple host. The regulatory impact of RprA on virulence would seem to mostly occur via direct interactions with mRNAs of transcriptional regulators of the associated virulence factor. For example, we demonstrated that RprA activates *hrpS* mRNA at a posttranscriptional level, likely via a direct interaction with *hrpS* mRNA. As the enhancer binding protein HrpS functions to activate the transcription of *hrpL*, encoding the alternative sigma factor HrpL, that is required for the transcription of all other genes within the Hrp regulon, the translational stimulation of *hrpS* due to *rprA* overexpression therefore explained its positive effects on the promoter activity of the downstream T3SS genes, including *hrpL*, *hrpA*, and *dspE*. Of note, RprA appeared to only affect the 129-nt 5' UTR but not the 227-nt 5' UTR of *hrpS*, suggesting that the longer 5'UTR of *hrpS* forms a distinct structure that is inaccessible to RprA and may or may not require an additional but yet unidentified factor(s) to regulate translation of HrpS.

We also found that RprA is a positive regulator of amylovoran production through a positive effect on the promoter of *amsG*, the first gene of the amylovoran biosynthetic gene

operon, and also has a negative effect on the expression of the levansucrase gene *lsc*. Transcriptional regulation of the 12-gene *ams* operon, encoding amylovoran biosynthesis, is highly complex. This is likely due to many reasons including that the amylovoran EPS is required for pathogenicity (Norelli et al. 2003), is the most important EPS component of *E. amylovora* biofilms (Koczan et al. 2009), and also reflects the inverse regulation of biofilm formation and expression of the T3SS (Edmunds et al. 2013). Positive transcriptional regulators of the *ams* operon include the RcsCDB phosphorelay via direct interaction with an Rcs box (Wang et al. 2009; Zhao et al. 2009b); *ams* operon expression is also positively regulated by the second messenger molecule cyclic di-GMP via an as yet unknown transcriptional regulator (Edmunds et al. 2013). Negative transcriptional regulators of the *ams* operon include the EnvZ/OmpR and GrrA/GrrS two component systems (Zhao et al. 2009b), and AmyR, a member of the enterobacterial YbjN family (Wang et al. 2012a). Thus, there are many potential targets that RprA might interact with to positively impact transcription of the *ams* operon.

It is noteworthy that the functions of RprA are majorly implied from the overexpression studies but not from the mutagenesis studies. Compared with the WT strain, the Ea1189Δ*rprA* mutant had little or negligible effects on swimming motility, levansucrase activity, and cellulose production. This suggests that the basal level of RprA in *E. amylovora* cells grown in a rich medium is too low to have strong effects on the measured phenotypes. Indeed, the promoter activity of *rprA* was very low in *E. amylovora* cells grown in LB as indicated by the dim red fluorescence using the dual reporter system. These observations are reminiscent of previous studies of RprA in *E. coli*. Through assays of an *rprA-lacZ* fusion or northern blot, several studies have shown that *rprA* is nearly undetectable in WT *E. coli* cells grown in a rich medium (Madhugiri et al. 2010; Majdalani et al. 2001; Majdalani et al. 2005). In line with this, known

targets of RprA in *E. coli*, including *rpoS*, *csgD*, and *ydaM*, were consistently identified through overexpression of this sRNA whereas a *rprA* knockout mutation hardly affected any of these targets (Majdalani et al. 2002; Mika et al. 2012). Therefore, a basal level of RprA in the bacteria grown in a rich medium functions minimally in affecting its targets, that are nevertheless strongly perturbed by overproduction of this sRNA.

We demonstrated that *rprA* expression was under the tight regulation of the Rcs phosphorelay, as *rprA* expression was reduced by about one half in the Ea1189*ΔrcsB* mutant compared with the WT Ea1189 strain. A similar level of decrease of the transcriptional activity of *rprA* in *E. coli* was previously reported in the Ea1189*ΔrcsB* mutant (Majdalani et al. 2002). In *E. coli*, *rprA* was shown to be positively regulated by RcsB when the protein was phosphorylated, and negatively regulated by RcsB when the protein was acetylated (Hu et al. 2013; Majdalani et al. 2002; Szczesny et al. 2018), which is consistent with our observation of the full activation of *rprA* expression in Ea1189*ΔrcsB*(prcsB-D56E) but loss of *rprA* expression in Ea1189*ΔrcsB*(prcsB-K154Q) in *E. amylovora*. We also examined *rprA* expression levels in *E. amylovora* cultures under conditions that are known to strongly activate *rprA* expression in *Salmonella enterica* serovar Typhimurium or *E. coli*, including low pH stress, osmotic shock, and high population density (Madhugiri et al. 2010; Srikumar et al. 2015). None of these conditions significantly altered *rprA* expression in *E. amylovora*. Nevertheless, we found that *rprA* expression was strongly stimulated in *E. amylovora* cultures grown in HrpMM medium, a low nutrient and low pH medium that mimics the plant apoplast (Huynh et al. 1989), and was induced in greater extend during infection of immature pears. Of note, we also found differential expression of several virulence factor genes in *E. amylovora* cells from emerged oozes of the inoculated immature pears in the same direction as that grown in LB broth with *rprA*

overexpression, suggesting the critical roles of RprA during *E. amylovora* pathogenesis on immature pears. Thus, although *E. amylovora*, *Escherichia coli*, and *Salmonella enterica* serovar Typhimurium are all phylogenetically closely-related members of the Enterobacteriaceae family, *rprA* regulation responds to different environmental cues, and is likely optimized for the regulation of specific virulence traits in each of these organisms.

The final stage of biofilm development is dispersal, that allows subpopulations of cells to be detached from the biofilm and resume the planktonic mode of growth (Koczan et al. 2011; Rumbaugh and Sauer 2020). Although biofilm dispersal in *E. amylovora*, to the best of our knowledge, has not been previously genetically or phenotypically characterized, dispersal is evidently an important step in *E. amylovora* pathogenesis from several lines of evidence: First, *E. amylovora* is capable of migrating systemically within host xylem (Thomson 2000); that clearly requires cells in the sessile mode of growth to switch back to the planktonic mode of growth to move to new infection sites. Using scanning electron microscopy analyses of longitudinal sections of the central vein of infected apple leaves, we previously visualized the discontinuous aggregation of *E. amylovora* microcolonies (Koczan et al. 2011), suggesting that a cycle of dispersal and re-establishment of biofilms contributes to the systemic movement of *E. amylovora* in apple leaf xylem. In addition, masses of *E. amylovora* cells have been demonstrated to break out of xylem vessels to reach the surrounding intercellular spaces of the cortical parenchyma cells (Bogs et al. 1998), which is a further example of dispersal from the biofilm and transitioning back to T3SS-mediated pathogenesis.

Our evidence suggests that RprA activates biofilm dispersal in *E. amylovora* and regulates several virulence traits associated with a transition from biofilm development to T3SS-mediated pathogenesis. The induction of motility has been observed during biofilm dispersal in

bacteria such as *Escherichia coli* and *Pseudomonas aeruginosa* (Jackson et al. 2002; Purevdorj-Gage et al. 2005; Sauer et al. 2002), and we found that motility is also positively regulated by RprA in *E. amylovora*. Cellulose and levan are important EPS constituents of the biofilm matrix of *E. amylovora* (Castiblanco and Sundin 2018; Koczan et al. 2009); thus, RprA-mediated down-regulation of both cellulose and levan production also suggests a cellular transition away from biofilm development. In contrast to the reduction in cellulose and levan we observed when *rprA* was overexpressed in *E. amylovora* Ea1189, amylovoran production was significantly increased (Figure 2.2). This seemingly paradoxical observation can be resolved by the knowledge that amylovoran is a pathogenicity factor in *E. amylovora* (Bellemann and Geider 1992), and this further indicates that amylovoran production of peripheral cells that are dispersing from biofilms may not be at the level necessary for continuing planktonic stage T3SS-mediated pathogenesis.

In summary, we demonstrated that the Hfq-dependent sRNA RprA exhibits important regulatory roles in orchestrating virulence factors of *E. amylovora* and affects transcriptional or post-transcriptional activity of the virulence factor genes. We showed that *rprA* has a very low basal level in a rich medium and can be activated by RcsB phosphorylation and by the host apoplast environment. Finally, we provided evidence that RprA plays an important role in the dispersal of *E. amylovora* cells from biofilms. This study sheds light on future mechanistic research of this important biological process during pathogenesis that has not yet been characterized in most phytopathogenic bacteria.

2.5 Materials and methods

2.5.1 Bacterial strains, plasmids, and media

The *E. amylovora* strains, plasmids, and oligonucleotide primers used in this are listed in Table A.1. All strains were routinely maintained in 15% glycerol at – 80°C. Single colonies were grown overnight in Luria Bertani (LB) at 28°C with shaking at 200 rpm for 20 h. The following antibiotics were amended to media as needed: ampicillin (100 μg ml^{-1}), chloramphenicol (30 μg ml^{-1}), gentamicin (15 μg ml^{-1}), and kanamycin (50 μg ml^{-1}).

2.5.2 DNA manipulations

To generate the pJP-*rprA* construct for *rprA* complementation, the *rprA* gene along with its native promoter region was cloned into the low-copy plasmid pBBR1MCS5. To generate the *rprA* overexpression construct, the *rprA* full-length gene sequence was cloned into pHM-*tac* immediate downstream the isopropyl β-D-1-thiogalactopyranoside (IPTG)-inducible *tac* promoter. To generate the construct p*rcsBD* for *rcsB* complementation, the *rcsBD* operon along with its native promoter region was cloned into pBBR1MCS5. The p*rcsB*-D56E and p*rcsB*-K154Q constructs, which allow expression of *rcsB* with a D56E substitution or a K154Q substitution, respectively, were generated through site-directed mutagenesis using the QuikChange Lightning kit (Santa Clara, CA). To generate the transcriptional fusion constructs, including pPROBE-NT:*hrpL*, pPROBE-NT:*hrpA*, pPROBE-NT:*dspE*, pPROBE-NT:*amsG*, and pPROBE-NT:*lsc*, the promoter region of the corresponding genes (~500-bp amplicons upstream of the start codon) were cloned immediately upstream of the promoter-less *gfp* gene in pPROBE-NT (Miller et al. 2000). To generate the translation fusion constructs pxg-20:*hrpS129* and pxg-20:*hrpS227*, the 5' UTR regions of *hrpS* were amplified from the two transcriptional start sites to 90 nt into the coding region and were cloned in-frame with *gfp* in pXG-20 (Urban and Vogel

2007). The transcription start sites of *hrpS* were identified previously (Lee and Zhao 2018). To generate p*NptII-gfp-rprA-mCherry*, the *Dickeya dadantii hrpA* promoter region in *nptII-gfp-hrpA-mCherry* (Cui et al. 2018) was replaced with the promoter region of *E. amylovora rprA*. Constructs were cloned using the standard ligation-dependent approach (Sambrook 2001) or a ligation-independent cloning approach (Li et al. 2011). The strains or plasmids used in this study are listed in Table A.1. The oligonucleotide primers used are listed in Table A.2. Constructs were transformed into *E. coli* Turbo cells using the TSS solution (Chung et al. 1989) and/or into *E. amylovora* through electroporation.

2.5.3 Bioinformatics

The secondary structure of RprA was predicted using the minimum free energy model of RNAfold (http://rna.tbi.univie.ac.at/cgi-bin/RNAWebSuite/RNAfold.cgi). The genome-wide targets of RprA were predicted using TargetRNA2 (http://cs.wellesley.edu/~btjaden/TargetRNA2/) with the default setting.

2.5.4 Quantification of amylovoran

The concentration of amylovoran was determined through a turbidity-based assay using cetylpyrimidinium chloride (CPC) with modifications (Bellemann et al. 1994). Briefly, overnight *E. amylovora* cultures grown in LB medium were washed twice and resuspended in MBMA medium supplemented with 1% galactose. Cultures were grown for 24 h at 28°C with shaking at 200 rpm. After centrifugation at ×16,000 g for 2 min, supernatant was harvested and mixed with 50 µl 50 mg ml^{-1} CPC (Sigma-Aldrich) per ml culture supernatant. The mixtures were incubated at room temperature for 5 min and their turbidity at the optical density of OD_{600} were measured using a spectrophotometer (Tecan; Männedorf, Switzerland) followed by normalization with the OD_{600} of the cultures.

2.5.5 Swimming motility assay

Swimming motility was examined following the method of Edmunds *et al.* with modifications (Edmunds et al. 2013). Briefly, 2 µl overnight *E. amylovora* culture was stab-inoculated into 0.3% agar LB plates and the inoculated plates were inoculated at 28°C for 48 h without any agitation. The motility area in radius was determined for the subsequent statistical analysis.

2.5.6 Cellulose assay

Cellulose biosynthesis was assessed following a previous described method (Castiblanco and Sundin 2018). In brief, 5 µl *E. amylovora* overnight culture was spotted on NaCl-free LB plates supplemented with Congo red (40 µg/ml). The inoculated plates were incubated for 48 h at 28°C without shaking. Red coloration of the *E. amylovora* colony is indicative of the production of cellulose that binds to Congo red.

2.5.7 Levansucrase activity

Levansucrase activity was quantified as described previously (Schachterle and Sundin 2019). In brief, supernatants of *E. amylovora* overnight cultures were mixed with 0.5× PBS buffer containing 2 M sucrose in a 1:1 ratio. The mixtures were incubated at 37°C for 4 h without shaking. The resultant turbidity from levan production, that is catalyzed by the levansucrase enzyme, was measured at the optical density of OD_{600} using a spectrophotometer (Tecan) followed by normalization with the OD_{600} values of the cultures.

2.5.8 Hypersensitive response (HR) assay

The HR assay followed the protocol of Zeng and Sundin (Zeng and Sundin 2014). In brief, overnight *E. amylovora* cultures were harvested, washed, and adjusted to the optical density OD_{600}=0.05 in 0.5× PBS buffer. Around 100 µl cell suspension was infiltrated into

Nicotiana benthamiana leaves of 10-week-old with a needle-less syringe. The HR symptom was observed and image-captured 16 h post infiltration.

2.5.9 Confocal microscopy

A FluoView 1000 (Olympus, Tokyo, Japan) laser scanning confocal microscope was used for examining *E. amylovora* cells expressing the *nptII-gfp-rprA-mCherry* contruct, which expressed gfp in a constitutive manner and mCherry under the control of the native promoter of *rprA*. To analyze *rprA* promoter activity *in vitro*, overnight cultures of *E. amylovora* Ea1189(*nptII-gfp-rprA-mCherry*) were washed and resuspended in fresh LB with the optical density OD_{600} adjusted to 1.0. To measure *in vivo rprA* promoter activity in pear ooze or pear flesh, *E. amylovora* Ea1189(*nptII-gfp-rprA-mCherry*) cultures were inoculated on immature pears as described previously (Edmunds et al. 2013), except that the starting amount of inoculum was approximately 2×10^5 colony forming units (CFUs) to accelerate the infection and ooze emergence. Pear ooze was harvested using a sterile inoculation loop and was resuspended in 0.5× PBS buffer to OD_{600}=1.0 immediately before imaging. Infected pear flesh tissue was dissected using a sterile razor blade immediately before imaging. The laser at 488 nm and the SDM560-BA505-525 emission filter were used for capturing the gfp fluorescence. The laser at 561 nm and the SDM640-BA560-620 emission filter were used for capturing the mCherry fluorescence. Sequential imaging recording method was used to avoid crosstalk between the fluorochromes.

2.5.10 Total RNA extraction and qRT-PCR

Overnight *E. amylovora* cultures were washed and diluted to OD_{600}=0.05 in fresh LB broth. The cultures were grown at 28°C with shaking until the optical density reached OD_{600}=0.5, corresponding to the exponential stage of bacterial growth. To examine the effect of environmental stressors on *rprA* expression, cultures of *E. amylovora* Ea1189 at OD_{600}=0.5 were

washed and resuspended in the same volume of the following media for 2 h: LB medium, LB medium (pH=5.1), LB medium amended 0.4M NaCl, and HrpMM (Huynh et al. 1989). To examine the effect of growth stage on *rprA* expression, late stationary phase cultures of *E. amylovora* were prepared by allowing cultures in exponential phase to continue to grow for another 16 h. To compare *in vivo* and *in vitro* expression of *rprA* and virulence factor genes in *E. amylovora* Ea1189, *E. amylovora* cells were grown and harvested from oozes of the inoculated pears or from overnight cultures following the same procedures as used for the confocal microscopic studies. To obtain enough starting materials for total RNA extraction and also to control the possible variations of *E. amylovora* gene expression in oozes of inoculated pears due to differences of pear size or maturity, oozes from six inoculated pears were pulled together as one biological replications and three biological replications were prepared as "Ooze 1", "Ooze 2", and "Ooze 3". Crude total RNA was extracted following a previous reported method (Rivas et al. 2001). Crude total RNA was purified using the RNA Clean & Concentrator-25 kit (Zymo Research; Irvine, CA) following the instructions of the manufacturer. Contaminating genomic DNA was eliminated using the TURBO DNA-free Kit (Thermo Fisher Scientific; Waltham, MA) according to the manufacturer's instructions. First-strand cDNA was synthesized with the High Capacity cDNA Reverse Transcription kit (Thermo Fisher Scientific) according to manufacturer's instructions. Expression levels of RprA were quantified routinely using a StepOne Plus Real-Time PCR system (Applied Biosystems; Foster City, CA) (Zeng et al. 2013). The reference gene *recA* was used as an endogenous control (Zeng et al. 2013). Relative expression values were calculated through the $2^{-\Delta\Delta C_T}$ method.

2.5.11 Biofilm assay

Overnight cultures of *E. amylovora* Ea1189(pHM-*tac*) and Ea1189(pOE-*rprA*) were washed and resuspended in ×0.5 LB with the optical density OD_{600} adjusted to 1.0. To enhance attachment of *E. amylovora* cells, wells of 96-well round-bottom microplates were etched with 200 µl acetone for 20 s to increase the roughness of the surface (Davies and Marques 2009a). After complete drying of the plates, resuspended *E. amylovora* cultures in 200 µl per well were inoculated and incubated at room temperature for 48 h with light horizontal shaking. After depletion of planktonic cultures, biofilm cells were stained by adding 250 µl 10% crystal violate solution for 1 h. Stained plates were washed twice by H_2O and dried. Distaining solution (40% methanol and 10% acetic acid) in 300 µl was added into each well incubated for 1 h at room temperature with light shaking. The absorbance A_{594} values of the suspensions were measured using a Tecan spectrophotometer.

2.5.12 Biofilm dispersal assay

Two ml washed overnight cultures at OD_{600} of 1.0 in ×0.5 LB were inoculated into 12-well plates without adding any IPTG. One polystyrene bead (7 mm) was added to each inoculated well. The inoculated plates were incubated at room temperature for 48 h with light shaking to allow even formation of biofilms on the beads. Each bead covered with biofilm cells was washed six times by 10 ml 0.5× PBS to remove any planktonic cells on the surface of the bead. Washed beads were transferred to wells in 2 ml fresh ×0.5 LB and 1 mM IPTG and incubated at room temperature without any shaking. Dispersed cells were quantified by withdrawing 10 µl of the culture suspension at one-hour intervals, and the CFUs were determined by dilution plating. To count the starting number of biofilm cells on the beads, beads with biofilm cells attached were added into 1.7-ml Eppendorf centrifuge tubes containing 1 ml

0.5× PBS followed by sonication for 5 min to release the attached cells. The CFUs of the suspension were counted through dilution plating.

CHAPTER 3

Chromosomally encoded *hok-sok* toxin-antitoxin system in the fire blight pathogen *Erwinia amylovora*: identification and functional characterization

This chapter has been accepted for publication and is accessible in its entirety at:

Peng, J.; Triplett, L.R.; Schachterle, J.K.; Sundin, G.W. (2019). Chromosomally encoded *hok-sok* toxin-antitoxin system in the fire blight pathogen *Erwinia amylovora*: identification and functional characterization. *Appl. Environ. Microbiol*.

10.1128/AEM.00724-19

3.1 Abstract

Toxin-antitoxin (TA) systems are genetic elements composed of a protein toxin and a counteracting antitoxin that is either a noncoding RNA or protein. In type I TA systems, the antitoxin is a noncoding small RNA (sRNA) that base pairs with the cognate toxin mRNA interfering with its translation. Although type I TA systems have been extensively studied in *Escherichia coli* and a few human or animal bacterial pathogens, they have not been characterized in plant-pathogenic bacteria. In this study, we characterized a chromosomal locus in the plant pathogen *Erwinia amylovora* Ea1189 that is homologous to the *hok-sok* type I TA system previously identified in the *Enterobacteriaceae*-restricted plasmid R1. Phylogenetic analysis indicated that the chromosomal location of the *hok-sok* locus is, thus far, unique to *E. amylovora*. We demonstrated that ectopic overexpression of *hok* is highly toxic to *E. amylovora* and that the sRNA *sok* reversed the toxicity of *hok* through *mok*, a reading frame presumably translationally coupled with *hok*. We also identified the region that is essential for maintenance of the main toxicity of Hok. Through a *hok-sok* deletion mutant (Ea1189Δ*hok-sok*), we determined the contribution of the *hok-sok* locus to cellular growth, micromorphology, and catalase activity. Combined, our findings indicate that the *hok-sok* TA system, besides being potentially self-toxic, provides fitness advantages to *E. amylovora*.

CHAPTER 4

Activation of metabolic and stress responses during subtoxic expression of the type I toxin *hok* in *Erwinia amylovora*

4.1 Abstract

Toxin-antitoxin (TA) systems, abundant in prokaryotes, are composed of a toxin gene and its cognate antitoxin. Several toxins are implied to affect the physiological state and stress tolerance of bacteria in a population. However, the molecular targets or regulatory roles of TA systems are largely unknown. Here, we examined the physiological and transcriptomic changes of *Erwinia amylovora* cells expressing *hok* at subtoxic levels that were confirmed to confer no cell death, and at toxic levels that resulted in killing of cells. In both conditions, *hok* caused membrane rupture and collapse of the proton motive force in a subpopulation of *E. amylovora* cells. We demonstrated that induction of *hok* resulted in upregulation of ATP biosynthesis genes and caused leakage of ATP from cells only at toxic levels. We showed that overexpression of the phage shock protein gene *pspA* largely reversed the cell death phenotype caused by high levels of *hok* induction. We also showed that induction of *hok* at a subtoxic level rendered a greater proportion of stationary phase *E. amylovora* cells tolerant to the antibiotic streptomycin. We characterized the molecular mechanism of toxicity by high-level of *hok* induction and demonstrated that low-level expression of *hok* primes the stress responses of *E. amylovora* against further membrane and antibiotic stressors.

4.2 Introduction

Toxin-antitoxin (TA) systems are simple genetic loci that encode a stable proteinaceous toxin and an unstable counteracting antitoxin. TA systems are widely found throughout the chromosomes and plasmids of free-living prokaryotes (Unterholzner et al. 2013). In type I TA systems, the antitoxins are small RNAs that inhibit the translation of or facilitate the degradation of the transcript encoding the corresponding toxin (reviewed in (Brantl 2012; Brielle et al. 2016)). Type I toxins, such as Hok, HokB, and TisB, tend to be small (≤60 amino acids)

hydrophobic proteins containing one transmembrane domain (Fozo et al. 2010; Pedersen and Gerdes 1999; Thisted and Gerdes 1992). A high induction level of the toxin genes *hok* or *tisB* causes drastic cell death of *E. coli* cells, accompanied by collapse of the proton motive force (PMF) (Gerdes et al. 1986; Gurnev et al. 2012b; Unoson and Wagner 2008). The gene products of both *hokB* and *tisB* form membrane pores in *Escherichia coli* (Gurnev et al. 2012b; Wilmaerts et al. 2018) and lead to leakage of cellular ATP during moderate (Wilmaerts et al. 2018) or high-level (Unoson and Wagner 2008) induction of the toxin genes. The PMF, the proton gradient generated via oxidation of NADH and $FADH_2$, is required to generate ATP through ATP synthase, as well as to power membrane-localized cell machinery, such as the flagellum (Ogawa and Lee 1984; Streif et al. 2008). The *hok/sok* TA system in *E. coli* has been suggested as a target for killing host bacterial cells (Chukwudi and Good 2020; Faridani et al. 2006). Through sequestering the sRNA *sok* from interacting with *hok* mRNA by addition of anti-Sok peptide nucleic acid (PNA) oligomers (Faridani et al. 2006) or doxycycline that inhibits RNase III degradation of the *hok-sok* dsRNA complex, *hok* mRNA is released and consequently causes cell death (Chukwudi and Good 2020).

The molecular targets and regulatory roles of many TA systems are still enigmatic. Although inactivation of a single type I TA system does not frequently result in a phenotype (Verstraeten et al. 2015), studies using low-level ectopic expression have revealed that a few membrane-associated TA systems can affect the physiological state and stress tolerance of bacteria in a population. In *E. coli*, expression of *hokB* or *tisB* at sub-toxic levels increased the proportion of persister cells with tolerance to multiple antibiotics, which was hypothesized to result from growth retardation following ATP leakage and the loss of the PMF (Dörr et al. 2010; Edelmann and Berghoff 2019; Gurnev et al. 2012b; Unoson and Wagner 2008; Verstraeten et

al. 2015). Plasmid expression of the *hok-sok* locus also increased T4 bacteriophage exclusion in *E. coli* (Pecota and Wood 1996). Interestingly, despite its role in compromising membrane integrity, moderate *hokB* expression was observed to increase metabolic activity in *E. coli*, determined via a fluorescent redox sensor (Wilmaerts et al. 2018).

Through transcriptomics and *in vitro* RNA degradation analyzes, Wang *et al*. demonstrated that the type V antitoxin GhoS cleaves the membrane-associated toxin *ghoT* mRNA (Wang et al. 2012c). However, the global transcriptional effects of a type I membrane-associated TA, to the best of our knowledge, have not been previously examined. It has been hypothesized that induction of *hokB* may activate phage shock protein (*psp*) genes, based on the protective effects of Psp proteins in mitigating various membrane stresses in *E. coli* (Gerdes 2016; Jovanovic et al. 2006). Though the effects vary in different bacteria, perturbation of the cell membrane seems to cause shared consequences in activating stress responses and downregulating genes that encode energy consuming machinery (Anes et al. 2019; Fallico et al. 2011; Han et al. 2019; Urfer et al. 2016; Zhao et al. 2016). Addition of polymyxin, an antibiotic that causes formation of membrane pores and cell death in bacteria, caused increased expression of genes associated with vancomycin resistance and decreased expression of virulence factor-related genes in *Staphylococcus aureus* (Zhao et al. 2016); exposure of *Klebsiella pneumoniae* to 1-(1-Naphthylmethyl)-piperazine depolarized the membrane PMF yet upregulated many envelope stress response genes (Anes et al. 2019). Still, it is not known whether endogenous pore-forming toxins also trigger stress response or influence the expression of virulence genes.

Recently, we identified a chromosomally encoded *hok-sok* type I TA system in *Erwinia amylovora* (Peng et al. 2019), a model enterobacterial plant-pathogenic bacterium that causes the

destructive fire blight disease of pome fruit trees including apple (*Malus* sp.) and pear (*Pyrus* sp.) (Chatterjee 2001; Malnoy et al. 2012). Episomal overexpression of the *hok* gene caused massive killing of *E. amylovora* cells and arrested cell division after septa were formed (Peng et al. 2019). We proposed that cell death due to *hok* induction at toxic levels in *E. amylovora* is likely to be associated with the disturbance of essential functions of the cell membrane. Although upregulation of toxin genes occurs under a variety of different stress conditions (Christensen-Dalsgaard et al. 2010; Keren et al. 2004; Ramage et al. 2009; Shah et al. 2006b; Shan et al. 2017), natively expressed toxin genes are not known to be induced to cell-killing levels in any environmental context, to the best of our knowledge. Therefore, we hypothesized that *hok* might actually confer a selective advantage to *E. amylovora* at moderate (subtoxic) levels of induction, when no cell death is observed. In this study, we compared the transcriptome profiles of *E. amylovora* cultures expressing *hok* at toxic, subtoxic, and wild-type levels. We found that Hok plays important roles in activating ATP biosynthesis and priming the tolerance of *E. amylovora* cells against membrane and antibiotic damage.

4.3 Results

4.3.1 Moderate overexpression of *hok* does not suppress bacterial growth

A *hok* overexpression construct, pOE-*hok*, was previously generated by cloning the *E. amylovora* Ea1189 *hok* gene into the *lac* promoter-containing plasmid pEVS143 (Peng et al. 2019). The *lac* promoter allows low levels of transcription in the absence of the inducer isopropyl β-D-1-thiogalactopyranoside (IPTG) (Oehler et al. 1990). We did not observe any growth defect in *E. amylovora* Ea1189 cells transformed with pOE-*hok*, suggesting that *E. amylovora* is able to tolerate leaky *hok* expression without inhibiting growth. Therefore, we hypothesized that Ea1189(pOE-*hok*) grown in the absence of IPTG induction may provide a

useful system to identify the physiological roles of Hok separate from those caused by its toxicity. We used quantitative real-time PCR (qRT-PCR) to measure the expression levels of *hok* in Ea1189(pEVS143) and Ea1189(pOE-*hok*) without IPTG and in four progressively increasing doses of IPTG, and monitored the growth of the cultures in the same conditions. In the absence of IPTG, expression of *hok* was approximately 40-fold higher in Ea1189(pOE-*hok*) compared to Ea1189(pEVS143), and expression of *hok* increased by another ~130-fold when 1mM IPTG was added to the Ea1189(pOE-*hok*) culture (Figure 4.1A). The expression levels of the small RNA antitoxin *sok* remained almost unchanged in these conditions (Figure 4.1A). Induction of *hok* did not result in cell death until expression reached about 60-fold induction or greater, induced by the addition of 0.01 mM IPTG (Figure 4.1B). Henceforth, we will define *hok* expression from the *lac* promoter with 0.01 mM, 0.1 mM or 1 mM IPTG as the "toxic" expression conditions for this study, while expression from the *lac* promoter with 0.001 mM or no IPTG will be defined as the "subtoxic" expression conditions.

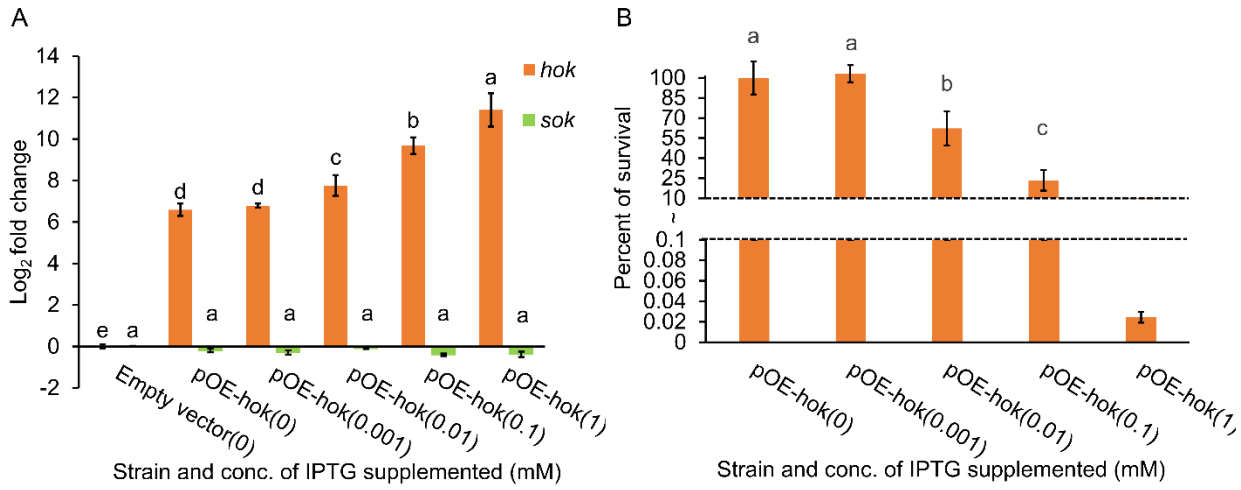

Figure 4.1. Induction of *hok* and its effect on cell survival in *E. amylovora*. (A) Expression levels of *hok* induced with four progressive doses (0.001 mM, 0.01 mM, 0.1 mM, and 1 mM) of isopropyl β-D-1-thiogalactopyranoside (IPTG) or with water. (B) The effect *hok* induction on survival rate of *E. amylovora*. The concentrations of IPTG supplemented are indicated in parentheses. After IPTG or water addition, cultures were incubated at 28°C with 200 rpm shaking for 1 h. Expression levels of *hok* were measured using quantitative real-time PCR (qRT-PCR), and fold changes were calculated using the $2^{-\Delta\Delta C_T}$ formula. The *recA* gene was used as an endogenous control. Survival rate was determined as the ratio of colony forming units (CFU)/ml in Ea1189(pOE-*hok*) after and before the addition of IPTG. Results represent the means of three replications, and error bars indicate the standard deviation. Different letters indicate significant differences ($P < 0.05$) using Tukey's HSD (honestly significant difference) test. The experiments were conducted three times with similar results.

4.3.2 Induction of *hok* causes PMF collapse and membrane rupture

Membrane-associated type I toxins of *E. coli*, including HokB and TisB, form membrane pores (Gurnev et al. 2012b; Wang et al. 2012c; Wilmaerts et al. 2018), and cause collapse of the PMF (Dörr et al. 2010; Gerdes et al. 1986; Wilmaerts et al. 2018). We therefore wondered if the transmembrane domain-containing *E. amylovora* Hok, sharing 48% and 14% amino acid identity to HokB and TisB, respectively, also causes membrane depolarization and rupture. To assess this possibility, we measured membrane potential using $DiBAC_4(3)$ (bis-(1,3-dibutylbarbituric acid) trimethine oxonol), a membrane potential-sensitive fluorescent dye. Fluorescence level

negatively correlates to membrane potential, meaning that higher fluorescence indicates a greater level of PMF collapse. Carbonyl cyanide-m-chlorophenylhydrazone (CCCP), a protonophore that uncouples the PMF, was used as a positive control for the $DiBAC_4(3)$ staining. Propidium iodide (PI) was used as an indicator of membrane rupture, which binds to nucleic acid and generates fluorescence in membrane integrity compromised cells. Ethanol disturbs the physical structure of cell membranes and was used as a positive control for the PI staining. Fluorescence was measured in single cells using a flow cytometer. We found that induction of *hok* to subtoxic levels caused membrane depolarization and rupture in a subpopulation of cells, though many cells remained unchanged in their membrane states (Figure 4.2A). More drastic membrane depolarization and rupture was observed when *hok* was induced to toxic levels (Figure 4.2A). At the highest level of *hok* induction, almost the entire population was shifted to the membrane depolarization state, with varied levels of membrane rupture. We next asked whether mannitol, a bacterial metabolite that feeds into glycolysis and was shown to stimulate the PMF in *E. coli* (Allison et al. 2011), was able to restore the collapsed PMF and rupture of cell membrane due to the toxicity of Hok in *E. amylovora*. In cells expressing *hok* with 0.1 mM IPTG induction, mannitol partially relieved the membrane stress (Figure 4.2A). Similarly, addition of mannitol significantly alleviated the inhibitory effect of bacterial growth during 0.01 or 0.1 mM induction of *hok* (Figure 4.2B). However, when 1 mM IPTG was supplemented, the protective effect of mannitol was not observed in any of these phenotypes (Figure 4.2A and Figure 4.2B). Arabinose, which does not contribute to the PMF (Allison et al. 2011), was used a negative control for the assays.

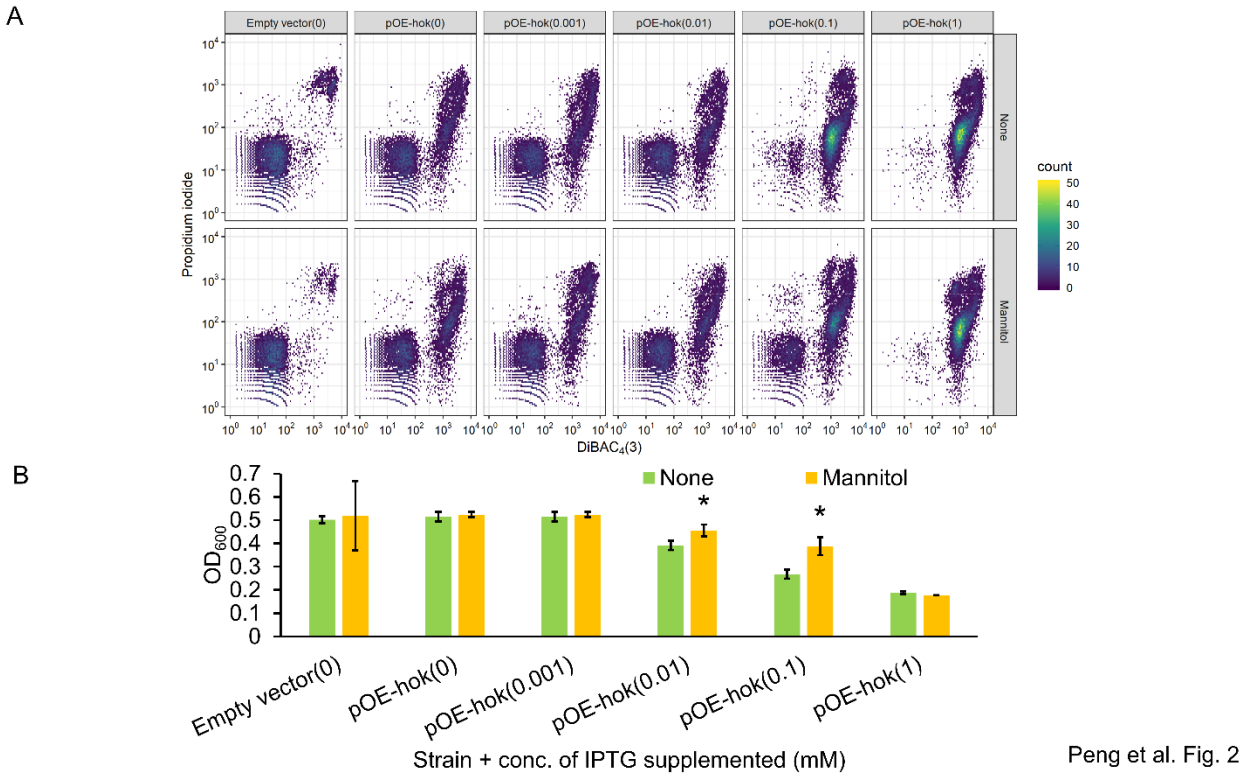

Figure 4.2. *hok* induction disturbs essential membrane functions of *E. amylovora*. Effect of *hok* induction on the proton motive force (PMF) and membrane integrity without (panel labelled as "None") or with the addition of 10 mM mannitol (panel labelled as "Mannitol") immediately before IPTG supplementation (A), and effect of mannitol in reversing the toxicity of Hok (B). *E. amylovora* cultures grown overnight for 20 h in LB broth were washed twice and diluted to OD_{600}=0.2 in fresh LB broth. The concentrations of IPTG supplemented are indicated in parentheses. After incubation at 28°C with 200 rpm shaking for 1 h, the PMF of cultures was examined using bis-(1,3-dibutylbarbituric acid) trimethine oxonol ($DiBAC_4(3)$), and membrane integrity was determined via propidium iodide (PI). Fluorescence was measured using a BD LSR II flow cytometer. Ten thousand events were examined with a 488 nm laser and a 530/30 emission filter ($DiBAC_4(3)$) staining and a 561 nm laser and a 620/15 emission filter (PI). Subsequent analyses were conducted on Flowing Software 2.5.1 and R v3.4.0. Increased fluorescence after treatment with $DiBAC_4(3)$ or PI indicates greater collapse of the PMF or compromised membrane integrity, respectively. To test the effect of bacterial metabolites on the toxicity of Hok, 10 mM mannitol or 10 mM arabinose was added to the cultures (OD_{600}=0.2) immediately before IPTG was added, and the OD_{600} was measured 4 h after the incubation using a Tecan spectrophotometer. Bacterial growth was monitored by measuring OD_{600} of the cultures using a Tecan spectrophotometer. Results represent the means of three biological replicates and error bars indicate the standard deviation. Different letters indicate significant differences ($P < 0.05$) using Student's *t*-test. The assays were done three times with similar results.

4.3.3 Transcriptomic analysis reveals that *hok* overexpression affects genes involved in stress responses and energy generation/consumption

While overexpression of *E. amylovora hok* causes extreme disturbance of essential membrane functions, it is not clear how the membrane disruption capacity of these toxins may affect bacterial physiology when *hok* is expressed in subtoxic or native expression conditions. To distinguish potential downstream effects of *E. amylovora* Hok from those resulting from toxicity, we compared the transcriptomes of *E. amylovora* cultures expressing *hok* at wild-type levels (i.e., wild-type strains carrying the empty vector) with cultures expressing *hok* at subtoxic (IPTG untreated) and toxic (1 mM IPTG treated) levels. Expression of each gene was quantified as counts per million reads (CPM), and differentially-expressed genes (DEGs) were defined as those having greater than 2-fold change of CPM values and less than 0.05 of the corresponding false discovery rate (FDR) values.

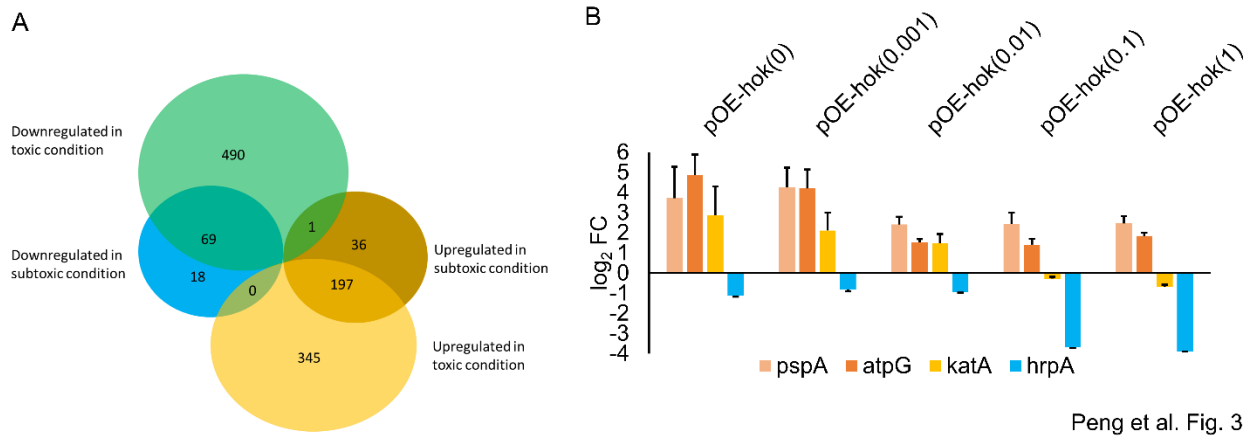

Figure 4.3. Comparative transcriptomic analysis of *E. amylovora* cells expressing *hok* at wild-type, subtoxic and toxic levels, respectively. (A) Venn diagram of the differentially-expressed genes (DEGs) in *E. amylovora* cells expressing *hok* at subtoxic or toxic level. (B) Expression of representative DEGs in subtoxic or toxic condition examined using qRT-PCR. Fold changes were calculated using the $2^{-\Delta\Delta C_T}$ formula. The *recA* gene was used as an endogenous control. The error bars indicate standard deviation. The concentrations of IPTG supplemented are indicated in parentheses.

Compared with Ea1189(pEVS143), which was also untreated with IPTG, 321 DEGs were identified in IPTG-untreated Ea1189(pOE-*hok*), of which 234 had increased expression and 87 had decreased expression (Figure 4.3A). After 1 mM IPTG treatment of Ea1189(pOE-*hok*), a much larger set of 541 and 560 genes were up- and down-regulated, respectively (Figure 4.3A). Approximately 83% of the DEGs identified in the subtoxic condition were differentially expressed in the same direction and to a greater extent in the toxic condition. Expression of representative genes in Ea1189(pOE-*hok*) in subtoxic and toxic conditions was validated through qRT-PCR (Figure 4.3B). The housekeeping gene *recA* was used as an endogenous control, that had negligible differences in expression among *E. amylovora* cultures expressing wild-type, subtoxic, or toxic levels of *hok* in our transcriptomic analysis. Based on the read count, the ratio of *hok* to *sok* was approximately 18 in the wild-type condition, that increased to ~200 in the subtoxic condition and ~6,000 in the toxic condition. Gene ontology (GO) enrichment analysis of the DEGs further revealed that *hok* exerts substantial effects in the essential metabolism of *E. amylovora* (Figure 4.4). Oxidative phosphorylation-related genes (GO:0006119), that include NADH-coenzyme Q oxidoreductase (complex I), Succinate-Q oxidoreductase (complex II), Cytochrome c oxidase (complex IV) and F_1F_o-ATPase (complex V), were enriched among the higher expressed genes in both toxic and subtoxic conditions. Specifically, in the toxic condition, higher expressed genes were also significantly associated with the “tricarboxylic acid cycle” GO term (GO:0006099).

Several genes with demonstrated importance to bacterial plant pathogenesis were negatively affected by elevated *hok* expression. Specifically, *hrpA* and *flhD*, encoding a T3SS protein and a flagellar transcriptional activator, respectively, decreased in expression at both levels of *hok* induction. In toxic but not subtoxic conditions, down-regulated genes were

primarily comprised of flagellar genes and “protein secretion” (GO:0009306) genes, which included type II secretion system (T2SS) and type III secretion system (T3SS)-related genes.

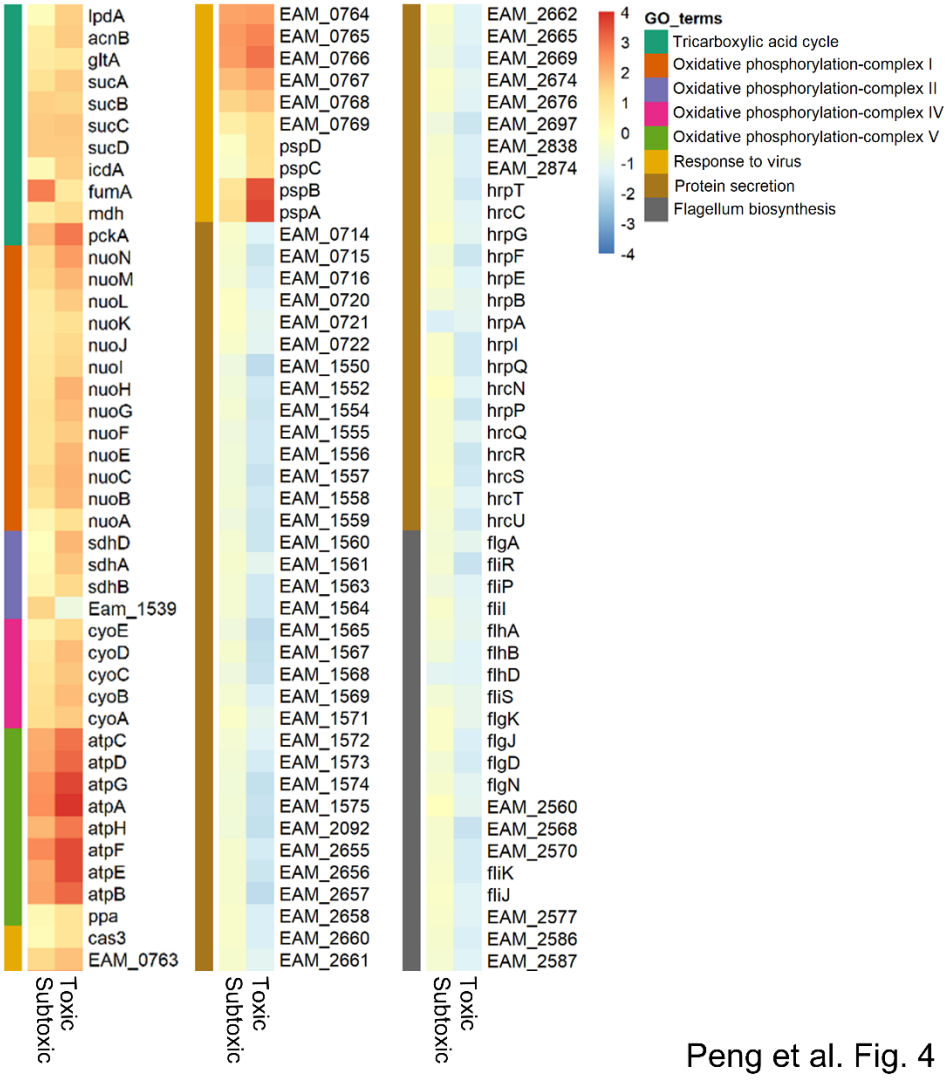

Figure 4.4. Overrepresented Gene Ontology (GO) terms enriched in the GO enrichment analysis with a cutoff FDR of 0.01. Scale bar indicates the color key of $\log_2$ fold-change values.

Induction of *hok* also activated multiple genes involved in stress responses. Several genes with known roles in antibiotic persistence and other stress responses, i.e. *groS*, *groL*, *dnaK*, *dnaJ*, *skp*, *surA*, *sucB* and *lon* (Christensen et al. 2004; Costello et al. 2016; Goltermann et al. 2013;

Hansen et al. 2008; Ma et al. 2010; Singh et al. 2007), were consistently more highly expressed in both *hok* induction conditions. Also upregulated were genes in the "response to virus" ontology (GO:0009615), including genes encoding phage shock proteins, i.e. *pspABCD*, and CRISPR-associated proteins. The catalase gene *katA* showed increased expression in the subtoxic condition, consistent with our previous observation that catalase activity is significantly compromised in a *hok-sok* deletion mutant (Peng et al. 2019). The stress-induced ATP-dependent chaperone gene *clpB* was also more highly expressed in the subtoxic but not the toxic condition. Together, these results show that different *hok* expression levels exert diverse and overlapping effects on the *E. amylovora* transcriptome, enhancing expression of metabolic and stress-related traits while suppressing genes required for infection.

4.3.4 *hok* positively affects ATP biosynthesis

Membrane-associated type I toxins have been shown to cause leakage of cellular ATP as indicated by either decrease level of intracellular ATP or increase level of extracellular ATP (Unoson and Wagner 2008; Wang et al. 2012c; Wilmaerts et al. 2018). In this study, we found that genes associated with oxidative phosphorylation, the process of ATP generation through electron transfer, were higher expressed in the subtoxic condition and were higher expressed to a greater extent in the toxic condition (Figure 4.5). We hypothesized that the upregulation of ATP biogenesis-related genes could be part of a response to compensate for the possible leakage of intracellular ATP through increased ATP synthesis in Ea1189(pOE-*hok*) cultures in both subtoxic and toxic conditions. To determine whether ATP leakage was occurring, we performed simultaneous measurements of both the intracellular and the extracellular levels of ATP in both subtoxic and toxic conditions. When induced with 0.1 or 1 mM IPTG, conditions causing more than 70% dieoff (Figure 4.1B), *E. amylovora* Hok caused dramatic leakage of ATP from the

cells, indicated by the decreased level of intracellular ATP and increased level of extracellular ATP (Figure 4.5). In contrast, a significant increase in intracellular ATP was measured after induction with 0.01 mM or less IPTG (Figure 4.5), expression conditions that were associated with minimal or no cell death of *E. amylovora* (Figure 4.1B). No ATP leakage was observed in these subtoxic conditions.

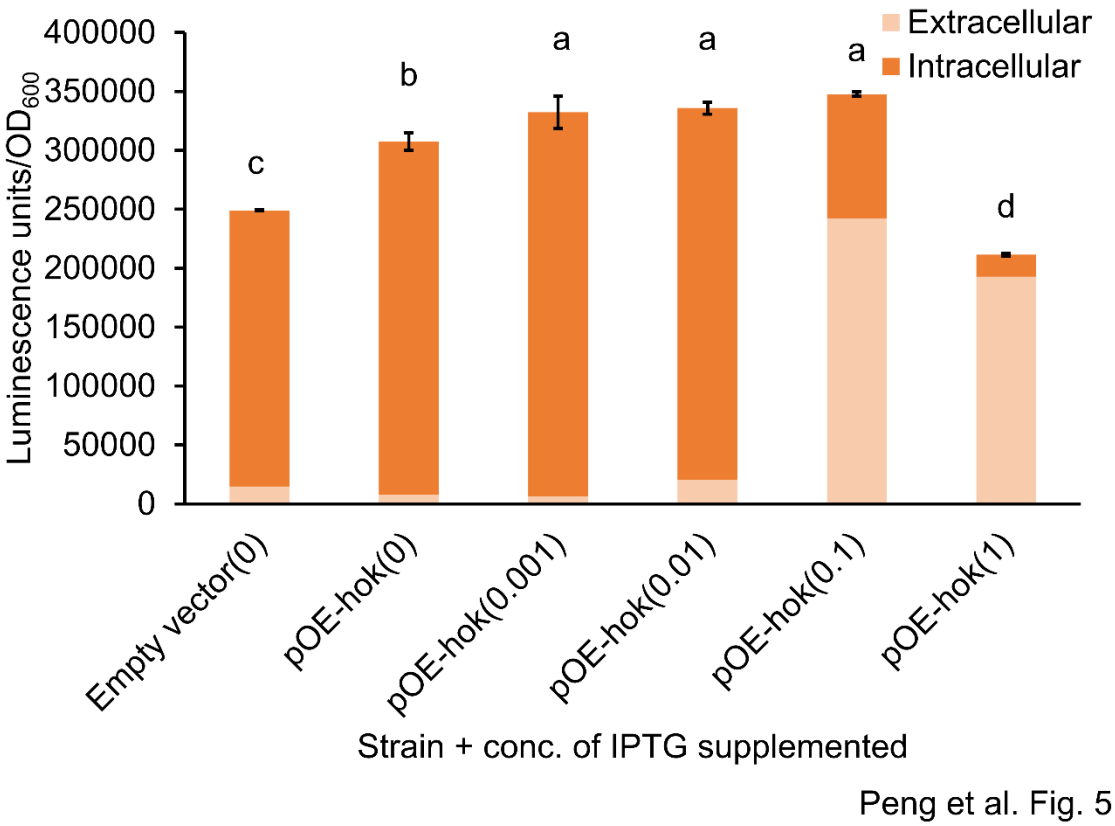

Figure 4.5. Effect of *hok* induction on ATP biosynthesis in *E. amylovora*. Both extracellular and intracellular levels of ATP were simultaneously quantified using a luciferase reporter system. Results represent the means of three biological replications and error bars indicate the standard deviation. Different letters indicate significant differences ($P < 0.05$) using Tukey's HSD test. The assays were done twice with similar results.

Combining intercellular and extracellular ATP measurements allowed us to assess the total ATP concentration under each expression condition. In the absence of IPTG, total ATP was greater in Ea1189(pOE-*hok*) cultures than Ea1189(pEVS143). Total ATP in Ea1189(pOE-*hok*) increased with IPTG addition at concentrations up to 0.1 mM (Figure 4.5). At the highest concentration of IPTG tested, 1 mM, the total ATP in Ea1189(pOE-*hok*) cultures started to decrease compared with lower levels of inducer, likely due to the massive kill-off of ATP-generating cells at this induction level. Taken together, our results suggest that *hok* positively affects the biosynthesis of ATP, and leakage of ATP only occurs when *hok* was induced at toxic levels.

Overexpression of the ATP synthase gene *atpB* is toxic to *E. coli* cells; it allows leakage of protons through the F_0 sector of F_1F_o-ATPase (Arechaga et al. 2003; Chen et al. 2018; Na et al. 2015; von Meyenburg et al. 1985). Given that *hok* positively affects ATP synthase gene expression and ATP biosynthesis in subtoxic conditions, we wondered if the toxicity of Hok was increased by the upregulation in ATP synthase genes. To test this hypothesis, we generated ATP synthase gene deletion mutants, Ea1189*ΔatpB* and Ea1189*ΔatpBEFHAGDC*. The growth of Ea1189*ΔatpB* and Ea1189*ΔatpBEFHAGDC* mutants was severely reduced, as overnight cultures only reached $OD_{600} \approx 0.3$ compared with $OD_{600} \approx 1.5$ in the wild-type Ea1189 strain (data not shown). pOE-*hok* was transformed into the ATP synthase mutants to generate Ea1189*ΔatpB*(pOE-*hok*) and Ea1189*ΔatpBEFHAGDC*(pOE-*hok*), respectively. Hok expression was induced in the wild-type and ATPase mutant backgrounds with 1 mM IPTG, and survival rates were measured. Hok killing efficiency was not changed between the wild-type and the mutants, suggesting that the toxicity of Hok is not affected by the increased expression of ATP biosynthesis genes.

4.3.5 Expression of *pspA* is induced in known PMF dissipation conditions and relieves the toxicity of Hok

Our transcriptome results indicated that *psp* genes were upregulated in both expression conditions. The *psp* genes are induced on exposure to conditions that dissipate the PMF, such as bacteriophage infection, alkaline pH, and addition of uncoupling agents, in both Gram-negative and -positive bacteria (reviewed in (Joly et al. 2010)). The protective roles of PspA in managing membrane stresses have been validated in *E. coli* and *Salmonella enterica* serovar Typhimurium (Becker et al. 2005; Kleerebezem et al. 1996; Kobayashi et al. 2007). As the functions of *psp* genes have not been previously investigated in *E. amylovora*, we constructed a transcriptional fusion of the promoter region of the *pspABCD* operon to a green fluorescence protein (*gfp*) reporter. As expected, the promoter activity of the *pspABCD* operon was significantly increased in *E. amylovora* cells after exposure to bacteriophage, and was increased to a lesser extent in the presence of CCCP, ethanol, or Triton X-100. To examine the possible protective role of *pspA* under the condition of membrane stress in *E. amylovora*, we generated the *pspA*-overexpression construct, pBAD33-*pspA*, through cloning the *pspA* gene into the pBAD33 plasmid, containing the arabinose-inducible P_{BAD} promoter. Compared with Ea1189(pBAD33), Ea1189(pBAD33-*pspA*) cultures were ~100 times more tolerant to CCCP (Figure 4.6A). Interestingly, without supplementing any IPTG, Ea1189(pOE-*hok*) cultures survived at significantly higher rates than Ea1189(pEVS143) (Figure 4.6A), suggesting that induction of *hok* at subtoxic levels protect *E. amylovora* cells from further membrane damage by activating the expression of *pspA*. Interestingly, *pspA* overexpression significantly alleviated the toxicity due to high levels of *hok* induction (Figure 4.6B), further validating the defensive role of *pspA* in response to membrane stress in *E. amylovora*.

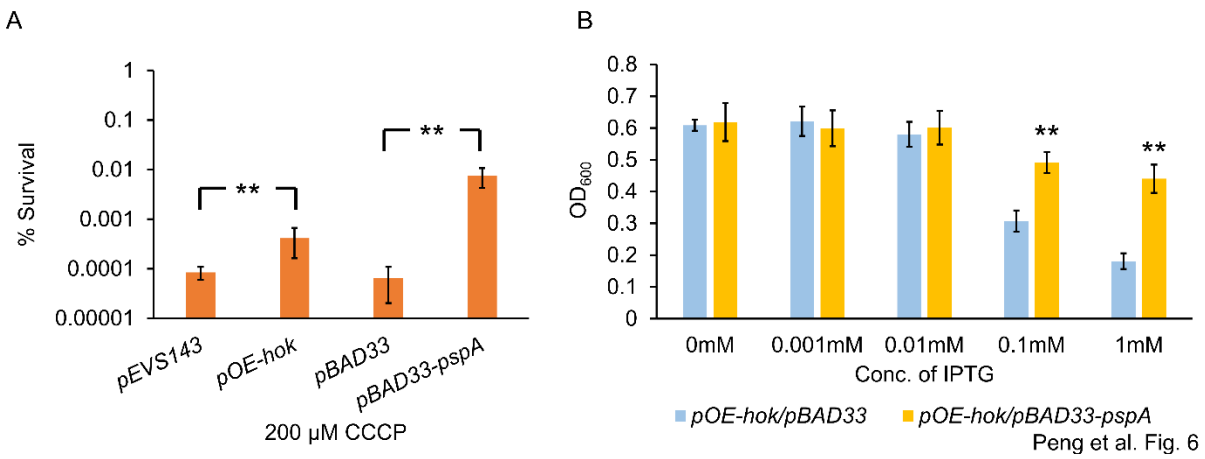

Figure 4.6. Effect of *pspA* in managing membrane stresses in *E. amylovora*. (A) Carbonyl cyanide-m-chlorophenylhydrazone (CCCP) was added to 200 μM to *E. amylovora* cultures and incubated for 5 h. Survival rate was determined as the ratio of CFU/ml after the treatment to that before the treatment. Arabinose at 10 mM, but no IPTG, was supplemented to the cultures. (B) Overexpression of *pspA* largely reverses the killing of *E. amylovora* cells expressing *hok* at toxic levels. Growth of cultures was determined by measuring OD_{600} using a Tecan spectrophotometer. Arabinose at 10 mM was supplemented to the cultures. Results represent the means of four biological replications and error bars indicate the standard deviation. Asterisk symbols indicate significant differences ($P < 0.05$ using Student's *t*-test). The assays were done three times with similar results.

4.3.6 Subtoxic expression of *hok* increases tolerance of stationary-phase *E. amylovora* cells to the aminoglycoside antibiotic streptomycin

Transcriptome results showed that *hok* expression upregulated several genes previously associated with antibiotic persistence, so we next asked whether *hok* has a role in antibiotic tolerance during stationary phase. Without addition of IPTG, stationary phase *E. amylovora* cultures expressing *hok* had 10 times the number of survivors to streptomycin exposure than the vector control strain (Figure 4.7). concentration that is routinely used for management of fire blight and screening of streptomycin-resistant *E. amylovora* isolates. Of note, we did not observe altered tolerance of *E. amylovora* cultures overexpressing *pspA*, suggesting that *hok* does not affect antibiotic tolerance through overproduction of PspA.

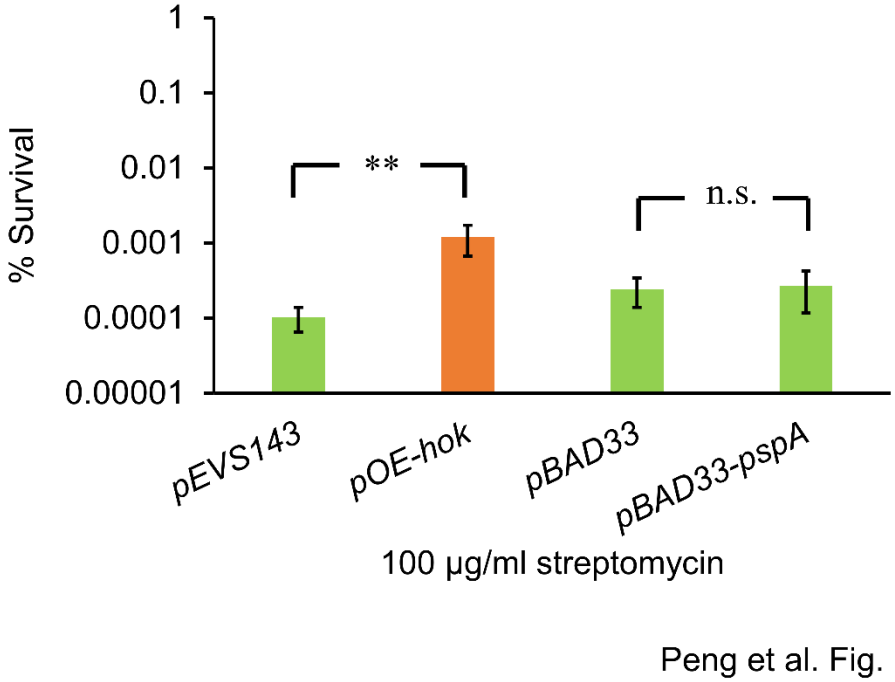

Figure 4.7. Subtoxic level of *hok* increases tolerance of stationary-phase *E. amylovora* cells to streptomycin. Single colonies of *E. amylovora* cultures were grown in LB broth amended with selective antibiotics for 20 h to reach stationary phase. Cultures were washed twice using fresh LB broth before streptomycin was added to 100 µg/ml; the culture was subsequently incubated at 28 °C with shaking for 5 h. Survival rate was determined as the ratio of CFU/ml after the treatment to that before the treatment. Arabinose at 10 mM and no IPTG was supplemented into the cultures. Results represent the means of four biological replications and error bars indicate the standard deviation. Asterisk symbols indicate significant differences ($P < 0.05$ using Student's *t*-test). The assays were done three times with similar results.

4.4 Discussion

In this study, by taking advantage of the "leaky" expression of the *lac* promoter, we showed that induction of the type I toxin *hok* disturbs essential functions of the cell membrane in both subtoxic and toxic conditions. In an effort to understand the physiological roles of *hok* in subtoxic and native expression conditions, we examined the transcriptomic changes in *E. amylovora* cells expressing *hok* at subtoxic and toxic levels. We demonstrated that subtoxic expression of *hok* in *E. amylovora* stimulates ATP biogenesis, activates *pspA* expression to

protect cells from further membrane damage, and renders stationary phase cell cultures more tolerant to streptomycin.

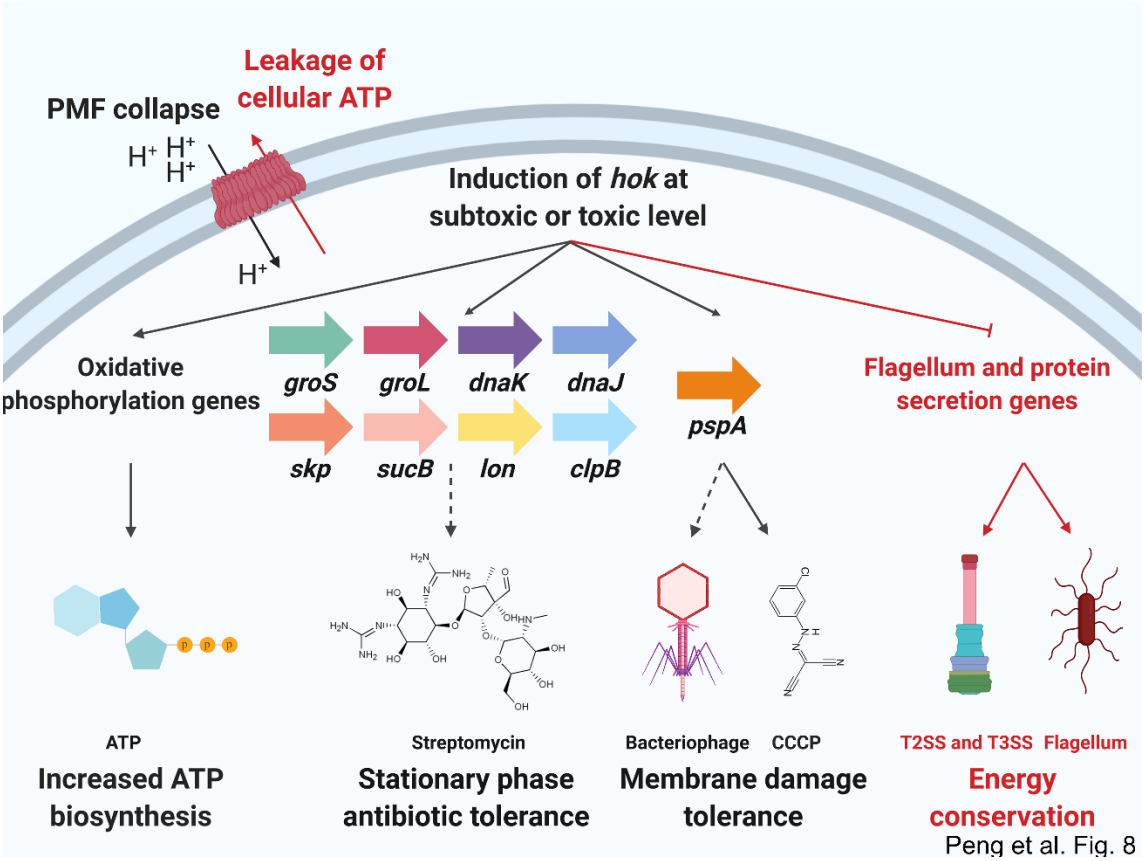

Figure 4.8. Working model of the effects of *hok* induction at subtoxic or toxic level. Induction of *hok* at a subtoxic level causes dissipation of the PMF, increased ATP biosynthesis, increased tolerance to antibiotics and further membrane stress (black arrows and letters). Induction of *hok* at a toxic level leads to leakage of cellular ATP and inactivation of energy-consuming cell machineries including T2SS, T3SS, and flagellum (red arrows and letters).

Consistent with observations in *E. coli* expressing *tisB* at a toxic level or *hokB* at a subtoxic level, induction of *E. amylovora hok* at both subtoxic and toxic levels caused collapse of the PMF and membrane rupture in a subpopulation of the cultures. Interestingly, although induction of *hok* with 1 mM IPTG killed more than 97% of *E. amylovora* cells, a significant subpopulation of cells retained low levels of membrane rupture under the same conditions. Therefore, the culturability of *E. amylovora* cells expressing a toxic level of *hok* is not entirely

correlated with the level of membrane rupture. Addition of mannitol alleviated the toxicity of Hok at lower induction levels, indicating that collapse of the PMF indeed contributes to the toxicity of Hok. However, mannitol did not reduce toxicity when Hok was expressed to the highest levels. Mannitol provides the PMF through glycolysis, and the massive killing due to high-level *hok* induction may severely impair the central metabolism machineries of *E. amylovora*.

Our transcriptomic profiling experiments demonstrate that induction of *hok* positively affects the expression of all the F_1F_o-ATPase genes. F_1F_o-ATPase, consist of a proton-conducting structure and a catalytic portion, exhibits a central role in energy transduction in bacteria. In line with the transcriptomic changes, quantification of intracellular and extracellular ATP showed that induction of *hok* positively affects ATP biogenesis, though leakage of ATP from cells was observed in toxic conditions. Although leakage of cellular ATP has also been suggested in a few other membrane-associated toxins at toxic conditions in *E. coli*, only intracellular (Cheng et al. 2014; Unoson and Wagner 2008) or extracellular ATP (Wilmaerts et al. 2018) alone was measured.

Though a subtoxic level of *hok* triggered primarily higher expression of genes in *E. amylovora*, a greater proportion of DEGs were negatively affected in cells expressing toxic levels of *hok*, including genes of flagellum, type II secretion system, and type III secretion system. A previous study of a Lon protease mutant in *E. amylovora* showed that Lon negatively affects the expression of pathogenesis-related genes *hrpA* and *flhD* (Lee et al. 2018). In this study, *lon* expression was increased, while *hrpA* and *flhD* expression was reduced, by more than two-fold in both *hok* expression conditions. This suggests that induction of *hok* inactivates these

energy-consuming cell machineries that are important for the pathogenesis of *E. amylovora,* and this favors energy conservation during the stress.

The transcriptome analysis in this study showed that *hok* triggers higher expression of *psp* genes in *E. amylovora*. Though not previously studied in *E. amylovora*, Psp proteins and homologs are widely found in bacteria, archaea, and plants (Joly et al. 2010). Bacterial Psp proteins are activated in response to phage, extreme temperature, ethanol, mislocalization of outer membrane secretins, and other events that cause membrane dissipation (Armstrong et al. 2016; Brissette et al. 1990; Darwin 2005; Fallico et al. 2011; Flores-Kim and Darwin 2016; Keren et al. 2004; Model et al. 1997; Shah et al. 2006b; Srivastava et al. 2017). We demonstrated that the promoter activity of *E. amylovora pspA* was induced upon exposure to several membrane stress-inducing substances, and that overexpression of *pspA* increased tolerance to Hok. These results show that in addition to protection from external stresses, PspA can serve a protective function from the effects of bacterially-produced stresses, such as toxin-antitoxin systems.

We found that subtoxic *hok* induction increased tolerance of stationary cultures of *E. amylovora* to the aminoglycoside antibiotic streptomycin. This is consistent with a previous report that low-level expression of the hok homolog *hokB* confers increased antibiotic tolerance to *E. coli* (Wilmaerts et al. 2018). Although energy state is an important factor for persister development in different bacteria (Conlon et al. 2016; Shan et al. 2017), we did not observe any leakage of ATP from *E. amylovora* cells expressing subtoxic levels of *hok*. Instead, ATP levels were significantly higher in these conditions. Given that several other genes associated with persistence were also upregulated during hok overexpression (Christensen et al. 2004; Hansen et al. 2008; Ma et al. 2010; Singh et al. 2007; Wu et al. 2015), it is possible that *hok* affects

antibiotic tolerance in *E. amylovora* through multiple mechanisms. While the importance of type II TA systems in antibiotic survival is still being debated, this study adds to the body of evidence that Type I systems may play such a role.

To our knowledge, this is the first study of the transcriptomic response to a type I membrane-disrupting toxin. Overall, the response of *E. amylovora* to *hok* expression appears highly congruent with bacterial responses to other PMF-dissipating stresses. Alkaline conditions, in which the PMF is dissipated to maintain the inverted pH gradient, results in upregulation of ATP synthases and downregulation of chemotaxis genes in *E. coli* (Maurer et al. 2005). The membrane-targeting antibiotic polymyxin strongly upregulates metabolic pathways while repressing key virulence factor genes in *Staphylococcus aureus* (Zhao et al. 2016). Exposure to the membrane destabilizer 1-(1-naphthylmethyl)-piperazine causes upregulation of many stress response genes, including *dnaJ*, *dnaK*, and *pspABCD* (Anes et al. 2019). These similarities indicate that membrane perturbation from diverse sources may activate overlapping downstream pathways to restore homeostasis.

A working model summarizing the effects of *hok* induced at subtoxic or toxic levels in *E. amylovora* is shown in Figure 4.8.

By examining the physiological and transcriptomic changes of *Erwinia amylovora* cells expressing the type I toxin/antitoxin system toxin gene *hok* at subtoxic or toxic levels, we demonstrated that low-level expression of *hok*, while not affecting bacterial culturability, triggers expression of the ATP synthase genes and overproduction of cellular ATP. Low-level expression of *hok* also activates multiple genes associated with stress response, and triggers expression of the phage shock protein gene *pspA*, which then functions to protect *E. amylovora* cells from further membrane stressors. This study contributes to the idea that stress management is an

important selective advantage of TA systems when these systems are under low level expression conditions. Although the *E. coli* Hok has been implied as a target for killing host bacterial cells(Chukwudi and Good 2020; Faridani et al. 2006), the significant transcriptomic and physiological changes during *E. amylovora hok* overexpression presented in this study suggest that additional considerations are requisite in applying this toxin to fire blight disease management.

4.5 Materials and methods

4.5.1 Bacterial strains, plasmids, and growth conditions

The bacterial strains and plasmids used in this study are listed in Table A.3. *E. amylovora* strains were routinely grown at 28°C in Luria-Bertani (LB) agar or broth. Unless stated otherwise, the following antibiotics were supplemented in the medium at the concentrations indicated: ampicillin (Ap; 100 µg/ml), chloramphenicol (Cm; 15 µg/ml), or kanamycin (Km; 25 µg/ml). For tolerance screening, streptomycin was applied at 100 µg/ml.

4.5.2 DNA manipulations

The *atpB* gene or the chromosomal region that spanned the entire ATP synthase gene cluster (*atpB, atpE, atpF, atpH, atpA, atpG, atpD,* and *atpC*) was deleted from *E. amylovora* Ea1189 using the λ Red recombinase system (Datsenko and Wanner 2000; Edmunds et al. 2013), as previously described. The pBAD33-*pspA* and pPROBE-NT:*pspA* constructs were generated by cloning the coding region of *pspA* or the 500 bp upstream the coding region into pBAD33 and pPROBE-NT, respectively, using the FastCloning approach (Li et al. 2011). The oligonucleotide primers used in this study are listed in Table A.4. *E. coli* and *E. amylovora* cells were transformed routinely using heat shock and electroporation approaches, respectively.

4.5.3 Growth arrest assay

E. amylovora cultures grown overnight for 20 h in LB broth were washed twice and diluted to OD_{600}=0.2 in fresh LB broth. Serially diluted IPTG (1 mM, 0.1 mM, 0.01 mM, 0.001 mM) or H_2O was supplemented, and the cultures were incubated at 28°C with 200 rpm shaking for 1 h. Survival rate was determined by the ratio of colony forming units (CFUs) per ml calculated through dilution plating in Ea1189(pOE-*hok*) to that in Ea1189(pEVS143). To test the effect of bacterial metabolites on the toxicity of Hok, cultures were prepared the same as the growth arrest assay, except that 10 mM mannitol or 10 mM arabinose was added to the cultures right before IPTG was added, and the OD_{600} was measured 4 h after the incubation using a spectrophotometer plate reader (Tecan; Männedorf, Switzerland).

4.5.4 Measurement of membrane polarity and membrane integrity through flow cytometry

Changes in membrane polarity and membrane integrity was measured using bis-(1,3-dibutylbarbituric acid) trimethine oxonol ($DiBAC_4(3)$; Thermo Fisher Scientific; Waltham, MA) and propidium iodide (PI; Thermo Fisher Scientific), respectively, following a published protocol (Clementi et al. 2014) with minor modifications. $DiBAC_4(3)$ is a slow-response potential-sensitive dye that enters depolarized cells and exhibits fluorescence (excitation/emission=490 nm/516 nm) after binding to membrane proteins. Propidium iodide exhibits fluorescence (excitation/emission, 535 nm/617 nm) after binding to DNA of membrane integrity-compromised cells. Briefly, *E. amylovora* cultures grown for 20 h were washed twice with fresh LB and adjusted to OD_{600}=0.5. Mannitol or arabinose at 10 mM or H_2O was supplemented followed by addition of serially diluted IPTG (1 mM, 0.1 mM, 0.01 mM, 0.001 mM) or H_2O of the same volume for 1 h at 28 °C with shaking. Cells were washed twice with

0.5× Phosphate-Buffered Saline (PBS) to the original volume, and 250 nM DiBAC4(3) or 20 μg/ml PI was added. The mixtures were incubated in a 28°C incubator for 1 h without shaking. Fluorescence was measured using a BD LSR II flow cytometer (BD Biosciences; Franklin Lakes, NJ) equipped with a 488 nm laser and a 530/30 emission filter for $DiBAC_4(3)$ staining and a 561 nm laser and a 620/15 emission filter for PI staining. A minimum of 10,000 events were collected for each sample. Subsequent analyses were conducted using Flowing Software 2.5.1 and R v3.4.0.

4.5.5 Total RNA extraction

Cultures of Ea1189(pEVS143) and Ea1189(pOE-*hok*) grown for 20 h were washed twice and diluted to OD_{600}=0.2 in fresh LB broth. H_2O or 1mM IPTG was supplemented to Ea1189(pOE-*hok*) cultures, representing induction of *hok* at subtoxic and toxic level, respectively. Ea1189(pEVS143) cultures supplemented with H_2O of the same volume represented cells expressing wild-type level of *hok*. Each treatment had three biological replicates. Bacterial cells were harvested 1 h after the addition of IPTG or H_2O. Total RNA extraction was modified from a previous reported method (Rivas et al. 2001). Briefly, cell pellets of *E. amylovora* cultures were resuspended in 200 μl of 0.1% N-lauroyl sarcosine sodium salt followed by centrifugation at 13,000× g for one min. The cell pellets were resuspended in 100 μl acetate/SDS solution (1% SDS in 10 mM EDTA and 50 mM sodium acetate, pH 5.1) and incubated for 5 min in boiling water. After centrifugation, RNA was extracted from the supernatants using the RNA Clean & Concentrator-25 kit (Zymo Research; Irvine, CA) following manufacturer's instructions. Residual DNA contamination was removed by TURBO DNA-free Kit (Thermo Fisher Scientific) following the manufacturer's instructions.

4.5.6 Library preparation and sequencing

The quality of RNA was analyzed on a 2100 Bioanalyzer (Agilent Technologies; Santa Clara, CA). The integrity of RNA was examined via electrophoresis on a 1% agarose gel. RNA libraries were prepared by Illumina TruSeq Stranded Total RNA Library Prep Kit (bacteria) (Illumina; San Diego, CA). Sequencing was conducted with the 50 bp single-end format on the Illumina HiSeq 4000 platform at the Michigan State University Research Technology Support Facility.

4.5.7 Data analysis

Adaptor sequences and low-quality reads were filtered through Trimmomatic v0.32 with following parameters: ILLUMINACLIP:$ADAPTOR:2:30:10 LEADING:3 TRAILING:3 SLIDINGWINDOW:4:30 (Bolger et al. 2014). The remaining reads were mapped to the genome of *E. amylovora* ATCC 49964 using Bowtie 2 v2.3.4.3 (Langmead and Salzberg 2012). Counts of reads for each annotated gene were obtained using HTSeq v0.6.1 (Anders et al. 2015). TMM-normalized CPM were called via edgeR (Robinson and Smyth 2008). DEGs were defined as greater than 2-fold change of CPM value and less than 0.05 of the corresponding FDR value. GO enrichment analysis was conducted on AgriGO v2.0 (Tian et al. 2017), with a cutoff FDR of 0.01. Redundant GO terms were filtered through REVIGO using the default setting (Supek et al. 2011).

4.5.8 qRT-PCR

Cultures were grown in the same condition as the RNA-seq experiment and total RNA from three biological replicates was extracted and pooled together. cDNA was synthesized from 1,000 ng total RNA using the High Capacity cDNA Reverse Transcription kit (Thermo Fisher Scientific) following manufacturer's instructions. Gene expression levels were quantified via

qRT-PCR using a StepOne Plus Real-Time PCR system (Applied Biosystems, Foster City, CA, USA) under the routine condition (Zeng et al. 2013) with three replications. The housekeeping gene *recA* was used as an endogenous reference gene (Zeng et al. 2013). Fold changes of gene expression were quantified via the $2^{-\Delta\Delta C_T}$ method.

4.5.9 Quantification of intracellular and extracellular ATP

BacTiter-Glo™ reagent (Promega; Madison, WI) was prepared following the manufacturer's instructions. The BacTiter-Glo™ reagent supports bacterial lysis, ATP extraction, and ATP quantification based on the luminescent signal from a thermostable luciferase. *E. amylovora* cultures were grown and treated in the same condition as that of the growth arrest assay in this study. To measure intracellular ATP levels, cultures were washed twice and resuspended in 0.5× PBS of the same volume to remove any extracellular ATP. One hundred µl of the culture suspension was mixed with equal volume of the BacTiter-Glo™ reagent prepared in a 96-well plate. The mixtures were incubated at room temperature for 5 minutes before luminescence was measured. Extracellular ATP levels were measured following the same procedure for intracellular ATP measurement, except that supernatants of the cultures from the first centrifugation were used for quantification. Total ATP was defined as the sum up of the intracellular and the extracellular levels of ATP.

4.5.10 Promoter activity of *pspABCD* operon and CCCP tolerance assay

Promoter activity of *pspABCD* was monitored in *E. amylovora* Ea1189 cultures containing the transcriptional fusion construct pPROBE-NT:*pspA*. The overnight cultures of Ea1189(pPROBE-NT:*pspA*) were washed and resuspended in LB broth to a final OD_{600} of 1.0. The cultures were incubated with approximately 10^8 plaque forming units of bacteriophage ΦEa31-3 (Gill et al. 2003), 40 µM CCCP, 5% ethanol, or 0.1% Triton X-100 for 5 h. The Gfp

fluorescence was measured on a spectrophotometer plate reader (Tecan). To measure tolerance of *E. amylovora* cultures during membrane stress, 200 µM CCCP was supplemented to the washed *E. amylovora* cultures at OD_{600}=1.0 followed by incubation for 5h. Survival rate was determined as the ratio of CFU/ml after the treatment to that before the treatment.

4.5.11 Tolerance of stationary phase cultures to streptomycin

Single colonies of *E. amylovora* cultures were in grown in LB broth amended with selective antibiotics for 20 h to reach stationary phase. Cultures were washed twice by fresh LB broth before subjecting to 100 µg/ml streptomycin. After incubation at 28 °C with shaking for 5 h, cultures were washed once and serially diluted in 0.5× PBS buffer, and plated in LB plates without any antibiotics. Survival rate was determined as the ratio of CFU/ml after the treatment to that before the treatment.

CHAPTER 5

A method for the examination of SDHI fungicide resistance mechanisms in phytopathogenic fungi using a heterologous expression system in *Sclerotinia sclerotiorum*

5.1 Abstract

Succinate dehydrogenase inhibitors (SDHI) comprise a class of broad-spectrum fungicides utilized for management of a variety of diseases caused by phytopathogenic fungi. In many cases, reduced sensitivity to SDHI fungicides has been correlated with point mutations in the *SdhB* and *SdhC* target genes that encode components of the succinate dehydrogenase complex. The genetic basis of SDHI fungicide resistance mechanisms, however, has been functionally characterized in very few fungi. *Sclerotinia sclerotiorum* is a fast-growing and SDHI fungicide-sensitive phytopathogenic fungus that can be conveniently transformed. Given the high amino acid sequence similarity and putative structural similarity of SDHI protein target sites between *S. sclerotiorum* and other common phytopathogenic ascomycete fungi, we developed an *in vitro* heterologous expression system that used *S. sclerotiorum* as a reporter strain. With this system, we were able to demonstrate the function of mutant *SdhB* or *SdhC* alleles from several ascomycete fungi in conferring resistance to multiple SDHI fungicides. In total, we successfully validated the function of *Sdh* alleles that had been previously identified in field isolates of *Botrytis cinerea*, *Blumeriella jaapii*, and *Clarireedia homoeocarpa* in conferring resistance to boscalid, fluopyram or fluxapyroxad, and used site-directed mutagenesis to construct and phenotype a mutant allele that is not yet known to exist in *Monilinia fructicola* populations. We also examined the functions of these alleles in conferring cross-resistance to the recently introduced SDHIs including pyraziflumid, pydiflumetofen, and inpyrfluxam, that have not been tested in these organisms in most cases. The approach developed in this study can potentially be widely applied to interrogate SDHI fungicide resistance mechanisms in other phytopathogenic ascomycetes. Our results of cross-resistance among different SDHIs provides

important insights into the future development of SDHIs in managing fungal populations that are resistant to existing SDHIs.

5.2 Introduction

Succinate dehydrogenase inhibitor (SDHI) fungicides belong to a class of broad-spectrum respiration-inhibiting fungicides that has been rapidly adopted by the agricultural industry to manage a range of fungal diseases (Sang and Lee 2020; Sierotzki and Scalliet 2013). Recently, SDHI fungicides have come into prominence largely due to the evolution of resistance to two other major classes of fungicides, the quinone outside inhibitor (QoI) and the demethylation inhibitor (DMI) fungicides (Brent 2007; Sierotzki and Scalliet 2013). Currently, the SDHI class of fungal mitochondrial respiration inhibitors contains 23 different molecules in 11 different chemical groups (FRAC 2020) and is used to manage fungal diseases on grains, cereals, oilseeds, fruits, vegetables, and turf (FRAC, 2018a; Sang *et al.*, 2019). The target site of SDHIs is the ubiquinone-binding (Qp) site in complex II of the electron transport chain, which is formed by subunits B, C and D of succinate dehydrogenase (SDH) in phytopathogenic fungi. The binding of SDHIs to the Qp site blocks the access of the natural substrate and consequently inhibits mitochondrial respiration (Sierotzki and Scalliet 2013).

The current status of SDHI resistance risk is considered to be medium to high (FRAC 2020), and reduced sensitivity and/or field resistance to SDHIs has been reported in at least 20 fungal species, including economically-important plant pathogens such as *Alternaria* spp., *Botrytis cinerea, Blumeriella jaapii, Clarireedia homoeocarpa, Monilinia fructicola*, *Sclerotinia sclerotiorum,* and *Zymoseptoria tritici* (Avenot et al. 2014; Chen et al. 2013; Dooley et al. 2016; Fernández-Ortuño et al. 2017; FRAC 2018b; Outwater et al. 2019; Popko et al. 2018; Yong Wang et al. 2015). Functional studies using traditional genetic techniques have demonstrated that

target site mutations in the Sdh subunits (mostly SdhB and SdhC) can confer reduced sensitivity to SDHIs in a fungal species. For example, Lalève *et al.* (2014) used site-directed mutagenesis and gene replacement of *B. cinerea SdhB* to demonstrate that specific mutations of amino acids P225, N230, and H272 conferred different patterns of SDHI fungicide resistance to bixafen, boscalid, carboxin, and fluopyram. Functional characterization of SDHI resistance mechanisms has also been conducted in the wheat pathogen *Z. tritici* through *in trans* allele expression (Skinner et al. 1998), bulked segregant analysis (Steinhauer et al. 2019), generation of a chromosomal knockout (Steinhauer et al. 2019), and UV radiation-based random mutagenesis (Fraaije *et al.*, 2012; Scalliet *et al.*, 2012). In particular, mutations altering codon H267 in *Z. tritici* SdhB (corresponding to H272 in *B. cinerea*) have been characterized to cause reduced sensitivity to bixafen, boscalid, carboxin, fluopyram, and isopyrazam (Fraaije *et al.*, 2012; Scalliet *et al.*, 2012; Skinner *et al.*, 1998). Likewise, mutations altering codon H267 in *C. homoeocarpa* SdhB (H267Y, H267R), and codons G91 and G150 in SdhC (G91R, G150R), have been confirmed to confer reduced sensitivity to SDHIs through the expression of mutated *SdhB* or *SdhC* genes in an SDHI-sensitive *C. homoeocarpa* strain (Popko et al. 2018; Lee et al. 2020).

In other SDHI-resistant ascomycete fungi, mutations, mostly in *SdhB* and *SdhC*, and frequently in amino acids corresponding to H272 of SdhB and H146 of SdhC in *B. cinerea*, have been identified (FRAC 2015; Sierotzki and Scalliet 2013). A wider diversity of mutations has also been identified. For example, in studies of SDHI resistance in *B. cinerea*, field isolates carrying mutation(s) at codon 225, 230, 272 of *SdhB*, codon 85, 93, 158, 168 of *SdhC*, and codon 132 of *SdhD* exhibited reduced sensitivity to SDHIs (Amiri et al. 2020; Fernández-Ortuño et al. 2017; Leroux et al. 2010). However, the majority of more recent investigations of SDHI fungicide resistance have correlated mutations in *SdhB* or *SdhC* with resistance, without

demonstrating function. Also, it is largely unknown how well newer SDHIs, such as pyraziflumid, pydiflumetofen, and inpyrfluxam, work in managing phytopathogenic fungal populations that are resistant to the older SDHIs mentioned above.

Sclerotinia sclerotiorum (Lib.) de Bary is a devastating necrotrophic fungal pathogen that causes white mold on more than 400 plant species (Boland and Hall 1994; Bolton et al. 2006). Due to the importance of this fungal pathogen, different genetic transformation tools of *S. sclerotiorum* have been developed to understand host - *S. sclerotiorum* interactions and fungicide resistance mechanisms (Liang and Rollins 2018; Yong Wang et al. 2015). Both protoplast-mediated and *Agrobacterium*-mediated transformation tools have been developed in *S. sclerotiorum* (Rollins, 2003; Weld *et al.*, 2006). The *Agrobacterium*-mediated approach from Weld *et al.* (2006) relies on *S. sclerotiorum* ascospores, which are produced under certain conditions and are not always readily obtainable (Weld *et al*., 2006). In contrast, protoplasts of *S. sclerotiorum* can be easily produced from fungal hyphae by using cell-wall degrading enzymes, and a high transformation efficiency has been obtained using the protoplast-mediated transformation approach (Ge *et al*., 2013). Also, *S. sclerotiorum* is fast-growing and exhibits high sensitivity to different classes of fungicides including SDHIs (Duan et al. 2013; Yong Wang et al. 2015; Y. Wang et al. 2015).

The investigation of the function of each mutation in *Sdh* genes identified in field resistant isolates is critical to make accurate recommendations of fungicide applications for growers. Of additional importance is the potential for cross resistance of existing target site mutations in SDHI-resistant fungi to newer SDHI compounds that either have recently been introduced or are still in experimental stages. We hypothesized that we could utilize the high transformation efficiency and SDHI fungicide sensitivity of *S. sclerotiorum* to generate a system enabling the

functional examination of resistance to any SDHI fungicide of mutant *SdhB* or *SdhC* alleles isolated from ascomycete fungi with resistance to at least one SDHI compound. In this study, our objectives were to develop and test a method for phenotyping SDHI resistance, and to use this method to characterize the function of specific mutation(s) in *SdhB* and *SdhC* for improved understanding of SDHI resistance in phytopathogenic ascomycetes.

5.3 Results

5.3.1 *Sdh* genes in phytopathogenic ascomycetes share high amino acid similarity

To explore potentially shared SDHI fungicide resistance mechanisms in phytopathogenic ascomycetes, a heatmap was generated comparing the amino acid sequences of SdhB and SdhC in a representative group of phytopathogenic fungal species to those in *S. sclerotiorum*. *Ustilago maydis,* a basidiomycete, was used as an outlier for this analysis. The SdhB amino acid sequences were well-conserved (≥69% amino acid identity relative to *S. sclerotiorum*), and the SdhC amino acid sequences were less conserved (≥42% amino acid identity) among the fungal organisms included. SDHI-resistant isolates of these fungi commonly contained nonsynonymous mutations in four regions of SdhB and SdhC, denoted SdhB R1, SdhB R2, SdhC R1 and SdhC R2. SdhB R1, corresponding to S222-N231 of SdhB in *S. sclerotiorum*, is a cysteine-rich region of SdhB including a conserved proline (P), where mutations of this amino acid residue are found in SDHI-resistant isolates of several ascomycete fungi, including *Botrytis cinerea* P225L/T/F (Fernández-Ortuño et al. 2012; Veloukas et al. 2011; Yin et al. 2011) and *Stemphylium vesicarium* P225L (FRAC 2015). SdhB R2, corresponding to S268 -N277 of SdhB in *S. sclerotiorum*, is the second cysteine-rich region of SdhB, and contains a conserved histidine (H) residue, where mutations of the histidine and its surrounding amino acid residues are shown to be correlated with SDHI fungicide resistance, such as *A. alternata* H277Y/R (Avenot et al. 2008),

A. oryzae H249Y/L/N (Shima et al. 2009), *B. cinerea* H272Y/R/L (Fernández-Ortuño et al. 2012; Veloukas et al. 2011; Yin et al. 2011), *B. jaapii* H260R (Outwater et al. 2019), *C. homoeocarpa* H267Y/R (Popko et al. 2018), and *S. sclerotiorum* H273Y (FRAC 2015). SdhC R1 is a less conserved region of SdhC corresponding to W81-G91 of SdhC in *S. sclerotiorum*. SdhC R2 is centered on a well-conserved histidine (H) residue of SdhC corresponding to F143-L151 of SdhC in *S. sclerotiorum*. Mutation of this H residue is correlated with SDHI fungicide resistance in many cases, such as *A. solani* H134R (Mallik et al. 2013), *Pyrenophora teres* H134R (Stammler et al. 2014), *S. sclerotiorum* H146R (FRAC 2015), and *Zymoseptoria tritici* H152R (Dooley et al. 2016) (Figure 5.1). The comparative alignment of the SdhB R1, SdhB R2, SdhC R1, and SdhC R2 regions among the fungal organisms examined is shown (Figure 5.1). Both SdhB R1 and SdhB R2 regions are almost identical among all the organisms tested, including *Ustilago maydis*. In contrast, SdhC R1 and SdhC R2 are less conserved overall, except for the universally shared histidine residue in SdhC R2.

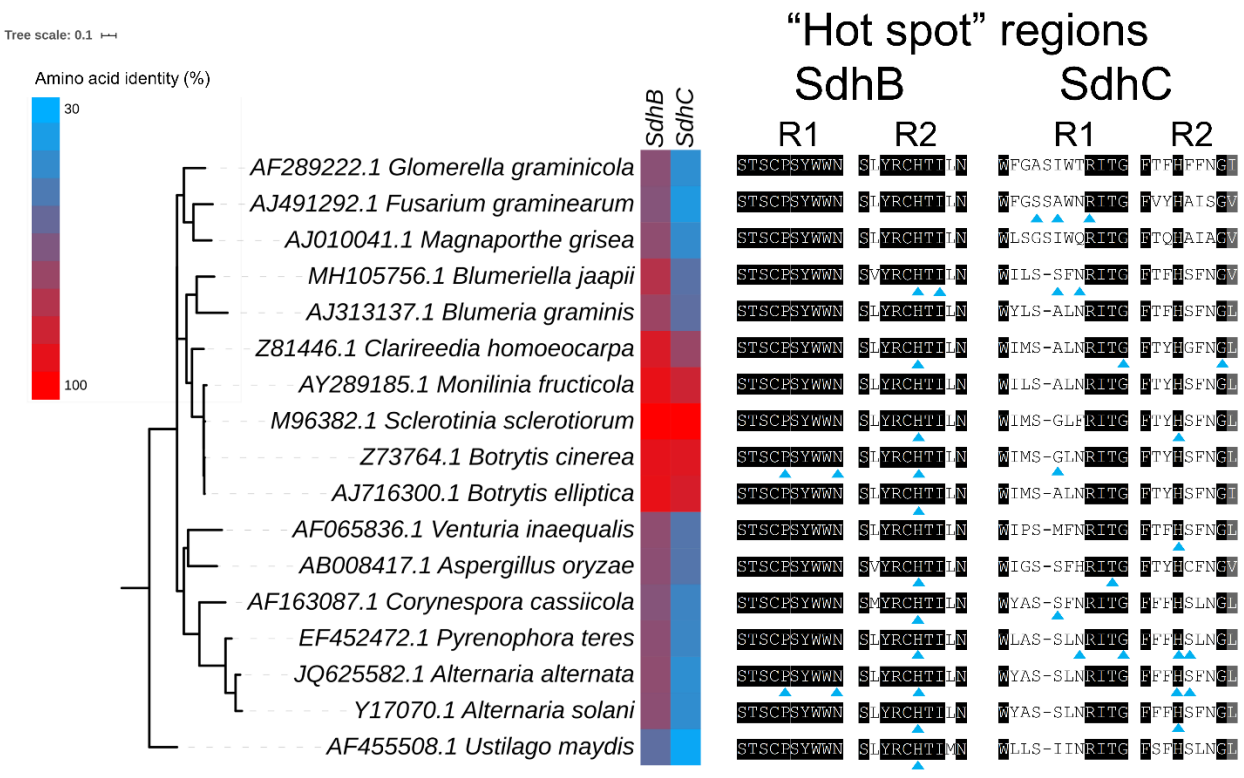

Figure 5.1. Alignment of SdhB and SdhC amino acid sequences in a representative group of phytopathogenic fungi. The heatmap displays the amino acid identity (%) of SdhB and SdhC in reference to that in *Sclerotinia sclerotiorum*. The regions spanning amino acids that are common “hot spots” for mutations that correlate with SDHI fungicide resistance are denoted SdhB R1, SdhB R2, SdhC R1 and SdhC R2. The highly conserved amino acid residues are highlighted. Amino acid residues that have been previously indicated to confer or correlate with SDHI fungicide resistance are marked with blue triangles. The phylogenetic tree was constructed by the maximum-likelihood method using the ITS sequences of the entries. The scale bar of the phylogenetic tree represents 1 substitutions in 100 bp.

5.3.2 Examination of SDHI fungicide resistance mechanisms using the *S. sclerotiorum* heterologous expression system

In this study, we developed a widely applicable heterologous expression system in *S. sclerotiorum* to examine the function of mutations in *SdhB* or *SdhC* from several ascomycete fungi in conferring resistance to different SDHI fungicides *in vitro*. The premise of the assay is to express putative mutant *SdhB* or *SdhC* alleles in *S. sclerotiorum* thus generating a strain containing both mutant *SdhB* or *SdhC* alleles and native *S. sclerotiorum SdhB* and *SdhC* alleles. We hypothesized that successful assembly and integration of the mutant *SdhB* or *SdhC* proteins in the otherwise native *S. sclerotiorum* Sdh complex would decrease the sensitivity of *S. sclerotiorum* to one or more SDHI fungicides, and that this phenotype could be visualized in a growth medium assay. An example workflow, in cloning and expressing a mutant *B. cinerea SdhB* allele using the *S. sclerotiorum* heterologous expression system, is shown (Figure 5.2). To express the extrinsic *SdhB* or *SdhC* gene of interest in *S. sclerotiorum*, the native promoters of the *SdhB* and the *SdhC* genes in *S. sclerotiorum* (1,500 bp upstream the coding region) were cloned into the pYHN3-ptrpC plasmid (Sang et al., 2018) to generate pProm-*SdhB* and pProm-*SdhC*, respectively. *SdhB or SdhC in the fungal organism of interest was subsequently cloned immediately downstream of the corresponding S. sclerotiorum* promoter region in pProm-*SdhB* or pProm-*SdhC*. The final construct was transformed into the WT SDHI-sensitive *S. sclerotiorum* scl02-05 strain. *In vitro* sensitivity of transformed strains to the SDHI fungicides boscalid 20 µg ml^{-1}, fluopyram 20 µg ml^{-1}, or fluxapyroxad 40 µg ml^{-1}, was examined by comparing the relative growth of the transformed *S. sclerotiorum* strain on amended and unamended medium. Using this approach, we examined the *in vitro* fungicide sensitivity of *S. sclerotiorum* expressing the WT or mutated *SdhB* or *SdhC* gene of *B. jaapii*, *B. cinerea*, *M.*

fructicola, or *C. homoeocarpa. The SdhB and SdhC* mutations examined in this study and their characterized or presumed correlation to *bos*calid, fluopyram, and fluxapyroxad resistance in the host organism is summarized (Table A.5). The strains generated in this study are listed in Table A.6.

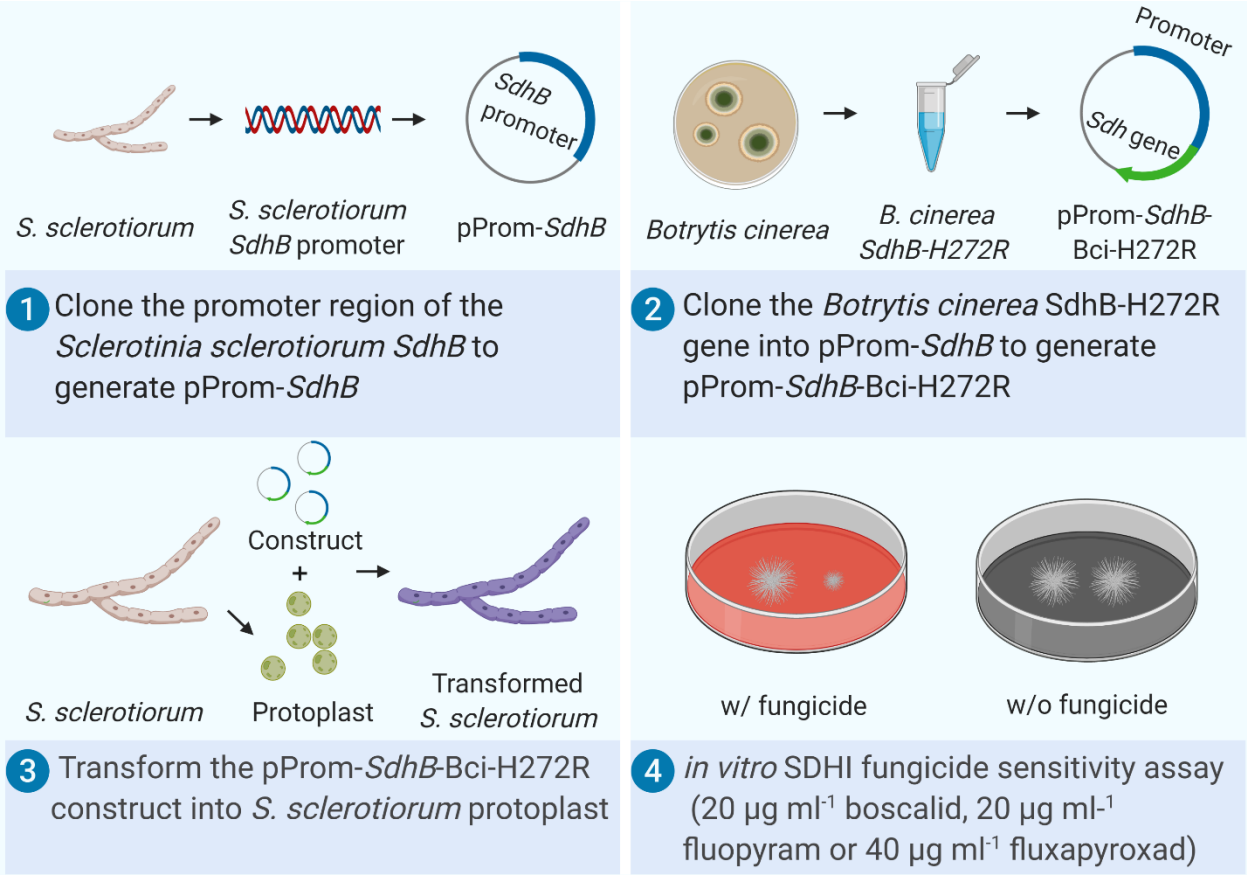

Figure 5.2. An example workflow in cloning and expressing a mutant *B. cinerea* SdhB allele using the S. sclerotiorum heterologous expression system. The native promoter region of *S. sclerotiorum SdhB* (1.5 kb upstream the coding region) was cloned into the pYHN3-ptrpC plasmid to generate pProm-SdhB (the constitutive promoter ptrpC was removed). The *B. cinerea SdhB* gene was cloned into pProm-SdhB and was inserted immediate downstream the promoter of *S. sclerotiorum SdhB*. The recombinant plasmid construct is transformed into the SDHI-sensitive *S. sclerotiorum* Scl02-05 strain. Agar plugs of 3-day old cultures grown on PDA plates were inoculated on PDA plates with or without the addition of the SDHI fungicides. The radius of mycelial growth was measured 48 h post inoculation, and relative growth was calculated and statistically analyzed.

B. cinerea is an important phytopathogenic fungus, that causes gray mold on more than 230 plant species including many fruits, vegetables, and ornamental plants (Price 1979). Multiple mutations in the *Sdh* genes have been shown to correlate with SDHI fungicide resistance (Amiri et al. 2020; De Miccolis Angelini et al. 2010; Fernández-Ortuño et al. 2012, 2017; Lalève et al. 2014; Leroux et al. 2010; Veloukas et al. 2011; Yin et al. 2011). In this study, we expressed the *B. cinerea SdhB-WT*, *SdhB-P225F* and *SdhB-H272R* genes in *S. sclerotiorum* and examined the *in vitro* fungicide sensitivity in the corresponding transformed *S. sclerotiorum* strains. *B. cinerea SdhB-P225F* conferred resistance to boscalid, fluopyram and fluxapyroxad in *S. sclerotiorum*, whereas *SdhB-H272R* conferred resistance to boscalid but not to fluopyram or fluxapyroxad in *S. sclerotiorum* (Figure 5.3). The *SdhB-P225F* mutation has been genetically characterized to confer resistance to boscalid and fluopyram in *B. cinerea* (De Miccolis Angelini et al. 2010; Lalève et al. 2014), and this mutation has been identified in natural isolates of *B. cinerea* that are resistant to boscalid, fluopyram, and fluxaproxad (Fernández-Ortuño et al. 2017; Veloukas et al. 2011). Though both the mutations contribute to boscalid resistance, *S. sclerotiorum* expressing *B. cinerea SdhB-P225F* was significantly more tolerant to boscalid compared with that expressing *B. cinerea SdhB-H272R* (Figure 5.4A). In agreement with our results, Lalève *et al.* (2014) demonstrated that *SdhB-P225F* exhibits greater inhibitory effect to germ-tube elongation and succinate-dehydrogenase activity than *SdhB-H272R* in *B. cinerea* field isolates and lab mutants. Similarly, the clear correlation between *SdhB-H272R* to boscalid resistance in *B. cinerea* has been previously shown in both natural isolates and lab mutants of *B. cinerea* (Fernández-Ortuño et al. 2012, 2017; Veloukas et al. 2011; Yin et al. 2011).

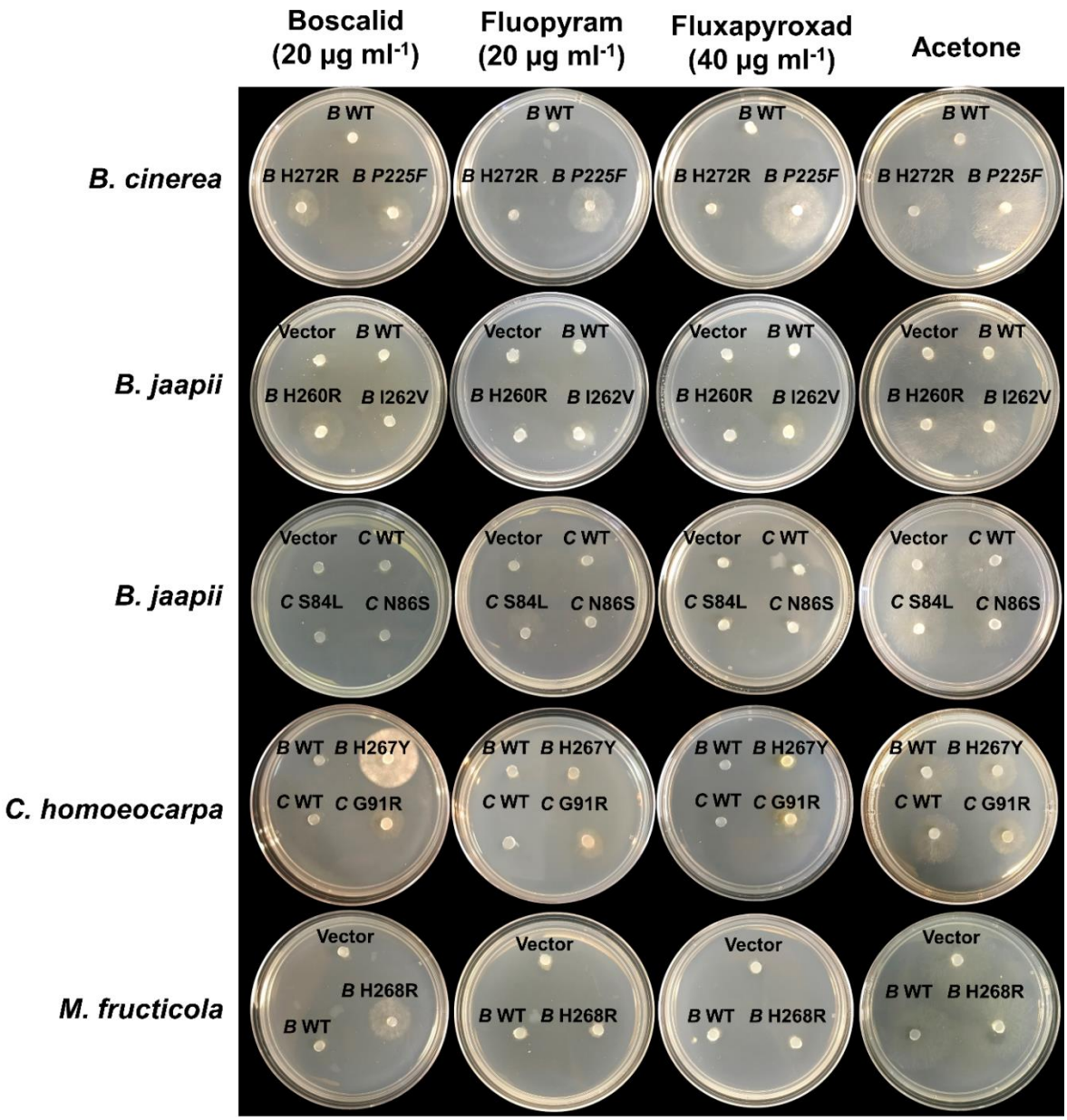

Figure 5.3. *In vitro* SDHI fungicide sensitivity of *S. sclerotiorum* Scl02-05 expressing *SdhB* or *SdhC* alleles of *B. cinerea*, *B. jaapii*, *C. homoeocarpa* and *M. fructicola* on PDA plates with or without the addition of the fungicides at the following concentrations (boscalid 20 µg ml^{-1}, fluopyram 20 µg ml^{-1} or fluxapyroxad 40 µg ml^{-1}). Images of *S. sclerotiorum growth* in the fungicide-free and fungicide-containing plates were collected 24 h and 48 h, respectively, post inoculation.

Cherry leaf spot (CLS), caused by *B. jaapii*, is one of the most important diseases of tart cherry in the Midwestern United States. Resistance to boscalid, fluopyram and fluxapyroxad has been observed in *B. jaapii* populations recovered from both research and commercial orchards (Outwater *et al.*, 2019; Peng *et al.*, unpublished). *B. jaapii* is slow-growing, and the *in vitro* fungicide sensitivity of an isolate is determined based on the minimum inhibitory concentration (MIC) of the fungicide (Outwater *et al*., 2006). Resistance to boscalid (MIC ≥ 25 μg ml^{-1}) is correlated with the *SdhB-H260R* mutation, which is commonly identified in the boscalid-resistant population of *B. jaapii* (Outwater et al. 2019). We recently identified three additional mutations, *SdhB-I262V*, *SdhC-S84L*, and *SdhC-N86S*, that are predominant in the current SDHI-resistant population of *B. jaapii* in Michigan (Table A.7 and Peng *et al.*, unpublished). To validate the correlation of the *SdhB-H260R*, *SdhB-I262V*, *SdhC-S84L*, and *SdhC-N86S* mutations to SDHI fungicide resistance, the *B. jaapii SdhB* or *SdhC* corresponding mutant alleles were expressed in *S. sclerotiorum*. As expected, the *B. jaapii SdhB-H260R* mutation conferred resistance to boscalid in *S. sclerotiorum* (Figure 5.3). The *B. jaapii SdhB-I262V* mutation conferred resistance to both fluopyram and fluxapyroxad in *S. sclerotiorum* (Figure 5.3), and the effect on fluopyram resistance was greater than that to fluxapyroxad (Figure 5.4B). The *S. sclerotiorum* strain expressing *B. jaapii SdhC-S84L* was significantly more resistant to fluopyram (Figure 5.3), and showed non-differential sensitivity to boscalid and fluxapyroxad (Figure 5.4C). Interestingly, the *B. jaapii SdhC-N86S* mutation, expected to confer resistance to boscalid, fluopyram and fluxapyroxad, did not increase resistance to any of these fungicides when expressed in *S. sclerotiorum* (Figure 5.4C).

C. homoeocarpa is the causal agent of dollar spot, a critical disease problem of turf grass. A previous study characterized the molecular mechanisms of SDHI fungicide resistance in *C.*

homoeocarpa (Popko et al. 2018). In particular, *SdhB-H267Y* confers resistance to boscalid but not to fluxapyroxad, whereas *SdhC-G91R* confers resistance to both boscalid and fluxapyroxad (Popko et al. 2018). To evaluate whether the correlation of these mutations to SDHI fungicide resistance holds true when they are expressed in *S. sclerotiorum*, the constructs expressing *C. homoeocarpa SdhB-WT, SdhB-H267, SdhC-WT,* or *SdhC-G91R* were transformed into *S. sclerotiorum* for *in vitro* fungicide sensitivity assays. As expected, both *C. homoeocarpa SdhB-H267Y* and *SdhC-G91R* conferred elevated resistance to boscalid in *S. sclerotiorum* (Figure 5.3), with *C. homoeocarpa SdhB-H267Y* showing a more significant effect on boscalid resistance (Figure 5.4D). *C. homoeocarpa SdhC-G91R* also conferred fluopyram and fluxapyroxad resistance (Figure 5.3). Noteworthy, though similar conclusions are made from this study and a previous study (Popko et al. 2018), *in vitro* sensitivity assays in *C. homoeocarpa* were conducted with the addition of boscalid, fluopyram, or fluxapyroxad at 1000 μg ml^{-1} into the media, and these concentrations of boscalid, fluopyram, and fluxapyroxad are 50 or 25 times higher than that used this study, suggesting the *S. sclerotiorum* is much more sensitive to these fungicides compared with *C. homoeocarpa in vitro*.

M. fructicola is the causal agent of brown rot in stone fruits, such as peach, cherry, and plum. Though sequence variations have been identified in the *Sdh* genes of the *M. fructicola* isolates, no varation was suggested to correlate with the boscalid-insensitive phenotype (Chen et al. 2013). In view of the high amino acid sequence identity (94%) of SdhB in *M. fructicola* and *S. sclerotiorum* (Figure 5.1), we wondered if these homologous alleles have shared active sites relevant to boscalid sensitivity. To access this possibility, we first generated p*Mfr-SdhB-WT*, a plasmid construct that allows the WT *M. fructicola sdhB* gene expression in *S. sclerotiorum*. The p*Mfr-SdhB-WT* construct was also used as the template to generate *pMfr-SdhB-H268R* through

site-directed mutagenesis, where a nonsynonymous mutation was introduced resulting in the amino acid substitution of a histidine to arginine at codon 268 in *M. fructicola* SdhB. Our result demonstrated that the *M. fructicola SdhB-H268R* mutation confers resistance to boscalid in *S. sclerotiorum* (Figure 5.3), where *S. sclerotiorum* expressing *M. fructicola SdhB-H268R* exhibited significantly greater relative fungal growth than that expressing *M. fructicola SdhB-WT* or the empty vector (Figure 5.4E). This is not unexpected since mutations in the orthologous histidine residue are correlated with the boscalid resistance phenotype in many fungi. However, whether this mutation exists in the field populations of *M. fructicola* and will be selected by field exposure to boscalid application remains to be investigated in the future.

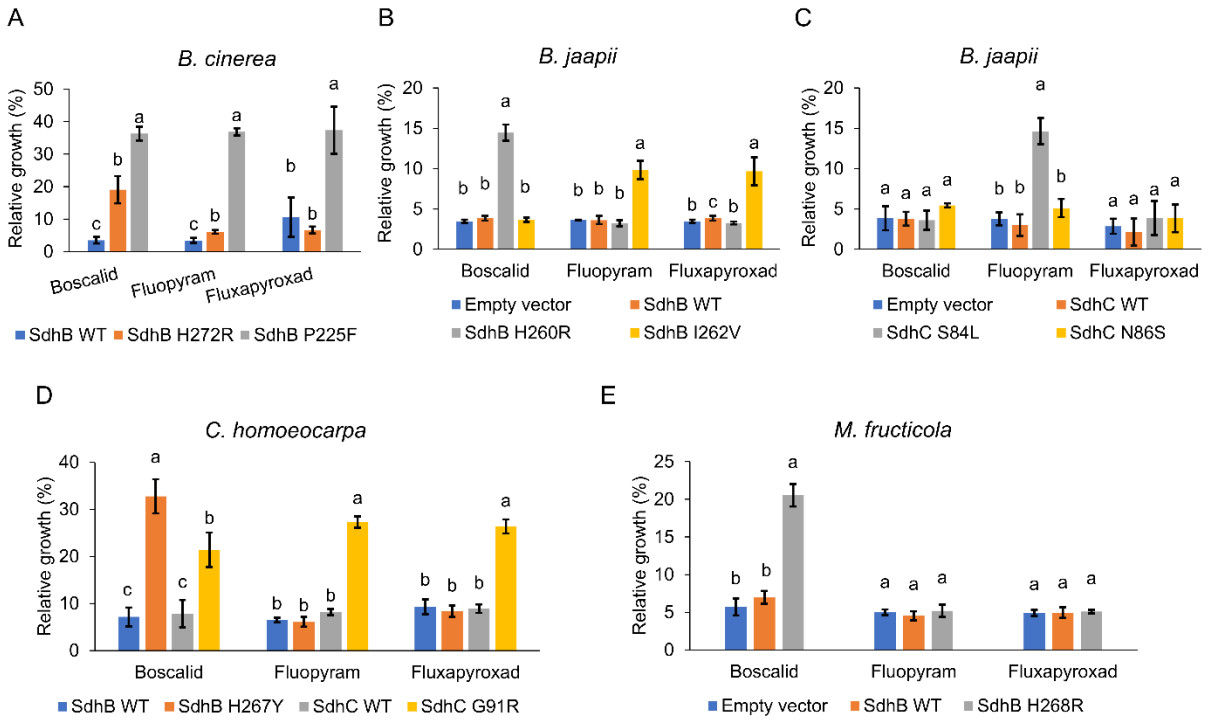

Figure 5.4. Statistical analysis of *in vitro* SDHI fungicide sensitivity assays. Two days post inoculation, the radius of mycelial growth was measured. Relative growth was determined as the ratio of the growth in the fungicide-containing plate to that in the fungicide-free plate. Results represent the means, and error bars are the standard error of the mean. Different letters indicate significant differences (Student's *t*-test; $P < 0.05$).

Due to the wide application of boscalid, fluopyram, and fluxapyroxad in recent years, the resistance mechanisms of these SDHIs have been relatively more intensively studied. However, the efficacy of newer SDHIs, i.e. pyraziflumid, pydiflumetofen, and inpyrfluxam, in managing different diseases has not been tested in most cases. More importantly, very little is known about whether these recently introduced SDHIs are able to manage fungal populations that are resistant to previous SDHIs. In an attempt to address these questions, we examined the *in vitro* sensitivity of pyraziflumid, pydiflumetofen, and inpyrfluxam in *S. sclerotiorum* strains expressing the mutant *Sdh* alleles investigated in this study. We found that the WT *S. sclerotiorum* strain or the *S. sclerotiorum* strain transformed with the empty vector had little mycelial growth in PDA plates supplemented with pyraziflumid, pydiflumetofen, and inpyrfluxam at the concentrations of 1 μg ml^{-1}, 1 μg ml^{-1}, and 4.25 μg ml^{-1}, suggesting the high sensitivity of *S. sclerotiorum* to these SDHIs (Figure 5.5). *S. sclerotiorum* expressing the WT *Sdh* alleles of *B. cinerea*, *B. jaapii*, *C. homoeocarpa*, and *M. fructicola* had similar levels of sensitivity to theses SDHIs compared with the vector control (Figure 5.5). We showed that *S. sclerotiorum* expressing *B. cinerea SdhB-P225F* was significantly more resistant to pyraziflumid, pydiflumetofen, and inpyrfluxam (Figure 5.5). For mutant alleles of the *B. jaapii Sdh* genes, pyraziflumid sensitivity was reduced in *S. sclerotiorum* strains expressing anyone of the four mutant *Sdh* alleles that have been identified in *B. jaapii* populations, with the greatest reduction of pyraziflumid sensitivity during *B. jaapii SdhB-H260R* or *SdhC-S84L* expression; *B jaapii SdhB-H260R* mutation also conferred increased resistance to pydiflumetofen; inpyrfluxam resistance was conferred only by the *B. jaapii SdhC-N86S* mutation (Figure 5.5). *S. sclerotiorum* expressing *C. homoeocarpa SdhB-H267Y* was significantly more resistant to pyraziflumid alone, whereas *C. homoeocarpa SdhC-G91R* expression in *S. sclerotiorum* lead to increased resistance to all the three newer SDHIs

(Figure 5.5). Expression of the *M. fructicola SdhB-H268R* mutation conferred resistance to pyraziflumid, but not to pydiflumetofen and inpyrfluxam in *S. sclerotiorum* (Figure 5.5).

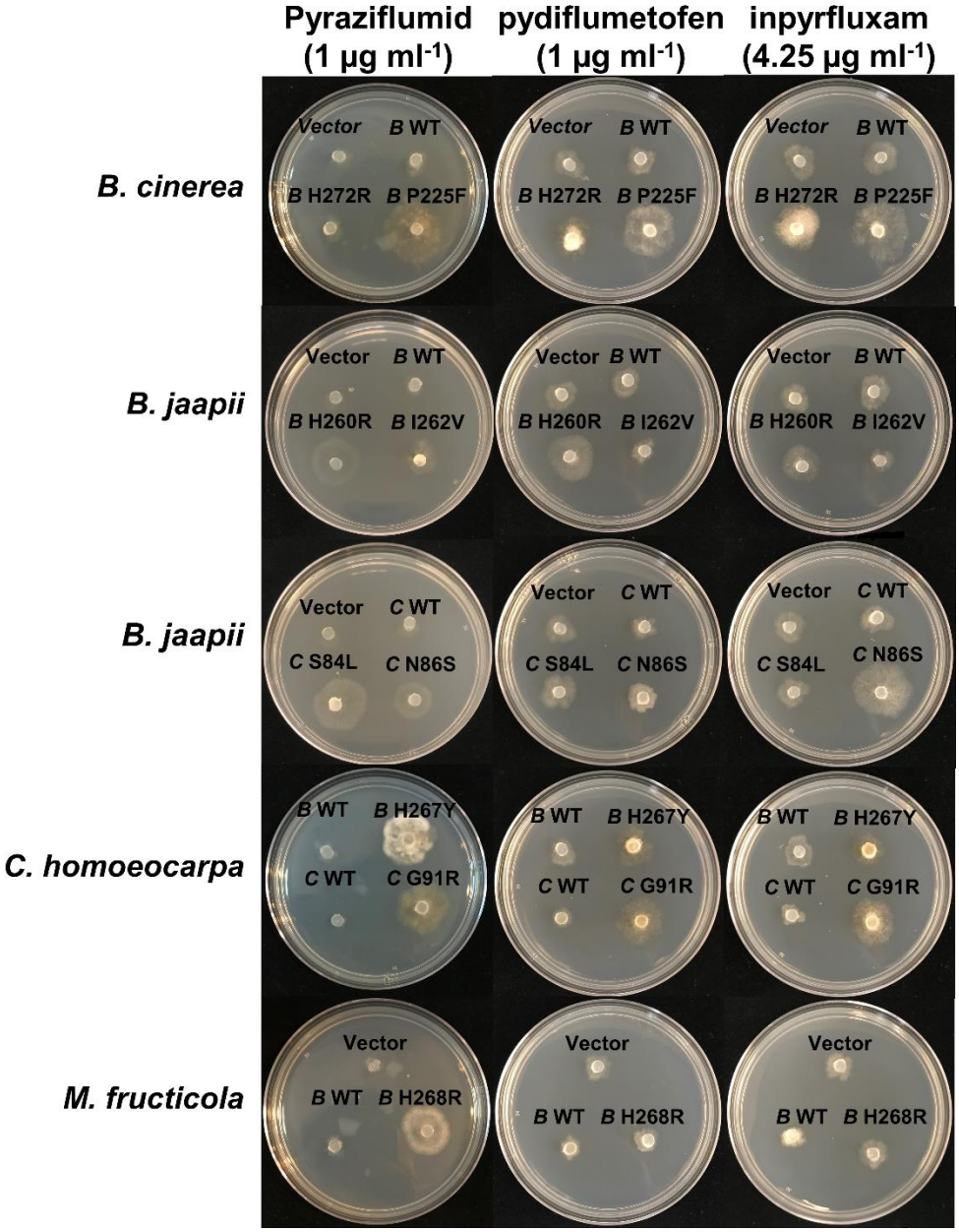

Figure 5.5. *In vitro* SDHI fungicide sensitivity of *S. sclerotiorum* Scl02-05 expressing *SdhB* or *SdhC* alleles of *B. cinerea, B. jaapii, C. homoeocarpa* and *M. fructicola* on PDA plates with or without the addition of the fungicides at the following concentrations (pyraziflumid 1 µg ml^{-1}, pydiflumetofen 1 µg ml^{-1}, or inpyrfluxam 4.25 µg ml^{-1}). Images of *S. sclerotiorum growth* in the fungicide-free and fungicide-containing plates were collected 24 h and 48 h, respectively, post inoculation.

5.4 Discussion

We functionally characterized the molecular mechanisms of SDHI fungicide resistance of several important phytopathogenic fungi through using the *S. sclerotiorum* heterologous expression system developed in this study. We successfully validated or characterized the correlation of previously identified *SdhB* or *SdhC* mutations in *B. cinerea*, *B. jaapii*, and *C. homoeocarpa* with resistance to boscalid, fluopyram, or fluxapyroxad. Coupled with site-directed mutagenesis, we showed that the *M. fructicola SdhB*-H268R mutation, a mutation not yet identified in natural populations of *M. fructicola*, rendered *S. sclerotiorum* insensitive to boscalid, suggesting a possible boscalid resistance mechanism in *M. fructicola*. Furthermore, we determined if the mutant alleles could confer cross-resistance to the newer SDHI fungicides inpyrfluxam, pydiflumetofen, and pyraziflumid.

To the best of our knowledge, characterization of SDHI fungicide resistance mechanisms through a heterologous expression system has not been successfully developed previously. In an attempt to characterize the binding properties of carboxamide SDHI fungicides in *Mycosphaerella graminicola*, the *M. graminicola Sdh* genes were expressed in *Escherichia coli* (Dehne *et al*., 2011). Under all of the conditions examined, the majority of *M. graminicola* Sdh proteins were found in inclusion bodies, indicating the incorrect folding of these enzymes in *E. coli* (Dehne *et al*., 2011). Yeast, a model fungal organism, has often been used as a host to study gene functions of filamentous fungi (Qiao, 2019). However, we examined a wild type *Saccharomyces cerevisiae* strain, and determined that this strain was highly resistant to boscalid, fluopyram, and fluxapyroxad at 1000 µg ml^{-1} (data not shown), and therefore unusable in SDHI sensitivity analyses. This is consistent with the previous observation of low binding potency of several carboxamides at the Qp site of the Sdh enzymes in yeast (Dehne *et al*., 2011).

Though SDHI fungicides have been deployed to manage many phytopathogenic fungi, genetic transformation tools are not currently available for the majority of them. Frequently, SDHI fungicide resistance mechanisms are extrapolated based on the overrepresented mutations in the SDHI-resistant populations, which requires enough sampling to eliminate the impact of genetic background differences among the isolates in addition to the mutations of interest. UV irradiation-based random mutagenesis has also been used frequently to generate mutants for SDHI sensitivity screening (De Miccolis Angelini *et al.*, 2010; Fraaije *et al.*, 2012; Shima *et al.*, 2009), which, though providing a near-isogenic background, still requires intensive sampling, phenotyping, and genotyping to obtain mutants relevant to field populations. The *S. sclerotiorum* heterologous expression approach presented in this study provides several advantages to studying SDHI fungicide resistance mechanisms. The *S. sclerotiorum* heterologous expression approach presented can be achieved using a minimal number of isolates, since the transformed *Sdh* alleles are expressed in an isogenic genetic background. In addition, *S. sclerotiorum* is fast-growing on laboratory media and therefore advantageous for studying *Sdh* mutations of a slow-growing fungus, such as *B. jaapii.* Combined with site-directed mutagenesis, the *S. sclerotiorum* heterologous expression approach can also be applied for studying the functions of a laboratory-generated mutation. As exemplified in this study, the *M. fructicola SdhB-H268R* mutation, a mutation not yet detected in field populations of *M. fructicola*, conferred resistance to boscalid when the mutated *M. fructicola SdhB* allele was expressed in *S. sclerotiorum*.

Though not examined in this study, the *S. sclerotiorum* heterologous expression system may be a convenient method to study SDHI fungicide resistance mechanisms of biotrophic fungi, such as *Blumeria graminis* and *Erysiphe necator*, which require *in vivo* tests to study fungicide resistance mechanisms (Rehfus et al. 2016; Wyand and Brown 2005). The *S. sclerotiorum*

heterologous expression system can also be helpful to study SDHI fungicide resistance mechanisms in a fungus that is highly tolerant to SDHI fungicides *in vitro*, such as *C. homoeocarpa* as examined in this study. The high sensitivity of *S. sclerotiorum* to the six SDHI fungicides screened in this study avoids the requirement of higher concentrations of these fungicides which typically crystallize out of the aqueous solid medium plates and cause uneven distribution in the medium.

Besides functional characterization of the mutant *Sdh* alleles of *B. cinerea*, *B. jaapii*, *C. homoeocarpa*, and *M. fructicola* in conferring resistance to boscalid, fluopyram, and/or fluxapyroxad, we also adapted the *S. sclerotiorum* heterologous expression system to interrogate the risk of using newer SDHIs, i.e. pyraziflumid, pydiflumetofen, and inpyrfluxam, to manage the existing SDHI-resistant populations. Pyraziflumid, discovered in 2016, is a broad-spectrum SDHI fungicide that has been shown to exhibit high fungicidal activities against *S. sclerotiorum* (Hou et al. 2018) and other phytopathogenic fungal pathogens including *B. cinerea*, *Blumeria graminis* f. sp. *hordei*, and *Puccinia recondite* (Oda et al. 2017). However, we showed that all the mutant *Sdh* alleles studied here excepted *B. cinerea SdhB-H272R* conferred resistance to pyraziflumid, suggesting concerning efficacy of using this fungicide to manage fungal populations in field sites with history of applying other SDHIs. In line with this, a recent study of the cucumber powdery mildew pathogen *Podosphaera xanthii* showed that four out of the five mutations identified in *Sdh* genes of this fungus correlated with increased resistance of pyraziflumid (Miyamoto et al. 2020). Pydiflumetofen, recently released by Syngenta Crop Protection AG, has been shown to have high antifungal efficacy at very low dosages against *B. cinerea* (He et al. 2020), *Didymella bryoniae* (Mao et al. 2020), *Fusarium asiaticum* (Chen et al. 2020), *Fusarium graminearum* (Sun et al. 2020), *S. sclerotiorum* (Gao et al. 2020; Duan et al.

2018; Huang et al. 2019), and *Venturia inaequalis* (Ayer et al. 2018). Although resistance mechanisms of pydiflumetofen have not been examined in most cases, the *SdhB-P225F* mutation in *B. cinerea* has been suggested to correlate with reduced sensitivity of this fungus to pydiflumetofen (He et al. 2020), that is consistent with the observation in this study using the *S. sclerotiorum* heterologous expression system. Inpyrfluxam is a novel SDHI fungicide discovered by Sumitomo that was approved by the United States Environmental Protection Agency in August, 2020 (https://www.federalregister.gov/documents/2020/08/26/2020-18661/inpyrfluxam-pesticide-tolerances). To the best of our knowledge, the efficacy of inpyrfluxam against *S. sclerotiorum* has not been previously investigated. In this study, we showed that inpyrfluxam was effective in inhibiting the *in vitro* mycelial growth of *S. sclerotiorum* at a low dosage. We also showed that expression of a WT *SdhB* or *SdhC* gene of *B. jaapii*, *B. cinerea*, *M. fructicola*, or *C. homoeocarpa* in *S. sclerotiorum* did not cause any significant reduction of inpyrfluxam sensitivity compared with the empty vector control, suggesting promising efficacy of applying inpyrfluxam to manage these fungal pathogens and other phylogenetically closely related organisms. Strikingly, *SdhB-P225F* of *B. cinerea* and *SdhC-G91R* of *C. homoeocarpa* conferred resistance to all the SDHIs examined in this study, suggesting an overall high risk of using the SDHI fungicide class to manage fungal populations with high frequency of these mutations. Together, our results indicate that newer SDHIs, i.e. pyraziflumid, pydiflumetofen, and inpyrfluxam, though may exhibit high antifungal activities at low dosages against the WT population of *S. sclerotiorum* and possibly many other ogranisms, they may still fail to manage fungal populations that have shifted towards the accumulation of certain mutations with historical applications of other SDHIs.

Several aspects need to be considered while using the *S. sclerotiorum* heterologous expression system for studying SDHI fungicide resistance mechanisms in a fungal organism of interest. The *S. sclerotiorum* heterologous expression approach may provide limited insights into the functions of amino acid residues in Sdh enzymes that are not conserved between *S. sclerotiorum* and the fungus of interest. In this study, both *SdhC*-S84 and *SdhC*-N86 amino acid residues of *B. jaapii* are not present in *S. sclerotiorum.* In agreement with our expectation, the *B.jaapii SdhC*-S84L mutation conferred resistance to fluopyram but not to boscalid and fluxapyroxad in *S. sclerotiorum.* However, the *SdhC*-N86S mutation, identified in many *B. jaapii* isolates that are resistant to boscalid, fluopyram, and fluxapyroxad, did not confer increased resistance to any of the three fungicides in *S. sclerotiorum.* These results suggest that a mutated *Sdh* allele that is not conserved between the organism of interest and *S. sclerotiorum* may have different functions when expressed in *S. sclerotiorum.*

Using the *S. sclerotiorum* heterologous expression approach described in this study, we have improved our understanding of resistance mechanisms to SDHI fungicides in several important phytopathogenic filamentous fungi. Our study reiterates the importance of conducting studies to functionally characterize different *Sdh* mutations in conferring resistance to SDHIs that are currently widely used or in testing phase to provide scientific recommendations of premixed or rotational uses of SDHIs. In view of the high and intermediate sequence similarity of SdhB and SdhC, respectively, between *S. sclerotiorum* and other major phytopathogenic ascomycetes, the *S. sclerotiorum* heterologous expression approach reported in this study is expected to be widely applicable to characterize molecular mechanisms of SDHI fungicide resistance in various filamentous fungi, and could potentially be adapted to interrogate alleles encoding resistance to other site-specific fungicides.

5.5 Materials and methods

5.5.1 Plasmid construction

The promoters of *S. sclerotiorum SdhB* and *SdhC (*1,500-bp upstream the coding regions) were amplified from the genomic DNA of *S. sclerotinium* scl02-05 with the oligonucleotide primer sets ApaI_PScl_SDHB_F/KpnI_PScl_SDHB_R and ApaI_PScl_SDHC_F/KpnI_PScl_SDHC_R, respectively. The purified PCR products were digested with ApaI and KpnI, and ligated to the plasmid pYHN3-ptrpC digested with the same restriction enzymes (the constitutive promoter ptrpC was removed), to generate pProm-*SdhB* or pProm-*SdhC*, respectively. *SdhB genes* of *B. jaapii, B. cinerea, C. homoeocarpa and M. fructicola* were amplified from gDNA of the host organisms and cloned into pProm-*SdhB* or pProm-*SdhC* through FastCloning, a ligation-independent PCR cloning approach (Li et al. 2011). Briefly, the pProm-*SdhB* and pProm-*SdhC* plasmid backbone were amplified and mixed with the corresponding *SdhB* or *SdhC* PCR productions at 1:1 ratio. The mixtures in 5 µl were transformed into *E. coli* DH5α using the heat shock approach. Site directed mutagenesis was performed with the QuikChange Lightning Site-Directed Mutagenesis Kit following manufacturer's instructions (Agilent Technologies; Santa Clara, CA).

5.5.2 Protoplast preparation and transformation of *S. sclerotiorum*

S. sclerotiorum protoplast preparation and transformation followed the method conducted by Sang *et al.* (Sang et al. 2016) with some modifications. Briefly, 4-day old *S. sclerotiorum* mycelium grown on potato dextrose agar (Thermo Fisher Scientific; Waltham, MA) plates was inoculated into 25 ml potato dextrose broth in a 50-mL falcon tube, and incubated for 4 days at 25 °C without shaking. The *S. sclerotiorum* mycelium was then washed with ddH_2O and subsequently with protoplast buffer (0.8 M MgSO4·7H_2O and 0.2 M $C_6H_5Na_3O_7·2H_2O$,

pH=5.5). The washed mycelium was chopped into small pieces with a sterile razor blade followed by addition of 3 mL lysing buffer (200 mg VinoTaste Pro lysing enzyme (Novozymes; Franklinton, NC), 1 M sorbitol, 50 mM sodium citrate, pH=5.8) and 17 ml protoplast buffer in a 50-ml falcon tube. The mixture was incubated at 28°C with gentle agitation for 3 h. The resultant solution containing protoplast and debris was passed through four-layers of cheesecloth in a funnel and collected in a 50-ml falcon tube. A solution of 0.6 M KCl in 30 ml was poured over the cheesecloth and collected in the falcon tube. After centrifugation at 3,000 × g for 10 min at 4°C, the protoplast pellet was washed twice in 10 ml STC buffer (1 M sorbitol; 50 mM Tris, pH 8; 50 mM $CaCl_2 \cdot 2H_2O$). Protoplasts were resuspended in the mixture containing 500 µl of protoplast solution, 6.25 µl of dimethyl sulfoxide, and 125 µl of polyethylene glycol (PEG) solution (40% [wt/vol] PEG 8000; 0.6 M KCl; 50 mM Tris, pH 8; 50 mM $CaCl_2$). Protoplasts were transformed immediately or were stored at -70°C until use.

For transformation of *S. sclerotiorum*, 4 µg of the plasmid construct (~10 µl) was added to 500 µl protoplast-containing solution and the mixture was incubated on ice for 60 min. Then, 1 ml PEG solution was supplemented to the mixture. After incubation at room temperature for 20 min, the mixture was pelleted by centrifugation at 2,500 × g for 10 min at 4°C and resuspended in 200 µl STC buffer. The suspension was mixed with 10 ml regeneration medium (per liter: 239.6 g of sucrose, 15 g of agar, 0.5 g of yeast extract) that was autoclaved and cooled to approximately 45°C and was immediately poured in plates. After incubation at 25°C for 24 h, 15 ml regeneration medium containing 100 µg ml^{-1} of hygromycin B (Sigma-Aldrich; St. Louis, MO) was poured on top of the plates and the plates were incubated at 25°C for 4-5 days. Single mycelia germinating on the surface plates were picked and transferred to potato dextrose agar

(PDA) plates containing 100 µg ml^{-1} of hygromycin B for selection of the vector-encoded resistance.

5.5.3 *In vitro* fungicide sensitivity assay

Agar plugs from the margins of 3-day-old cultures grown on PDA plates were inoculated onto PDA plates amended with SDHI fungicides at the following concentrations (boscalid 20 µg ml^{-1}, fluopyram 20 µg ml^{-1} or fluxapyroxad 40 µg ml^{-1}, pyraziflumid 1 µg ml^{-1}, pydiflumetofen 1 µg ml^{-1}, or inpyrfluxam 4.25 µg ml^{-1}).

An unamended PDA plate with acetone, the solvent used for the fungicide stock solutions, was inoculated as the control. The inoculated plates were incubated in complete darkness at 25°C without shaking. Mycelia growth in radius in PDA plates with or without the fungicide was measured at 48 h post inoculation. Relative growth was calculated as the ratio of the growth in the fungicide-containing plate to that in the fungicide-free plate. Results represent the means of three biological replications, and error bars are the standard error of the mean. Statistical analyses were performed using JMP Pro 14 software (SAS Institute Inc.; Cary, NC). Images of *S. sclerotiorum growth* in the fungicide-containing plates were collected 48 h post inoculation. For *S. sclerotiorum strains growing* in the fungicide-free plates, images were taken 24 h post inoculation before different colonies started to overlap in growth.

APPENDIX

Table A.1. Bacteria strains or plasmids used in this CHAPTER 2

	Strain or plasmid	Genotype	Reference
Strains	Ea1189	Wild type	(Yu *et al.*)
	Ea1189*ΔrprA*	*rprA* deletion mutant,Cm^R	(Zeng et al., 2013)
	Ea1189*ΔrcsB*	*rcsB* deletion mutant,Cm^R	(Wang et al., 2009)
Plasmids	pBBR1MCS5	Broad-host-range cloning vector, Gm^R	(Kovach *et al.*, 1995)
	pJP-*rprA*	A region spanning the *rprA* gene and its corresponding native promoter in pBBR1MCS-5; Gm^R	This study
	p*rcsB*	A region spanning the *rcsBD* operon along with its native promoter region in pBBR1MCS5; Gm^R	This study
	p*rcsB*-D56E	p*rcsB* with an allele change resulting in the amino acid substitution of aspartic acid to glutamic acid at codon 56 in RcsB	This study
	p*rcsB*-K154Q	p*rcsB* with an allele change resulting in the amino acid substitution of lysine to glutamine at codon 154 in RcsB	This study
	pHM-*tac*	IPTG-inducible sRNA overexpression vector, Ap^R	(Park *et al.*, 2013)
	pOE-*rprA*	pHM-*tac*::*rprA*; overexpression vector; Ap^R	This study
	pPROBE-NT	Broad-host-range promoter-probe vector; Km^R	(Miller et al., 2000)
	pPROBE-*hrpS*	pPROBE-NT::*hrpS*; native promoter of *hrpS* in pPROBE-NT; Km^R	This study
	pPROBE-*hrpL*	pPROBE-NT::*hrpL*; native promoter of *hrpL* in pPROBE-NT; Km^R	This study
	pPROBE-*hrpA*	pPROBE-NT::*hrpA*; native promoter of *hrpA* in pPROBE-NT; Km^R	This study
	pPROBE-*dspE*	pPROBE-NT::*dspE*; native promoter of *dspE* in pPROBE-NT; Km^R	This study
	pPROBE-*amsG*	pPROBE-NT::*amsG*; native promoter of *amsG* in pPROBE-NT; Km^R	This study
	pPROBE-*lsc*	pPROBE-NT::*lsc*; native promoter of *lsc* in pPROBE-NT; Km^R	This study
	pxg-20	Broad-host-range translational fusion vector; Cm^R	(Urban & Vogel, 2007)
	pxg-20:*hrpS129*	5' UTR (129 nt) of *hrpS* and 90 nt into the coding region of *hrpS* in pxg-20; Cm^R	This study
	pxg-20:*hrpS227*	5' UTR (227 nt) of *hrpS* and 90 nt into the coding region of *hrpS* in pxg-20; Cm^R	This study

Table A.2. Oligonucleotide primers used in this CHAPTER 2

Primer name	Sequence (5'-3')	Purpose
com_rprAF	TAGGAATTCGCAATAATCTGGCTTTACTGGA	Primers used for rprA complementation
com_rprAR	ATATCTAGATCGGTTCACCGATCGTCC	
com_RcsBD_F	CCCGACTGGAAAGCGGGCAGTGCTAGCACAATTCACAAGGTTGG	Primer used for rcsB complementation
com_RcsBD_R	GTTGCGTCGCGGTGCATGGCTCCTAATGAACTGCCGCTACT	
backbone_pBBR1MCS5_F	CACTGCCCGCTTTCCAGTCGGG	
backbone_pBBR1MCS5_R	CCATGCACCGCGACGCAAC	
RcsB_D56E_F	CCAGGCATCGAAAGCTCGGTGACCAGCAC	Primers used for site-directed mutagenesis of prcsB
RcsB_D56E_R	GTGCTGGTCACCGAGCTTTCGATGCCTGG	
RcsB_K154Q_F	GCGCAGAACTTCGCTCTCCTGCGGTGACAAACGCTTATC	
RcsB_K154Q_R	GATAAGCGTTTGTCACCGCAGGAGAGCGAAGTTCTGCGC	
hrpS_tsc_F	CGACCTGAATGGAAGCCGGCAGATTGTCTTTGCCGAGTACA	Primers used for transcriptional fusion constructions
hrpS_tsc_R	GAGCTCGGTACCCGGGGATCCTCAAAAAATTACCCCTGCCCTATC	
tsc_hrpL_F	CGACCTGAATGGAAGCCGGCTAAACGCGCATGCTGCGGAT	
tsc_hrpL_R	GAGCTCGGTACCCGGGGATCCTCGGCTTGCTCCGTTACTAAATCA	
tsc_dspE_F	CGACCTGAATGGAAGCCGGCCTGACTGTCAGACTGCGGAGTGG	
tsc_dspE_R	GAGCTCGGTACCCGGGGATCCTCGACCCGTTGCCCCCACCCTCT	
tsc_hrpA_F	CGACCTGAATGGAAGCCGGCCTGGTGAAGGCGCACCGGGAT	
tsc_hrpA_R	GAGCTCGGTACCCGGGGATCCTCATTAATCTCTCCAATTATTGAGGTTG TGTTCC	
tsc_lsc_F	CGACCTGAATGGAAGCCGGCAAGTGCACCTCCGCAAGGT	
tsc_lsc_R	GAGCTCGGTACCCGGGGATCCTC AAATATCCTCACAGGTTATTTCG	
backbone_pPROBE-NT_F	GAGGATCCCCGGGTACCGAGCTC	
backbone_pPROBE-NT_R	GCCGGCTTCCATTCAGGTCG	
tsc_amsG_F	CGACCTGAATGGAAGCCGGCCCTTAATGAGATGGTTGATAAATCCAT	
tsc_amsG_R	GAGCTCGGTACCCGGGGATCCTCAATTAGCTCTTAATTTTATCTCAGG	
tln_dspE_F	GAGATTGACATCCCTATCAGTGATAGAGATACTGAGCACAAAAATATC TAATGTTTACGGCAGAGG	Primers used for translational fusion constructs
tln_dspE_R	AGTTCTTCTCCTTTGCTCATGAATTCGCCAGAACCCTGCTGTAAGGCAA CACC	
tln_hrpS129_F	GAGATTGACATCCCTATCAGTGATAGAGATACTGAGCACACAGCGTAA ACTCAGAGTAAATA	
tln_hrpS227_F	GAGATTGACATCCCTATCAGTGATAGAGATACTGAGCACAATGTAGGG TAATCCCTACATTGC	
tln_hrpS_R	AGTTCTTCTCCTTTGCTCATGAATTCGCCAGAACCGATATCGATGGGTT GTTCTTCTGT	
backbone_pxg20_F	GAAGGTTCTGGCGAATTCATGAGCAAAGGAGAAGAACT	
backbone_pxg20_R	TGTGCTCAGTATCTCTATCACTGATAGGGATGTCAATCTC	
NptII-gfp-rprA-mCherry_F	GTTGGATCCGCAATAATCTGGCTTTACTG	Primers used for generating pNptII-gfp-rprA-mCherry
NptII-gfp-rprA-mCherry_R	GGTGAGCTCGTAACCATAGTATGAAAAGGTG	

Table A.3. List of strains generated and used in CHAPTER 4

Strain or plasmid		Genotype	Reference
Strains	Ea1189	Wild type	(Edmunds et al. 2013)
	Ea1189Δ*atpB*	*atpB* deletion mutant	This study
	Ea1189Δ*atpBC*	Deletion of the chromosomal region that spans the *atpB*, *atpE*, *atpF*, *atpH*, *atpA*, *atpG*, *atpD*, and *atpC* genes	This study
Plasmids	pKD3	Contains FRT-flanked Cm^r cassette sites; R6K *ori*; Cm^r	(Datsenko and Wanner 2000)
	pKD46	Contains lambda Red recombinase induced by L-Arabinose; R101 *ori*; Ap^r	(Datsenko and Wanner 2000)
	pEVS143	Broad-host-range cloning vector; IPTG inducible Cm^r; pES213 *ori*; Km^r	(Dunn et al. 2006)
	pOE-*hok*	pEVS143 cmR::*hok*; overexpression vector; Km^r	(Peng et al. 2019)
	pBAD33	Broad-host-range cloning vector; arabinose inducible Cm^r; pACYC18 *ori*	(Guzman et al. 1995)
	pBAD33-*pspA*	pBAD33 cmR::*pspA*; overexpression vector; Cm^r	This study
	pPROBE-NT	Broad-host-range promoter-probe vector; pBBR1 *ori*; Km^r	(Miller et al. 2000)
	pPROBE-*pspA*	pPROBE-NT::*pspA*; native promoter of *pspA* in pPROBE-NT; Km^r	This study

Table A.4. List of oligonucleotide primers used in CHAPTER 4

Primer Name	Sequence (5'-3')	Reference
Primers used for making knockout mutants		
atpBC_F	ATGGCTGCAGGAGAAATCTCTACGCCGCAAGAGTACATAGG TCATCATCTGTGTAGGCTGGAGCTGCTTC	This study
atpBC_R	TTACATCGCGTTTTTGGTCAACTCGATCACGCGCAGTTTGGC GATCGCTTCATATGAATATCCTCCTTA	This study
atpB_R	TCAATGTTCTTCAGATGCCATCGACAGATAGACAATCGTTAA GACCATGACATATGAATATCCTCCTTA	This study
Primers used for the overexpression construct of *pspA*		
pBAD_FC_F	GGCTGTTTTGGCGGATGAGA	This study
pBAD_FC_R	AATTCGCTAGCCCAAAAAAACGG	This study
pspA_FC_F	CCGTTTTTTTGGGCTAGCGAATTATGGGTATTTTTTCACGTTT TGCCG	This study
pspA_FC_R	TCTCATCCGCCAAAACAGCCTTATTCACCGATACGCCGGTT	This study
Primers used for confirming knockout of genes		
atpBC_CF	CCGGCTGTAATTAACAACAAAG	This study
atpBC_CR	TTTCCTGACTGGCCTTCT	This study
atpB_CR	CCATGTACAGCAGATCCATATT	This study
Primers used for the transcriptional fusion construct of *pspA*		
pspA_tsc_F	CGACCTGAATGGAAGCCGGCGCCAGTTCGTCGAGAAACAAC	This study
pspA_tsc_R	GAGCTCGGTACCCGGGGATCCTCAATCAAATTCCTCATCAGT CTGG	This study
pPROBE-NT_tsc_F	GAGGATCCCCGGGTACCGAGCTC	(Peng et al. 2019)
pPROBE-NT_tsc_R	GCCGGCTTCCATTCAGGTCG	(Peng et al. 2019)
Primers used for qRT-PCR		
qhok_F	TGGTGCGTACTTATAGTGTGTG	This study
qhok_R	CCGGATTCGTAAGCCATGAA	This study
qpspA_F	GACCTGATTGCTGCTTTGC	This study
qpspA_R	GGTTTCAGCCAGTTTACTTTCC	This study
qatpG_F	GTCGGCTATCTGGTCGTATCT	This study
qatpG_R	GCCTTTATCAGCCCAGGATTT	This study
qkatA_F	CGCGACTGGGTGTTAACTATAA	This study
qkatA_R	TGGATCAGAGGCAAGATCAATAC	This study
qhrpA_F	AGCACTTCAGCATCCAAGAC	This study
qhrpA_R	CGAGTTCTGCGTATCCATCTTC	This study

Table A.5. Relationship between *SdhB* or *SdhC* mutations and SDHI fungicide resistance examined through correlative analyses of field isolates or functional genetic characterization

Organism	Mutation	Method	SDHI fungicide resistance			References
			Boscalid	Fluopyram	Fluxapyroxad	
Botrytis cinerea	*SdhB* H272R	Correlative	R	S	S	(Fernández-Ortuño *et al.*, 2017)
		Functional	R	S	n.a	(Lalève *et al.*, 2014)
		Correlative	R	n.a	n.a	(Fernández-Ortuño *et al.*, 2012; Veloukas *et al.*, 2011; Yin *et al.*, 2011)
		Correlative	R	S	n.a	(Amiri *et al.*, 2020)
	SdhB P225F	Functional	R	R	n.a	(Lalève *et al.*, 2014)
		Functional	R	n.a	n.a	(De Miccolis Angelini *et al.*, 2010)
Blumeriella jaapii	*SdhB* H260R	Correlative	R	S	S	(Outwater *et al.*, 2019)
	SdhB I262V	Correlative	S	R	R	(Peng *et al.*, unpublished)
	SdhC S84L	Correlative	S	R	S	
	SdhC N86S	Correlative	R	R	R	
Clarireedia homoeocarpa	*SdhB* H267Y	Functional	R	S	S	(Popko *et al.*, 2018)
	SdhC G91R	Functional	R	S	R	
	SdhB H267R	Functional	R	S	S	(Lee et al. 2020)
	SdhC G150R	Functional	R	R	R	
Monilinia fructicola	*SdhB* H268R	n.a.	n.a.	n.a.	n.a.	This study

Table A.6. Strains or plasmids used in CHAPTER 5

Strain or plasmids	Relevant characteristics	Reference
Sclerotinia sclerotiorum scl02-05	Wild type strain	(Sang *et al.*, 2019)
pYHN3-ptrpC	Overexpression plasmid	(Sang et al. 2018)
pProm-*SdhB*	Plasmid containing the upstream (1500 bp) of *S. sclerotiorum SdhB*	This study
pProm-*SdhC*	Plasmid containing the upstream (1500 bp) of *S. sclerotiorum SdhC*	This study
pProm-*SdhB*-Bci-WT	Plasmid for *B. cinerea* wild type *SdhB* expression	This study
pProm-*SdhB*-Bci-H272R	Plasmid for *B. cinerea SdhB*-H272R expression	This study
pProm-*SdhB*-Bci-P225L	Plasmid for *B. cinerea SdhB*-P225L expression	This study
pProm-*SdhB*-Bja-WT	Plasmid for *B. jaapii* wild type *SdhB* expression	This study
pProm-*SdhB*-Bja-H260R	Plasmid for *B. jaapii SdhB*-H260R expression	This study
pProm-*SdhB*-Bja-I262V	Plasmid for *B. jaapii SdhB*-I262V expression	This study
pProm-*SdhC*-Bja-WT	Plasmid for *B. jaapii* wild type *SdhC* expression	This study
pProm-*SdhC*-Bja-S84L	Plasmid for *B. jaapii SdhC*-S84L expression	This study
pProm-*SdhC*-Bja-N86S	Plasmid for *B. jaapii SdhC*-N86S expression	This study
pProm-*SdhB*-Sho-WT	Plasmid for *C. homoeocarpa* wild type *SdhB* expression	This study
pProm-*SdhB*-Sho-H267Y	Plasmid for *C. homoeocarpa SdhB*-H267R expression	This study
pProm-*SdhC*-Sho-WT	Plasmid for *C. homoeocarpa* wild type *SdhC* expression	This study
pProm-*SdhC*-Sho-G91R	Plasmid for *C. homoeocarpa SdhC*-G91R expression	This study
pProm-*SdhB*-Mfr-WT	Plasmid for *M. fructicola* wild type *SdhB* expression	This study
pProm-*SdhB*-Mfr-H268R	Plasmid for *M. fructicola SdhB*-H268R expression	This study

Table A.7. Draft genome sequence resource for *Blumeriella jaapii*, the cherry leaf spot pathogen

Genome Size (bp)	47,419,685
GC content (%)	43.0%
Contigs	95
N50 (bp)	1,484,584
Coverage	56×
BUSCO[a]	98.6%
Protein-encoding genes	7,898
NCBI-nr	6,845
Swiss-Prot	2,579
KEGG[b]	6,822
KOG[c]	1,787
TCDB[d]	355
GO[e]	4,841
tRNA[f]	124
rRNA[g]	32
Transposable elements[h]	11,764

REFERENCES

REFERENCES

Aakre, C. D., Phung, T. N., Huang, D., and Laub, M. T. 2013. A bacterial toxin inhibits DNA replication elongation through a direct interaction with the β sliding clamp. Molecular cell 52:617-628.

Ackrell, B. A. 2000. Progress in understanding structure-function relationships in respiratory chain complex II. FEBS letters 466:1-5.

Allison, K. R., Brynildsen, M. P., and Collins, J. J. 2011. Metabolite-enabled eradication of bacterial persisters by aminoglycosides. Nature 473:216-220.

An, S., Wu, J., and Zhang, L. H. 2010. Modulation of *Pseudomonas aeruginosa* biofilm dispersal by a cyclic-Di-GMP phosphodiesterase with a putative hypoxia-sensing domain. Applied and environmental microbiology 76:8160-8173.

Ancona, V., Chatnaparat, T., and Zhao, Y. 2015. Conserved aspartate and lysine residues of RcsB are required for amylovoran biosynthesis, virulence, and DNA binding in *Erwinia amylovora*. Molecular genetics and genomics 290:1265-1276.

and, M. B. M., and Bassler, B. L. 2001. Quorum Sensing in Bacteria. Annual review of microbiology 55:165-199.

Anders, S., Pyl, P. T., and Huber, W. 2015. HTSeq--a Python framework to work with high-throughput sequencing data. Bioinformatics (Oxford, England) 31:166-169.

Andreassen, P. R., Pettersen, J. S., Szczerba, M., Valentin-Hansen, P., Møller-Jensen, J., and Jørgensen, M. G. 2018. sRNA-dependent control of curli biosynthesis in *Escherichia coli*: McaS directs endonucleolytic cleavage of *csgD* mRNA. Nucleic acids research 46:6746-6760.

Anes, J., Sivasankaran, S. K., Muthappa, D. M., Fanning, S., and Srikumar, S. 2019. Exposure to Sub-inhibitory Concentrations of the Chemosensitizer 1-(1-Naphthylmethyl)-Piperazine Creates Membrane Destabilization in Multi-Drug Resistant Klebsiella pneumoniae. Frontiers in microbiology 10:92.

Arechaga, I., Miroux, B., Runswick, M. J., and Walker, J. E. 2003. Over-expression of *Escherichia coli* $F_1F_{(o)}$-ATPase subunit a is inhibited by instability of the *uncB* gene transcript. FEBS letters 547:97-100.

Armstrong, R. M., Adams, K. L., Zilisch, J. E., Bretl, D. J., Sato, H., Anderson, D. M., and Zahrt, T. C. 2016. Rv2744c Is a PspA Ortholog That Regulates Lipid Droplet Homeostasis and Nonreplicating Persistence in *Mycobacterium tuberculosis*. Journal of bacteriology 198:1645-1661.

Avenot, H., Morgan, D. P., and Michailides, T. J. 2008a. Resistance to pyraclostrobin, boscalid and multiple resistance to Pristine (pyraclostrobin + boscalid) fungicide in *Alternaria alternata* causing alternaria late blight of pistachios in California. Plant Pathology 57:135-140.

Avenot, H. F., and Michailides, T. J. 2010. Progress in understanding molecular mechanisms and evolution of resistance to succinate dehydrogenase inhibiting (SDHI) fungicides in phytopathogenic fungi. Crop Protection 29:643-651.

Avenot, H. F., Sellam, A., Karaoglanidis, G., and Michailides, T. J. 2008b. Characterization of mutations in the iron-sulphur subunit of succinate dehydrogenase correlating with Boscalid resistance in Alternaria alternata from California pistachio. Phytopathology 98:736-742.

Baharoglu, Z., and Mazel, D. 2014. SOS, the formidable strategy of bacteria against aggressions. FEMS microbiology reviews 38:1126-1145.

Bak, G., Lee, J., Suk, S., Kim, D., Young Lee, J., Kim, K.-s., Choi, B.-S., and Lee, Y. 2015. Identification of novel sRNAs involved in biofilm formation, motility and fimbriae formation in *Escherichia coli*. Scientific reports 5:15287.

Bardill, J. P., Zhao, X., and Hammer, B. K. 2011. The *Vibrio cholerae* quorum sensing response is mediated by Hfq-dependent sRNA/mRNA base pairing interactions. Molecular microbiology 80:1381-1394.

Barraud, N., Hassett, D. J., Hwang, S.-H., Rice, S. A., Kjelleberg, S., and Webb, J. S. 2006. Involvement of Nitric Oxide in Biofilm Dispersal of *Pseudomonas aeruginosa*. Journal of bacteriology 188:7344-7353.

Barraud, N., Schleheck, D., Klebensberger, J., Webb, J. S., Hassett, D. J., Rice, S. A., and Kjelleberg, S. 2009. Nitric oxide signaling in *Pseudomonas aeruginosa* biofilms mediates phosphodiesterase activity, decreased cyclic di-GMP levels, and enhanced dispersal. Journal of bacteriology 191:7333-7342.

Bayot, R. G., and Ries, S. M. 1986. Role of motility in apple blossom infection by *Erwinia amylovora* and studies of fire blight control with attractant and repellent compounds. Phytopathology 76:441-445.

Becker, L. A., Bang, I. S., Crouch, M. L., and Fang, F. C. 2005. Compensatory role of PspA, a member of the phage shock protein operon, in *rpoE* mutant *Salmonella enterica* serovar Typhimurium. Molecular microbiology 56:1004-1016.

Bellemann, P., and Geider, K. 1992. Localization of transposon insertions in pathogenicity mutants of *Erwinia amylovora* and their biochemical characterization. Microbiology (Reading, England) 138:931-940.

Bellemann, P., Bereswill, S., Berger, S., and Geider, K. 1994. Visualization of capsule formation by *Erwinia amylovora* and assays to determine amylovoran synthesis. International journal of biological macromolecules 16:290-296.

Berghoff, B. A., and Wagner, E. G. H. 2017. RNA-based regulation in type I toxin-antitoxin systems and its implication for bacterial persistence. Current genetics 63:1011-1016.

Bernard, P., Kézdy, K. E., Van Melderen, L., Steyaert, J., Wyns, L., Pato, M. L., Higgins, P. N., and Couturier, M. 1993. The F plasmid CcdB protein induces efficient ATP-dependent DNA cleavage by gyrase. Journal of molecular biology 234:534-541.

Black, D. S., Kelly, A. J., Mardis, M. J., and Moyed, H. S. 1991. Structure and organization of hip, an operon that affects lethality due to inhibition of peptidoglycan or DNA synthesis. Journal of bacteriology 173:5732-5739.

Bogdanove, A. J., Bauer, D. W., and Beer, S. V. 1998. *Erwinia amylovora* secretes DspE, a pathogenicity factor and functional AvrE homolog, through the Hrp (type III secretion) pathway. Journal of bacteriology 180:2244-2247.

Bogs, J., Bruchmüller, I., Erbar, C., and Geider, K. 1998. Colonization of host plants by the fire blight pathogen *Erwinia amylovora* marked with genes for bioluminescence and fluorescence. Phytopathology 88:416-421.

Bokinsky, G., Baidoo, E. E., Akella, S., Burd, H., Weaver, D., Alonso-Gutierrez, J., García-Martín, H., Lee, T. S., and Keasling, J. D. 2013. HipA-triggered growth arrest and β-lactam tolerance in Escherichia coli are mediated by RelA-dependent ppGpp synthesis. Journal of bacteriology 195:3173-3182.

Bolger, A. M., Lohse, M., and Usadel, B. 2014. Trimmomatic: a flexible trimmer for Illumina sequence data. Bioinformatics (Oxford, England) 30:2114-2120.

Brantl, S. 2012. Bacterial type I toxin-antitoxin systems. RNA biology 9:1488-1490.

Brauner, A., Fridman, O., Gefen, O., and Balaban, N. Q. 2016. Distinguishing between resistance, tolerance and persistence to antibiotic treatment. Nature Reviews Microbiology 14:320-330.

Brielle, R., Pinel-Marie, M. L., and Felden, B. 2016. Linking bacterial type I toxins with their actions. Current opinion in microbiology 30:114-121.

Brissette, J. L., Russel, M., Weiner, L., and Model, P. 1990. Phage shock protein, a stress protein of *Escherichia coli*. Proceedings of the National Academy of Sciences of the United States of America 87:862-866.

Brown, J. M., and Shaw, K. J. 2003. A novel family of *Escherichia coli* toxin-antitoxin gene pairs. Journal of bacteriology 185:6600-6608.

Bugert, P., and Geider, K. 1995. Molecular analysis of the ams operon required for exopolysaccharide synthesis of *Erwinia amylovora*. Molecular microbiology 15:917-933.

Cashel, M., and Gallant, J. 1969. Two Compounds implicated in the Function of the RC Gene of Escherichia coli. Nature 221:838-841.

Castiblanco, L. F., and Sundin, G. W. 2018. Cellulose production, activated by cyclic di-GMP through BcsA and BcsZ, is a virulence factor and an essential determinant of the three-dimensional architectures of biofilms formed by *Erwinia amylovora* Ea1189. Molecular plant pathology 19:90-103.

Castro-Roa, D., Garcia-Pino, A., De Gieter, S., van Nuland, N. A. J., Loris, R., and Zenkin, N. 2013. The Fic protein Doc uses an inverted substrate to phosphorylate and inactivate EF-Tu. Nature chemical biology 9:811-817.

Cecchini, G. 2003. Function and structure of complex II of the respiratory chain. Annual review of biochemistry 72:77-109.

Chaignon, P., Sadovskaya, I., Ragunah, C., Ramasubbu, N., Kaplan, J. B., and Jabbouri, S. 2007. Susceptibility of staphylococcal biofilms to enzymatic treatments depends on their chemical composition. Applied microbiology and biotechnology 75:125-132.

Chambers, J. R., and Sauer, K. 2013. Small RNAs and their role in biofilm formation. Trends in Microbiology 21:39-49.

Chatterjee, A. 2001. Fire Blight: The Disease and its Causative Agent, *Erwinia amylovora*. Edited by J.L. Vanneste. European Journal of Plant Pathology 107:569-569.

Chen, H., Venkat, S., Wilson, J., McGuire, P., Chang, A. L., Gan, Q., and Fan, C. 2018. Genome-Wide Quantification of the Effect of Gene Overexpression on *Escherichia coli* Growth. Genes 9.

Cheng, H. Y., Soo, V. W., Islam, S., McAnulty, M. J., Benedik, M. J., and Wood, T. K. 2014. Toxin GhoT of the GhoT/GhoS toxin/antitoxin system damages the cell membrane to reduce adenosine triphosphate and to reduce growth under stress. Environmental microbiology 16:1741-1754.

Cherny, K. E., and Sauer, K. 2019. *Pseudomonas aeruginosa* Requires the DNA-Specific Endonuclease EndA To Degrade Extracellular Genomic DNA To Disperse from the Biofilm. Journal of bacteriology 201:e00059-00019.

Christensen-Dalsgaard, M., Jørgensen, M. G., and Gerdes, K. 2010. Three new RelE-homologous mRNA interferases of *Escherichia col*i differentially induced by environmental stresses. Molecular microbiology 75:333-348.

Christensen, S. K., Mikkelsen, M., Pedersen, K., and Gerdes, K. 2001. RelE, a global inhibitor of translation, is activated during nutritional stress. Proceedings of the National Academy of Sciences of the United States of America 98:14328-14333.

Christensen, S. K., Maenhaut-Michel, G., Mine, N., Gottesman, S., Gerdes, K., and Van Melderen, L. 2004. Overproduction of the Lon protease triggers inhibition of translation in *Escherichia coli*: involvement of the *yefM-yoeB* toxin-antitoxin system. Molecular microbiology 51:1705-1717.

Chua, S. L., Liu, Y., Yam, J. K. H., Chen, Y., Vejborg, R. M., Tan, B. G. C., Kjelleberg, S., Tolker-Nielsen, T., Givskov, M., and Yang, L. 2014. Dispersed cells represent a distinct stage in the transition from bacterial biofilm to planktonic lifestyles. Nature Communications 5:4462.

Chukwudi, C. U., and Good, L. 2020. The *hok/sok* toxin/antitoxin locus enhances bacterial susceptibility to doxycycline. bioRxiv:2020.2002.2013.948752.

Chung, C. T., Niemela, S. L., and Miller, R. H. 1989. One-step preparation of competent *Escherichia coli*: transformation and storage of bacterial cells in the same solution. Proceedings of the National Academy of Sciences of the United States of America 86:2172-2175.

Chung, M.-C., Dean, S., Marakasova, E. S., Nwabueze, A. O., and van Hoek, M. L. 2014. Chitinases Are Negative Regulators of Francisella novicida Biofilms. PloS one 9:e93119.

Clementi, E. A., Marks, L. R., Roche-Håkansson, H., and Håkansson, A. P. 2014. Monitoring Changes in Membrane Polarity, Membrane Integrity, and Intracellular Ion Concentrations in *Streptococcus pneumoniae* Using Fluorescent Dyes. JoVE:e51008.

Conlon, B. P., Rowe, S. E., Gandt, A. B., Nuxoll, A. S., Donegan, N. P., Zalis, E. A., Clair, G., Adkins, J. N., Cheung, A. L., and Lewis, K. 2016. Persister formation in *Staphylococcus aureus* is associated with ATP depletion. Nature microbiology 1:16051.

Costello, S. M., Plummer, A. M., Fleming, P. J., and Fleming, K. G. 2016. Dynamic periplasmic chaperone reservoir facilitates biogenesis of outer membrane proteins. Proceedings of the National Academy of Sciences 113:E4794-E4800.

Costerton, J. W., Lewandowski, Z., Caldwell, D. E., Korber, D. R., and Lappin-Scott, H. M. 1995. Microbial biofilms. Annual review of microbiology 49:711-745.

Cui, Z., Yuan, X., Yang, C. H., Huntley, R. B., Sun, W., Wang, J., Sundin, G. W., and Zeng, Q. 2018. Development of a method to monitor gene expression in single bacterial cells during the interaction with plants and use to study the expression of the type III secretion system in single cells of *Dickeya dadantii* in potato. Frontiers in microbiology 9:1429.

Dalebroux, Z. D., Svensson, S. L., Gaynor, E. C., and Swanson, M. S. 2010. ppGpp conjures bacterial virulence. Microbiology and molecular biology reviews : MMBR 74:171-199.

Danhorn, T., and Fuqua, C. 2007. Biofilm Formation by Plant-Associated Bacteria. Annual review of microbiology 61:401-422.

Darwin, A. J. 2005. The phage-shock-protein response. Molecular microbiology 57:621-628.

Datsenko, K. A., and Wanner, B. L. 2000. One-step inactivation of chromosomal genes in *Escherichia coli* K-12 using PCR products. Proceedings of the National Academy of Sciences of the United States of America 97:6640-6645.

Davies, D. 2003. Understanding biofilm resistance to antibacterial agents. Nature Reviews Drug Discovery 2:114-122.

Davies, D. G., and Marques, C. N. 2009a. A fatty acid messenger is responsible for inducing dispersion in microbial biofilms. Journal of bacteriology 191:1393-1403.

Davies, D. G., and Marques, C. N. H. 2009b. A Fatty Acid Messenger Is Responsible for Inducing Dispersion in Microbial Biofilms. Journal of bacteriology 191:1393-1403.

Dean, R. E., Ireland, P. M., Jordan, J. E., Titball, R. W., and Oyston, P. C. F. 2009. RelA regulates virulence and intracellular survival of *Francisella novicida*. Microbiology (Reading, England) 155:4104-4113.

Dean, S. N., Chung, M. C., and van Hoek, M. L. 2015. Burkholderia Diffusible Signal Factor Signals to *Francisella novicida* To Disperse Biofilm and Increase Siderophore Production. Applied and environmental microbiology 81:7057-7066.

Deising, H. B., Reimann, S., and Pascholati, S. F. 2008. Mechanisms and significance of fungicide resistance. Brazilian journal of microbiology : [publication of the Brazilian Society for Microbiology] 39:286-295.

Dörr, T., Vulić, M., and Lewis, K. 2010. Ciprofloxacin Causes Persister Formation by Inducing the TisB toxin in *Escherichia coli*. PLoS biology 8:e1000317.

Dow, J. M., Crossman, L., Findlay, K., He, Y. Q., Feng, J. X., and Tang, J. L. 2003. Biofilm dispersal in *Xanthomonas campestris* is controlled by cell-cell signaling and is required for full virulence to plants. Proceedings of the National Academy of Sciences of the United States of America 100:10995-11000.

Dunn, A. K., Millikan, D. S., Adin, D. M., Bose, J. L., and Stabb, E. V. 2006. New *rfp*- and pES213-derived tools for analyzing symbiotic *Vibrio fischeri* reveal patterns of infection and *lux* expression *in situ*. Applied and environmental microbiology 72:802-810.

Edelmann, D., and Berghoff, B. A. 2019. Type I toxin-dependent generation of superoxide affects the persister life cycle of *Escherichia coli*. Scientific reports 9:14256.

Edmunds, A. C., Castiblanco, L. F., Sundin, G. W., and Waters, C. M. 2013. Cyclic Di-GMP modulates the disease progression of *Erwinia amylovora*. Journal of bacteriology 195:2155-2165.

Fallico, V., Ross, R. P., Fitzgerald, G. F., and McAuliffe, O. 2011. Genetic response to bacteriophage infection in *Lactococcus lactis* reveals a four-strand approach involving induction of membrane stress proteins, D-alanylation of the cell wall, maintenance of proton motive force, and energy conservation. Journal of virology 85:12032-12042.

Faridani, O. R., Nikravesh, A., Pandey, D. P., Gerdes, K., and Good, L. 2006. Competitive inhibition of natural antisense Sok-RNA interactions activates Hok-mediated cell killing in *Escherichia coli*. Nucleic acids research 34:5915-5922.

Fazli, M., Almblad, H., Rybtke, M. L., Givskov, M., Eberl, L., and Tolker-Nielsen, T. 2014. Regulation of biofilm formation in *Pseudomonas* and *Burkholderia* species. Environmental microbiology 16:1961-1981.

Fernández De Henestrosa, A. R., Ogi, T., Aoyagi, S., Chafin, D., Hayes, J. J., Ohmori, H., and Woodgate, R. 2000. Identification of additional genes belonging to the LexA regulon in *Escherichia coli*. Molecular microbiology 35:1560-1572.

Fineran, P. C., Blower, T. R., Foulds, I. J., Humphreys, D. P., Lilley, K. S., and Salmond, G. P. C. 2009. The phage abortive infection system, ToxIN, functions as a protein–RNA toxin–antitoxin pair. Proceedings of the National Academy of Sciences 106:894.

Flemming, H.-C., and Wingender, J. 2010. The biofilm matrix. Nature Reviews Microbiology 8:623-633.

Flores-Kim, J., and Darwin, A. J. 2016. The Phage Shock Protein Response. Annual review of microbiology 70:83-101.

Fozo, E. M., Makarova, K. S., Shabalina, S. A., Yutin, N., Koonin, E. V., and Storz, G. 2010. Abundance of type I toxin-antitoxin systems in bacteria: searches for new candidates and discovery of novel families. Nucleic acids research 38:3743-3759.

Fraaije, B. A., Bayon, C., Atkins, S., Cools, H. J., Lucas, J. A., and Fraaije, M. W. 2012. Risk assessment studies on succinate dehydrogenase inhibitors, the new weapons in the battle to control Septoria leaf blotch in wheat. Molecular plant pathology 13:263-275.

Frac. 2020. FRAC code list 2020.https://www.frac.info/knowledge-database/downloads-teams/working-groups/sdhi-fungicides/recommendations-for-sdhi.

Gefen, O., and Balaban, N. Q. 2009. The importance of being persistent: heterogeneity of bacterial populations under antibiotic stress. FEMS microbiology reviews 33:704-717.

Geier, G., and Geider, K. 1993. Characterization and influence on virulence of the levansucrase gene from the fireblight pathogen *Erwinia amylovora*. Physiological and Molecular Plant Pathology 42:387-404.

Gerdes, K. 2016. Hypothesis: type I toxin-antitoxin genes enter the persistence field-a feedback mechanism explaining membrane homoeostasis. Philosophical transactions of the Royal Society of London. Series B, Biological sciences 371:20160189.

Gerdes, K., Nielsen, A., Thorsted, P., and Wagner, E. G. H. 1992. Mechanism of killer gene activation. Antisense RNA-dependent RNase III cleavage ensures rapid turn-over of the stable Hok, SrnB and PndA effector messenger RNAs. Journal of molecular biology 226:637-649.

Gerdes, K., Bech, F. W., Jørgensen, S. T., Løbner-Olesen, A., Rasmussen, P. B., Atlung, T., Boe, L., Karlstrom, O., Molin, S., and von Meyenburg, K. 1986. Mechanism of postsegregational killing by the *hok* gene product of the *parB* system of plasmid R1 and its homology with the *relF* gene product of the *E. coli relB* operon. The EMBO journal 5:2023-2029.

Germain, E., Castro-Roa, D., Zenkin, N., and Gerdes, K. 2013. Molecular Mechanism of Bacterial Persistence by HipA. Molecular cell 52:248-254.

Gill, J. J., Svircev, A. M., Smith, R., and Castle, A. J. 2003. Bacteriophages of *Erwinia amylovora*. Applied and environmental microbiology 69:2133-2138.

Gjermansen, M., Ragas, P., Sternberg, C., Molin, S., and Tolker-Nielsen, T. 2005. Characterization of starvation-induced dispersion in *Pseudomonas putida* biofilms. Environmental microbiology 7:894-906.

Glättli, A., Stammler, G., and Schlehuber, S. 2009. Mutations in the target proteins of succinate-dehydrogenase inhibitors (SDHI) and 14α-demethylase inhibitors (DMI) conferring changes in the sensitivity - structural insights from molecular modelling. Pages 670-681 Association Française de Protection des Plantes (AFPP), Alfortville.

Glättli, A., Grote, T., and Stammler, G. 2011. SDH-inhibitors: history, biological performance and molecular mode of action. Pages 159-169 Deutsche Phytomedizinische Gesellschaft e.V. Selbstverlag.

Goltermann, L., Good, L., and Bentin, T. 2013. Chaperonins fight aminoglycoside-induced protein misfolding and promote short-term tolerance in *Escherichia coli*. The Journal of biological chemistry 288:10483-10489.

Goodman, R. N., Huang, J. S., and Huang, P.-Y. 1974. Host-specific phytotoxic polysaccharide from apple tissue infected by *Erwinia amylovora*. Science (New York, N.Y.) 183:1081-1082.

Goodwine, J., Gil, J., Doiron, A., Valdes, J., Solis, M., Higa, A., Davis, S., and Sauer, K. 2019. Pyruvate-depleting conditions induce biofilm dispersion and enhance the efficacy of antibiotics in killing biofilms *in vitro* and *in vivo*. Scientific reports 9:3763.

Gross, M., Geier, G., Rudolph, K., and Geider, K. 1992. Levan and levansucrase synthesized by the fireblight pathogen *Erwinia amylovora*. Physiological and Molecular Plant Pathology 40:371-381.

Gurnev, P. A., Ortenberg, R., Dorr, T., Lewis, K., and Bezrukov, S. M. 2012a. Persister-promoting bacterial toxin TisB produces anion-selective pores in planar lipid bilayers. FEBS letters 586:2529-2534.

Gurnev, P. A., Ortenberg, R., Dörr, T., Lewis, K., and Bezrukov, S. M. 2012b. Persister-promoting bacterial toxin TisB produces anion-selective pores in planar lipid bilayers. FEBS letters 586:2529-2534.

Guzman, L. M., Belin, D., Carson, M. J., and Beckwith, J. 1995. Tight regulation, modulation, and high-level expression by vectors containing the arabinose pBAD promoter. Journal of bacteriology 177:4121-4130.

Hammer, B. K., and Bassler, B. L. 2009. Distinct Sensory Pathways in *Vibrio cholerae* El Tor and Classical Biotypes Modulate Cyclic Dimeric GMP Levels To Control Biofilm Formation. Journal of bacteriology 191:169-177.

Han, M. L., Zhu, Y., Creek, D. J., Lin, Y. W., Gutu, A. D., Hertzog, P., Purcell, T., Shen, H. H., Moskowitz, S. M., Velkov, T., and Li, J. 2019. Comparative Metabolomics and Transcriptomics Reveal Multiple Pathways Associated with Polymyxin Killing in *Pseudomonas aeruginosa*. mSystems 4.

Hansen, S., Lewis, K., and Vulić, M. 2008. Role of Global Regulators and Nucleotide Metabolism in Antibiotic Tolerance in *Escherichia coli*. Antimicrobial agents and chemotherapy 52:2718-2726.

Harms, A., Maisonneuve, E., and Gerdes, K. 2016. Mechanisms of bacterial persistence during stress and antibiotic exposure. Science (New York, N.Y.) 354:aaf4268.

Harms, A., Brodersen, D. E., Mitarai, N., and Gerdes, K. 2018. Toxins, Targets, and Triggers: An Overview of Toxin-Antitoxin Biology. Molecular cell 70:768-784.

Harms, A., Fino, C., Sørensen, M. A., Semsey, S., and Gerdes, K. 2017. Prophages and Growth Dynamics Confound Experimental Results with Antibiotic-Tolerant Persister Cells. mBio 8:e01964-01917.

Harrison, J. J., Wade, W. D., Akierman, S., Vacchi-Suzzi, C., Stremick, C. A., Turner, R. J., and Ceri, H. 2009. The chromosomal toxin gene *yafQ* is a determinant of multidrug tolerance for *Escherichia coli* growing in a biofilm. Antimicrobial agents and chemotherapy 53:2253-2258.

Hauryliuk, V., Atkinson, G. C., Murakami, K. S., Tenson, T., and Gerdes, K. 2015. Recent functional insights into the role of (p)ppGpp in bacterial physiology. Nature Reviews Microbiology 13:298-309.

Helaine, S., Cheverton, A. M., Watson, K. G., Faure, L. M., Matthews, S. A., and Holden, D. W. 2014. Internalization of Salmonella by macrophages induces formation of nonreplicating persisters. Science (New York, N.Y.) 343:204-208.

Hengge, R. 2009. Principles of c-di-GMP signalling in bacteria. Nature reviews. Microbiology 7:263-273.

Horsefield, R., Yankovskaya, V., Sexton, G., Whittingham, W., Shiomi, K., Omura, S., Byrne, B., Cecchini, G., and Iwata, S. 2006. Structural and computational analysis of the quinone-binding site of complex II (succinate-ubiquinone oxidoreductase): a mechanism of electron transfer and proton conduction during ubiquinone reduction. The Journal of biological chemistry 281:7309-7316.

Hu, L. I., Chi, B. K., Kuhn, M. L., Filippova, E. V., Walker-Peddakotla, A. J., Bäsell, K., Becher, D., Anderson, W. F., Antelmann, H., and Wolfe, A. J. 2013. Acetylation of the response regulator RcsB controls transcription from a small RNA promoter. Journal of bacteriology 195:4174-4186.

Huang, L.-s., Sun, G., Cobessi, D., Wang, A. C., Shen, J. T., Tung, E. Y., Anderson, V. E., and Berry, E. A. 2006. 3-Nitropropionic Acid Is a Suicide Inhibitor of Mitochondrial Respiration That, upon Oxidation by Complex II, Forms a Covalent Adduct with a Catalytic Base Arginine in the Active Site of the Enzyme. Journal of Biological Chemistry 281:5965-5972.

Huynh, T. V., Dahlbeck, D., and Staskawicz, B. J. 1989. Bacterial blight of soybean: regulation of a pathogen gene determining host cultivar specificity. Science (New York, N.Y.) 245:1374-1377.

Ishii, H., Miyamoto, T., Ushio, S., and Kakishima, M. 2011. Lack of cross-resistance to a novel succinate dehydrogenase inhibitor, fluopyram, in highly boscalid-resistant isolates of *Corynespora cassiicola* and *Podosphaera xanthii*. Pest management science 67:474-482.

Jackson, D. W., Suzuki, K., Oakford, L., Simecka, J. W., Hart, M. E., and Romeo, T. 2002. Biofilm formation and dispersal under the influence of the global regulator CsrA of *Escherichia coli*. Journal of bacteriology 184:290-301.

Jenal, U., and Malone, J. 2006. Mechanisms of Cyclic-di-GMP Signaling in Bacteria. Annual review of genetics 40:385-407.

Jiang, Y., Pogliano, J., Helinski, D. R., and Konieczny, I. 2002. ParE toxin encoded by the broad-host-range plasmid RK2 is an inhibitor of *Escherichia coli* gyrase. Molecular microbiology 44:971-979.

Joly, N., Engl, C., Jovanovic, G., Huvet, M., Toni, T., Sheng, X., Stumpf, M. P., and Buck, M. 2010. Managing membrane stress: the phage shock protein (Psp) response, from molecular mechanisms to physiology. FEMS microbiology reviews 34:797-827.

Jones, A. J., and Hirst, J. 2013. A spectrophotometric coupled enzyme assay to measure the activity of succinate dehydrogenase. Analytical biochemistry 442:19-23.

Jørgensen, M. G., Pandey, D. P., Jaskolska, M., and Gerdes, K. 2009. HicA of Escherichia coli Defines a Novel Family of Translation-Independent mRNA Interferases in Bacteria and Archaea. Journal of bacteriology 191:1191.

Jovanovic, G., Lloyd, L. J., Stumpf, M. P., Mayhew, A. J., and Buck, M. 2006. Induction and function of the phage shock protein extracytoplasmic stress response in *Escherichia coli*. The Journal of biological chemistry 281:21147-21161.

Kaplan, J. B. 2010. Biofilm dispersal: mechanisms, clinical implications, and potential therapeutic uses. Journal of dental research 89:205-218.

Kaplan, J. B., Ragunath, C., Ramasubbu, N., and Fine, D. H. 2003. Detachment of Actinobacillus actinomycetemcomitans biofilm cells by an endogenous beta-hexosaminidase activity. Journal of bacteriology 185:4693-4698.

Kaplan, J. B., Ragunath, C., Velliyagounder, K., Fine, D. H., and Ramasubbu, N. 2004. Enzymatic detachment of Staphylococcus epidermidis biofilms. Antimicrobial agents and chemotherapy 48:2633-2636.

Karatan, E., and Watnick, P. 2009. Signals, Regulatory Networks, and Materials That Build and Break Bacterial Biofilms. Microbiology and Molecular Biology Reviews 73:310-347.

Kawano, M., Aravind, L., and Storz, G. 2007. An antisense RNA controls synthesis of an SOS-induced toxin evolved from an antitoxin. Molecular microbiology 64:738-754.

Keren, I., Shah, D., Spoering, A., Kaldalu, N., and Lewis, K. 2004. Specialized persister cells and the mechanism of multidrug tolerance in *Escherichia coli*. Journal of bacteriology 186:8172-8180.

Kery, M. B., Feldman, M., Livny, J., and Tjaden, B. 2014. TargetRNA2: identifying targets of small regulatory RNAs in bacteria. Nucleic acids research 42:W124-129.

Kim, J.-S., and Wood, T. K. 2016. Persistent Persister Misperceptions. Frontiers in microbiology 7.

Kim, J. F., Wei, Z. M., and Beer, S. V. 1997. The hrpA and hrpC operons of *Erwinia amylovora* encode components of a type III pathway that secretes harpin. Journal of bacteriology 179:1690-1697.

Kim, Y., and Wood, T. K. 2010. Toxins Hha and CspD and small RNA regulator Hfq are involved in persister cell formation through MqsR in *Escherichia coli*. Biochemical and biophysical research communications 391:209-213.

Kleerebezem, M., Crielaard, W., and Tommassen, J. 1996. Involvement of stress protein PspA (phage shock protein A) of *Escherichia coli* in maintenance of the protonmotive force under stress conditions. The EMBO journal 15:162-171.

Kobayashi, R., Suzuki, T., and Yoshida, M. 2007. Escherichia coli phage-shock protein A (PspA) binds to membrane phospholipids and repairs proton leakage of the damaged membranes. Molecular microbiology 66:100-109.

Koczan, J. M., McGrath, M. J., Zhao, Y., and Sundin, G. W. 2009. Contribution of *Erwinia amylovora* exopolysaccharides amylovoran and levan to biofilm formation: implications in pathogenicity. Phytopathology 99:1237-1244.

Koczan, J. M., Lenneman, B. R., McGrath, M. J., and Sundin, G. W. 2011. Cell surface attachment structures contribute to biofilm formation and xylem colonization by *Erwinia amylovora*. Applied and environmental microbiology 77:7031-7039.

Koutsoudis, M. D., Tsaltas, D., Minogue, T. D., and von Bodman, S. B. 2006. Quorum-sensing regulation governs bacterial adhesion, biofilm development, and host colonization in *Pantoea stewartii* subspecies *stewartii*. Proceedings of the National Academy of Sciences 103:5983.

Kwan, B. W., Valenta, J. A., Benedik, M. J., and Wood, T. K. 2013. Arrested protein synthesis increases persister-like cell formation. Antimicrobial agents and chemotherapy 57:1468-1473.

Lalève, A., Gamet, S., Walker, A. S., Debieu, D., Toquin, V., and Fillinger, S. 2014. Site-directed mutagenesis of the P225, N230 and H272 residues of succinate dehydrogenase subunit B from *Botrytis cinerea* highlights different roles in enzyme activity and inhibitor binding. Environmental microbiology 16:2253-2266.

Langmead, B., and Salzberg, S. L. 2012. Fast gapped-read alignment with Bowtie 2. Nature methods 9:357-359.

Lee, J. H., and Zhao, Y. 2018. Integration of multiple stimuli-sensing systems to regulate HrpS and type III secretion system in *Erwinia amylovora*. Molecular Genetics and Genomics 293:187-196.

Lee, J. H., Sundin, G. W., and Zhao, Y. 2016. Identification of the HrpS binding site in the *hrpL* promoter and effect of the RpoN binding site of HrpS on the regulation of the type III secretion system in *Erwinia amylovora*. Molecular plant pathology 17:691-702.

Lee, J. H., Ancona, V., and Zhao, Y. 2018. Lon protease modulates virulence traits in *Erwinia amylovora* by direct monitoring of major regulators and indirectly through the Rcs and Gac-Csr regulatory systems. Molecular plant pathology 19:827-840.

Lenz, D. H., Mok, K. C., Lilley, B. N., Kulkarni, R. V., Wingreen, N. S., and Bassler, B. L. 2004. The small RNA chaperone Hfq and multiple small RNAs control quorum sensing in *Vibrio harveyi* and *Vibrio cholerae*. Cell 118:69-82.

Li, C., Wen, A., Shen, B., Lu, J., Huang, Y., and Chang, Y. 2011. FastCloning: a highly simplified, purification-free, sequence- and ligation-independent PCR cloning method. BMC biotechnology 11:92.

Li, Y., Heine, S., Entian, M., Sauer, K., and Frankenberg-Dinkel, N. 2013. NO-induced biofilm dispersion in *Pseudomonas aeruginosa* is mediated by an MHYT domain-coupled phosphodiesterase. Journal of bacteriology 195:3531-3542.

Ma, C., Sim, S., Shi, W., Du, L., Xing, D., and Zhang, Y. 2010. Energy production genes *sucB* and *ubiF* are involved in persister survival and tolerance to multiple antibiotics and stresses in *Escherichia coli*. FEMS microbiology letters 303:33-40.

Madhugiri, R., Basineni, S. R., and Klug, G. 2010. Turn-over of the small non-coding RNA RprA in *E. coli* is influenced by osmolarity. Molecular genetics and genomics : MGG 284:307-318.

Mah, T.-F. C., and O'Toole, G. A. 2001. Mechanisms of biofilm resistance to antimicrobial agents. Trends in Microbiology 9:34-39.

Maisonneuve, E., Shakespeare, L. J., Jørgensen, M. G., and Gerdes, K. 2011. Bacterial persistence by RNA endonucleases. Proceedings of the National Academy of Sciences of the United States of America 108:13206-13211.

Majdalani, N., Hernandez, D., and Gottesman, S. 2002. Regulation and mode of action of the second small RNA activator of RpoS translation, RprA. Molecular microbiology 46:813-826.

Majdalani, N., Heck, M., Stout, V., and Gottesman, S. 2005. Role of RcsF in signaling to the Rcs phosphorelay pathway in *Escherichia coli*. Journal of bacteriology 187:6770-6778.

Majdalani, N., Chen, S., Murrow, J., St John, K., and Gottesman, S. 2001. Regulation of RpoS by a novel small RNA: the characterization of RprA. Molecular microbiology 39:1382-1394.

Maklashina, E., and Cecchini, G. 2010. The quinone-binding and catalytic site of complex II. Biochimica et biophysica acta 1797:1877-1882.

Mallik, I., Arabiat, S., Pasche, J. S., Bolton, M. D., Patel, J. S., and Gudmestad, N. C. 2014. Molecular characterization and detection of mutations associated with resistance to succinate dehydrogenase-inhibiting fungicides in *Alternaria solani*. Phytopathology 104:40-49.

Malnoy, M., Martens, S., Norelli, J. L., Barny, M. A., Sundin, G. W., Smits, T. H., and Duffy, B. 2012. Fire blight: applied genomic insights of the pathogen and host. Annual review of phytopathology 50:475-494.

Margolis, J. J., El-Etr, S., Joubert, L. M., Moore, E., Robison, R., Rasley, A., Spormann, A. M., and Monack, D. M. 2010. Contributions of *Francisella tularensis* subsp. *novicida* chitinases and Sec secretion system to biofilm formation on chitin. Applied and environmental microbiology 76:596-608.

Martínez, L. C., and Vadyvaloo, V. 2014. Mechanisms of post-transcriptional gene regulation in bacterial biofilms. Frontiers in cellular and infection microbiology 4:38.

Maurer, L. M., Yohannes, E., Bondurant, S. S., Radmacher, M., and Slonczewski, J. L. 2005. pH regulates genes for flagellar motility, catabolism, and oxidative stress in *Escherichia coli* K-12. Journal of bacteriology 187:304-319.

McCullen, C. A., Benhammou, J. N., Majdalani, N., and Gottesman, S. 2010. Mechanism of positive regulation by DsrA and RprA small noncoding RNAs: pairing increases translation and protects mRNA from degradation. Journal of bacteriology 192:5559.

McNally, R. R., Toth, I. K., Cock, P. J., Pritchard, L., Hedley, P. E., Morris, J. A., Zhao, Y., and Sundin, G. W. 2012. Genetic characterization of the HrpL regulon of the fire blight

pathogen *Erwinia amylovora* reveals novel virulence factors. Molecular plant pathology 13:160-173.

Mika, F., Busse, S., Possling, A., Berkholz, J., Tschowri, N., Sommerfeldt, N., Pruteanu, M., and Hengge, R. 2012. Targeting of *csgD* by the small regulatory RNA RprA links stationary phase, biofilm formation and cell envelope stress in *Escherichia coli*. Molecular microbiology 84:51-65.

Miles, T. D., Miles, L. A., Fairchild, K. L., and Wharton, P. S. 2014. Screening and characterization of resistance to succinate dehydrogenase inhibitors in *Alternaria solani*. Plant Pathology 63:155-164.

Miller, W. G., Leveau, J. H., and Lindow, S. E. 2000. Improved *gfp* and *inaZ* broad-host-range promoter-probe vectors. Molecular plant-microbe interactions : MPMI 13:1243-1250.

Model, P., Jovanovic, G., and Dworkin, J. 1997. The Escherichia coli phage-shock-protein (psp) operon. Molecular microbiology 24:255-261.

Morgan, R., Kohn, S., Hwang, S.-H., Hassett, D. J., and Sauer, K. 2006. BdlA, a Chemotaxis Regulator Essential for Biofilm Dispersion in *Pseudomonas aeruginosa*. Journal of bacteriology 188:7335.

Motoba, K., Uchida, M., and Tada, E. 1988. Mode of Antifungal Action and Selectivity of Flutolanil. Agricultural and Biological Chemistry 52:1445-1449.

Moyed, H. S., and Bertrand, K. P. 1983. hipA, a newly recognized gene of *Escherichia coli* K-12 that affects frequency of persistence after inhibition of murein synthesis. Journal of bacteriology 155:768-775.

Muthuramalingam, M., White, J. C., and Bourne, C. R. 2016. Toxin-Antitoxin Modules Are Pliable Switches Activated by Multiple Protease Pathways. Toxins 8.

Na, Y. A., Lee, J. Y., Bang, W. J., Lee, H. J., Choi, S. I., Kwon, S. K., Jung, K. H., Kim, J. F., and Kim, P. 2015. Growth retardation of *Escherichia coli* by artificial increase of intracellular ATP. Journal of industrial microbiology & biotechnology 42:915-924.

Nimtz, M., Mort, A., Domke, T., Wray, V., Zhang, Y., Qiu, F., Coplin, D., and Geider, K. 1996. Structure of amylovoran, the capsular exopolysaccharide from the fire blight pathogen *Erwinia amylovora*. Carbohydrate Research 287:59-76.

Norelli, J. L., Jones, A. L., and Aldwinckle, H. S. 2003. Fire blight management in the twenty-first century: using new technologies that enhance host resistance in apple. Plant Dis. 87:756-765.

Oehler, S., Eismann, E. R., Krämer, H., and Müller-Hill, B. 1990. The three operators of the lac operon cooperate in repression. The EMBO journal 9:973-979.

Ogawa, S., and Lee, T. M. 1984. The relation between the internal phosphorylation potential and the proton motive force in mitochondria during ATP synthesis and hydrolysis. The Journal of biological chemistry 259:10004-10011.

Oh, C. S., Kim, J. F., and Beer, S. V. 2005. The Hrp pathogenicity island of *Erwinia amylovora* and identification of three novel genes required for systemic infectiondouble dagger. Molecular plant pathology 6:125-138.

Ōmura, S., and Shiomi, K. 2007. Discovery, chemistry, and chemical biology of microbial products. Pure and Applied Chemistry 79:581.

Orman, M. A., and Brynildsen, M. P. 2013. Dormancy Is Not Necessary or Sufficient for Bacterial Persistence. Antimicrobial agents and chemotherapy 57:3230.

Page, R., and Peti, W. 2016. Toxin-antitoxin systems in bacterial growth arrest and persistence. Nature chemical biology 12:208-214.

Pecota, D. C., and Wood, T. K. 1996. Exclusion of T4 phage by the *hok/sok* killer locus from plasmid R1. Journal of bacteriology 178:2044-2050.

Pedersen, K., and Gerdes, K. 1999. Multiple hok genes on the chromosome of *Escherichia coli*. Molecular microbiology 32:1090-1102.

Peng, J., Triplett, L. R., Schachterle, J. K., and Sundin, G. W. 2019. Chromosomally Encoded *hok-sok* Toxin-Antitoxin System in the Fire Blight Pathogen *Erwinia amylovora*: Identification and Functional Characterization. Applied and environmental microbiology 85.

Popko, J. T., Sang, H., Lee, J., Yamada, T., Hoshino, Y., and Jung, G. 2018. Resistance of *Sclerotinia homoeocarpa* Field Isolates to Succinate Dehydrogenase Inhibitor Fungicides. Plant Dis. 102:2625-2631.

Prysak, M. H., Mozdzierz, C. J., Cook, A. M., Zhu, L., Zhang, Y., Inouye, M., and Woychik, N. A. 2009. Bacterial toxin YafQ is an endoribonuclease that associates with the ribosome and blocks translation elongation through sequence-specific and frame-dependent mRNA cleavage. Molecular microbiology 71:1071-1087.

Pu, Y., Zhao, Z., Li, Y., Zou, J., Ma, Q., Zhao, Y., Ke, Y., Zhu, Y., Chen, H., Baker, M. A. B., Ge, H., Sun, Y., Xie, X. S., and Bai, F. 2016. Enhanced Efflux Activity Facilitates Drug Tolerance in Dormant Bacterial Cells. Molecular cell 62:284-294.

Purevdorj-Gage, B., Costerton, W. J., and Stoodley, P. 2005. Phenotypic differentiation and seeding dispersal in non-mucoid and mucoid *Pseudomonas aeruginosa* biofilms. Microbiology (Reading, England) 151:1569-1576.

Radzikowski, J. L., Vedelaar, S., Siegel, D., Ortega, A. D., Schmidt, A., and Heinemann, M. 2016. Bacterial persistence is an active sigmaS stress response to metabolic flux limitation. Molecular systems biology 12:882.

Ramage, H. R., Connolly, L. E., and Cox, J. S. 2009. Comprehensive Functional Analysis of *Mycobacterium tuberculosis* Toxin-Antitoxin Systems: Implications for Pathogenesis, Stress Responses, and Evolution. PLoS genetics 5:e1000767.

Rivas, R., Vizcaíno, N., Buey, R. M., Mateos, P. F., Martínez-Molina, E., and Velázquez, E. 2001. An effective, rapid and simple method for total RNA extraction from bacteria and yeast. Journal of microbiological methods 47:59-63.

Robinson, M. D., and Smyth, G. K. 2008. Small-sample estimation of negative binomial dispersion, with applications to SAGE data. Biostatistics (Oxford, England) 9:321-332.

Römling, U., Gomelsky, M., and Galperin, M. Y. 2005. C-di-GMP: the dawning of a novel bacterial signalling system. Molecular microbiology 57:629-639.

Roy, A. B., Petrova, O. E., and Sauer, K. 2012. The Phosphodiesterase DipA (PA5017) Is Essential for *Pseudomonas aeruginosa* Biofilm Dispersion. Journal of bacteriology 194:2904.

Rumbaugh, K. P., and Sauer, K. 2020. Biofilm dispersion. Nature Reviews Microbiology.

Ruprecht, J., Yankovskaya, V., Maklashina, E., Iwata, S., and Cecchini, G. 2009. Structure of *Escherichia coli* succinate:quinone oxidoreductase with an occupied and empty quinone-binding site. The Journal of biological chemistry 284:29836-29846.

Sambrook, J. 2001. Molecular cloning : a laboratory manual. Third edition. Cold Spring Harbor, N.Y. : Cold Spring Harbor Laboratory Press.

Sauer, K., Camper, A. K., Ehrlich, G. D., Costerton, J. W., and Davies, D. G. 2002. *Pseudomonas aeruginosa* displays multiple phenotypes during development as a biofilm. Journal of bacteriology 184:1140-1154.

Scalliet, G., Bowler, J., Luksch, T., Kirchhofer-Allan, L., Steinhauer, D., Ward, K., Niklaus, M., Verras, A., Csukai, M., Daina, A., and Fonné-Pfister, R. 2012. Mutagenesis and Functional Studies with Succinate Dehydrogenase Inhibitors in the Wheat Pathogen *Mycosphaerella graminicola*. PloS one 7:e35429.

Schachterle, J. K., and Sundin, G. W. 2019. The Leucine-responsive regulatory protein Lrp participates in virulence regulation downstream of small RNA ArcZ in *Erwinia amylovora*. mBio 10:e00757-00719.

Schleheck, D., Barraud, N., Klebensberger, J., Webb, J. S., McDougald, D., Rice, S. A., and Kjelleberg, S. 2009. *Pseudomonas aeruginosa* PAO1 Preferentially Grows as Aggregates in Liquid Batch Cultures and Disperses upon Starvation. PloS one 4:e5513.

Schmeling, B. V., and Kulka, M. 1966. Systemic fungicidal activity of 1,4-oxathiin derivatives. Science (New York, N.Y.) 152:659-660.

Shah, D., Zhang, Z., Khodursky, A. B., Kaldalu, N., Kurg, K., and Lewis, K. 2006a. Persisters: a distinct physiological state of E. coli. BMC microbiology 6:53.

Shah, D., Zhang, Z., Khodursky, A., Kaldalu, N., Kurg, K., and Lewis, K. 2006b. Persisters: a distinct physiological state of *E. coli*. BMC microbiology 6:53-53.

Shan, Y., Brown Gandt, A., Rowe, S. E., Deisinger, J. P., Conlon, B. P., and Lewis, K. 2017. ATP-Dependent Persister Formation in *Escherichia coli*. mBio 8.

Shidore, T., and Triplett, L. R. 2017. Toxin-Antitoxin Systems: Implications for Plant Disease. Annual review of phytopathology 55:161-179.

Shidore, T., Zeng, Q., and Triplett, L. R. 2019. Survey of Toxin-Antitoxin Systems in *Erwinia amylovora* Reveals Insights into Diversity and Functional Specificity. Toxins 11.

Short, F. L., Pei, X. Y., Blower, T. R., Ong, S.-L., Fineran, P. C., Luisi, B. F., and Salmond, G. P. C. 2013. Selectivity and self-assembly in the control of a bacterial toxin by an antitoxic noncoding RNA pseudoknot. Proceedings of the National Academy of Sciences 110:E241.

Sierotzki, H., and Scalliet, G. 2013. A review of current knowledge of resistance aspects for the next-generation succinate dehydrogenase inhibitor fungicides. Phytopathology 103:880-887.

Singh, S., Singh, S. K., Chowdhury, I., and Singh, R. 2017. Understanding the Mechanism of Bacterial Biofilms Resistance to Antimicrobial Agents. The open microbiology journal 11:53-62.

Singh, V. K., Utaida, S., Jackson, L. S., Jayaswal, R. K., Wilkinson, B. J., and Chamberlain, N. R. 2007. Role for *dnaK* locus in tolerance of multiple stresses in *Staphylococcus aureus*. Microbiology (Reading, England) 153:3162-3173.

Singletary, L. A., Gibson, J. L., Tanner, E. J., McKenzie, G. J., Lee, P. L., Gonzalez, C., and Rosenberg, S. M. 2009. An SOS-regulated type 2 toxin-antitoxin system. Journal of bacteriology 191:7456-7465.

Sjulin, T. M., and Beer, S. V. 1978. Mechanism of wilt induction by amylovorin in cotoneaster shoots and Its relation to wilting of shoots infected by *Erwinia amylovora*.

Slack, S. M., Zeng, Q., Outwater, C. A., and Sundin, G. W. 2017. Microbiological examination of *Erwinia amylovora* exopolysaccharide ooze. Phytopathology 107:403-411.

Srikumar, S., Kröger, C., Hébrard, M., Colgan, A., Owen, S. V., Sivasankaran, S. K., Cameron, A. D. S., Hokamp, K., and Hinton, J. C. D. 2015. RNA-seq brings new insights to the intra-macrophage transcriptome of *Salmonella Typhimurium*. PLoS pathogens 11:e1005262.

Srivastava, D., Moumene, A., Flores-Kim, J., and Darwin, A. J. 2017. Psp Stress Response Proteins Form a Complex with Mislocalized Secretins in the *Yersinia enterocolitica* Cytoplasmic Membrane. mBio 8:e01088-01017.

Steinhauer, D., Salat, M., Frey, R., Mosbach, A., Luksch, T., Balmer, D., Hansen, R., Widdison, S., Logan, G., Dietrich, R. A., Kema, G. H. J., Bieri, S., Sierotzki, H., Torriani, S. F. F., and Scalliet, G. 2019. A dispensable paralog of succinate dehydrogenase subunit C mediates standing resistance towards a subclass of SDHI fungicides in *Zymoseptoria tritici*. PLoS pathogens 15:e1007780.

Streif, S., Staudinger, W. F., Marwan, W., and Oesterhelt, D. 2008. Flagellar rotation in the archaeon *Halobacterium salinarum* depends on ATP. Journal of molecular biology 384:1-8.

Sun, F., Huo, X., Zhai, Y., Wang, A., Xu, J., Su, D., Bartlam, M., and Rao, Z. 2005. Crystal structure of mitochondrial respiratory membrane protein complex II. Cell 121:1043-1057.

Supek, F., Bošnjak, M., Škunca, N., and Šmuc, T. 2011. REVIGO Summarizes and Visualizes Long Lists of Gene Ontology Terms. PloS one 6:e21800.

Szczesny, M., Beloin, C., and Ghigo, J. M. 2018. Increased osmolarity in biofilm triggers RcsB-dependent lipid A palmitoylation in *Escherichia coli*. mBio 9.

Szeto, S. S., Reinke, S. N., Sykes, B. D., and Lemire, B. D. 2007. Ubiquinone-binding site mutations in the *Saccharomyces cerevisiae* succinate dehydrogenase generate superoxide and lead to the accumulation of succinate. The Journal of biological chemistry 282:27518-27526.

Tao, F., Swarup, S., and Zhang, L.-H. 2010. Quorum sensing modulation of a putative glycosyltransferase gene cluster essential for *Xanthomonas campestris* biofilm formation. Environmental microbiology 12:3159-3170.

Thisted, T., and Gerdes, K. 1992. Mechanism of post-segregational killing by the *hok/sok* system of plasmid R1. Sok antisense RNA regulates *hok* gene expression indirectly through the overlapping *mok* gene. Journal of molecular biology 223:41-54.

Thisted, T., Sørensen, N. S., Wagner, E. G., and Gerdes, K. 1994. Mechanism of post-segregational killing: Sok antisense RNA interacts with Hok mRNA via its 5′-end single-stranded leader and competes with the 3′-end of Hok mRNA for binding to the *mok* translational initiation region. The EMBO journal 13:1960-1968.

Thomson, S. V. 2000. Epidemiology of fire blight in: *Fire Blight: The Disease and its Causative Agent, Erwinia amylovora*. (Vanneste, J., ed.). New York: CABI publishing:pp. 9-36.

Thormann, K. M., Duttler, S., Saville, R. M., Hyodo, M., Shukla, S., Hayakawa, Y., and Spormann, A. M. 2006. Control of formation and cellular detachment from *Shewanella oneidensis* MR-1 biofilms by cyclic di-GMP. Journal of bacteriology 188:2681-2691.

Tian, T., Liu, Y., Yan, H., You, Q., Yi, X., Du, Z., Xu, W., and Su, Z. 2017. agriGO v2.0: a GO analysis toolkit for the agricultural community, 2017 update. Nucleic acids research 45:W122-w129.

Traxler, M. F., Summers, S. M., Nguyen, H. T., Zacharia, V. M., Hightower, G. A., Smith, J. T., and Conway, T. 2008. The global, ppGpp-mediated stringent response to amino acid starvation in *Escherichia coli*. Molecular microbiology 68:1128-1148.

Triplett, L. R., Melotto, M., and Sundin, G. W. 2009. Functional analysis of the N terminus of the *Erwinia amylovora* secreted effector DspA/E reveals features required for secretion, translocation, and binding to the chaperone DspB/F. Molecular Plant-Microbe Interactions 22:1282-1292.

Ulrich, J. T., and Mathre, D. E. 1972. Mode of action of oxathiin systemic fungicides. V. Effect on electron transport system of *Ustilago maydis* and *Saccharomyces cerevisiae*. Journal of bacteriology 110:628-632.

Unoson, C., and Wagner, E. G. 2008. A small SOS-induced toxin is targeted against the inner membrane in *Escherichia coli*. Molecular microbiology 70:258-270.

Unterholzner, S. J., Poppenberger, B., and Rozhon, W. 2013. Toxin-antitoxin systems: Biology, identification, and application. Mobile genetic elements 3:e26219.

Urban, J. H., and Vogel, J. 2007. Translational control and target recognition by *Escherichia coli* small RNAs *in vivo*. Nucleic acids research 35:1018-1037.

Urfer, M., Bogdanovic, J., Lo Monte, F., Moehle, K., Zerbe, K., Omasits, U., Ahrens, C. H., Pessi, G., Eberl, L., and Robinson, J. A. 2016. A Peptidomimetic Antibiotic Targets Outer Membrane Proteins and Disrupts Selectively the Outer Membrane in *Escherichia coli*. The Journal of biological chemistry 291:1921-1932.

Vanneste, J. L. 1995. *Erwinia amylovora*. In: Pathogenesis and host specificity in plant diseases: histopathological, biochemical, genetic and molecular bases (Singh, U. S., Singh, R. P., Kohmoto, K., eds.). Oxford and London: Pergammon Press.

Vázquez-Laslop, N., Lee, H., and Neyfakh, A. A. 2006. Increased persistence in *Escherichia coli* caused by controlled expression of toxins or other unrelated proteins. Journal of bacteriology 188:3494-3497.

Veloukas, T., Markoglou, A. N., and Karaoglanidis, G. S. 2013. Differential Effect of SdhB Gene Mutations on the Sensitivity to SDHI Fungicides in *Botrytis cinerea*. Plant Dis. 97:118-122.

Verstraeten, N., Knapen, W. J., Kint, C. I., Liebens, V., Van den Bergh, B., Dewachter, L., Michiels, J. E., Fu, Q., David, C. C., Fierro, A. C., Marchal, K., Beirlant, J., Versees, W., Hofkens, J., Jansen, M., Fauvart, M., and Michiels, J. 2015. Obg and Membrane Depolarization Are Part of a Microbial Bet-Hedging Strategy that Leads to Antibiotic Tolerance. Molecular cell 59:9-21.

Vogel, J., Argaman, L., Wagner, E. G., and Altuvia, S. 2004. The small RNA IstR inhibits synthesis of an SOS-induced toxic peptide. Current biology : CB 14:2271-2276.

Vogt, S. L., Evans, A. D., Guest, R. L., and Raivio, T. L. 2014. The Cpx envelope stress response regulates and is regulated by small noncoding RNAs. Journal of bacteriology 196:4229.

von Meyenburg, K., Jørgensen, B. B., Michelsen, O., Sørensen, L., and McCarthy, J. E. 1985. Proton conduction by subunit a of the membrane-bound ATP synthase of *Escherichia coli* revealed after induced overproduction. The EMBO journal 4:2357-2363.

Wang, D., Korban, S. S., and Zhao, Y. 2009. The Rcs phosphorelay system is essential for pathogenicity in *Erwinia amylovora*. Molecular plant pathology 10:277-290.

Wang, D., Korban, S. S., Pusey, P. L., and Zhao, Y. 2012a. AmyR is a novel negative regulator of amylovoran production in *Erwinia amylovora*. PloS one 7:e45038.

Wang, X., Lord, D. M., Hong, S. H., Peti, W., Benedik, M. J., Page, R., and Wood, T. K. 2013. Type II toxin/antitoxin MqsR/MqsA controls type V toxin/antitoxin GhoT/GhoS. Environmental microbiology 15:1734-1744.

Wang, X., Kim, Y., Hong, S. H., Ma, Q., Brown, B. L., Pu, M., Tarone, A. M., Benedik, M. J., Peti, W., Page, R., and Wood, T. K. 2011. Antitoxin MqsA helps mediate the bacterial general stress response. Nature chemical biology 7:359-366.

Wang, X., Lord, D. M., Cheng, H. Y., Osbourne, D. O., Hong, S. H., Sanchez-Torres, V., Quiroga, C., Zheng, K., Herrmann, T., Peti, W., Benedik, M. J., Page, R., and Wood, T. K. 2012b. A new type V toxin-antitoxin system where mRNA for toxin GhoT is cleaved by antitoxin GhoS. Nature chemical biology 8:855-861.

Wang, X., Lord, D. M., Cheng, H.-Y., Osbourne, D. O., Hong, S. H., Sanchez-Torres, V., Quiroga, C., Zheng, K., Herrmann, T., Peti, W., Benedik, M. J., Page, R., and Wood, T. K. 2012c. A new type V toxin-antitoxin system where mRNA for toxin GhoT is cleaved by antitoxin GhoS. Nature chemical biology 8:855-861.

Waters, C. M., Lu, W., Rabinowitz, J. D., and Bassler, B. L. 2008. Quorum sensing controls biofilm formation in *Vibrio cholerae* through modulation of cyclic di-GMP levels and repression of vpsT. Journal of bacteriology 190:2527-2536.

Wei, Z., Kim, J. F., and Beer, S. V. 2000. Regulation of *hrp* genes and type III protein secretion in *Erwinia amylovora* by HrpX/HrpY, a novel two-component system, and HrpS. Molecular plant-microbe interactions : MPMI 13:1251-1262.

Wei, Z. M., and Beer, S. V. 1995. *hrpL* activates *Erwinia amylovora hrp* gene transcription and is a member of the ECF subfamily of sigma factors. Journal of bacteriology 177:6201-6210.

Wilmaerts, D., Bayoumi, M., Dewachter, L., Knapen, W., Mika, J. T., Hofkens, J., Dedecker, P., Maglia, G., Verstraeten, N., and Michiels, J. 2018. The Persistence-Inducing Toxin HokB Forms Dynamic Pores That Cause ATP Leakage. mBio 9:e00744-00718.

Wu, N., He, L., Cui, P., Wang, W., Yuan, Y., Liu, S., Xu, T., Zhang, S., Wu, J., Zhang, W., and Zhang, Y. 2015. Ranking of persister genes in the same *Escherichia coli* genetic background demonstrates varying importance of individual persister genes in tolerance to different antibiotics. Frontiers in microbiology 6:1003.

Yankovskaya, V., Horsefield, R., Törnroth, S., Luna-Chavez, C., Miyoshi, H., Léger, C., Byrne, B., Cecchini, G., and Iwata, S. 2003. Architecture of Succinate Dehydrogenase and Reactive Oxygen Species Generation. Science (New York, N.Y.) 299:700.

Zeng, Q., and Sundin, G. W. 2014. Genome-wide identification of Hfq-regulated small RNAs in the fire blight pathogen *Erwinia amylovora* discovered small RNAs with virulence regulatory function. BMC genomics 15:414.

Zeng, Q., McNally, R. R., and Sundin, G. W. 2013. Global small RNA chaperone Hfq and regulatory small RNAs are important virulence regulators in *Erwinia amylovora*. Journal of bacteriology 195:1706-1717.

Zhang, C. Q., Yuan, S. K., Sun, H. Y., Qi, Z. Q., Zhou, M. G., and Zhu, G. N. 2007. Sensitivity of Botrytis cinerea from vegetable greenhouses to boscalid. Plant Pathology 56:646-653.

Zhao, J., Cheah, S.-E., Roberts, K. D., Nation, R. L., Thompson, P. E., Velkov, T., Du, Z., Johnson, M. D., and Li, J. 2016. Transcriptomic Analysis of the Activity of a Novel *Polymyxin against Staphylococcus* aureus. mSphere 1:e00119-00116.

Zhao, Y., Sundin, G. W., and Wang, D. 2009a. Construction and analysis of pathogenicity island deletion mutants of *Erwinia amylovora*. Canadian journal of microbiology 55:457-464.

Zhao, Y., Wang, D., Nakka, S., Sundin, G. W., and Korban, S. S. 2009b. Systems level analysis of two-component signal transduction systems in *Erwinia amylovora*: Role in virulence, regulation of amylovoran biosynthesis and swarming motility. BMC genomics 10:245.

Amiri, A., Zuniga, A. I., and Peres, N. A. 2020. Mutations in the membrane-anchored SdhC subunit affect fitness and sensitivity to succinate dehydrogenase inhibitors in *Botrytis cinerea* populations from multiple hosts. Phytopathol. 110:327–335.

Avenot, H. F., van den Biggelaar, H., Morgan, D. P., Moral, J., Joosten, M., and Michailides, T. J. 2014. Sensitivities of baseline isolates and boscalid-resistant mutants of *Alternaria alternata* from pistachio to fluopyram, penthiopyrad, and fluxapyroxad. Plant Dis. 98:197–205.

Avenot, H. F., Sellam, A., Karaoglanidis, G., and Michailides, T. J. 2008. Characterization of mutations in the iron-sulphur subunit of succinate dehydrogenase correlating with boscalid resistance in *Alternaria alternata* from California pistachio. Phytopathol. 98:736–742.

Ayer, K. M., Villani, S. M., Choi, M.-W., and Cox, K. D. 2018. Characterization of the *VisdhC* and *VisdhD* Genes in *Venturia inaequalis*, and sensitivity to fluxapyroxad, pydiflumetofen, inpyrfluxam, and benzovindiflupyr. Plant Dis. 103:1092–1100.

Boland, G., and Hall, R. 1994. Index of plant hosts of *Sclerotinia Sclerotiorum*. Can. J. Plant Pathol. 16:93–108.

Bolton, M. D., Thomma, B. P. H. J., and Nelson, B. D. 2006. *Sclerotinia sclerotiorum* (Lib.) de Bary: biology and molecular traits of a cosmopolitan pathogen. Mol. Plant Pathol. 7:1–16.

Brent, K. J. 2007. Fungicide resistance in crop pathogens: how can it be managed? Second edition. Fungicides Resistance action committee.

Chen, F., Liu, X., Chen, S., Schnabel, E., and Schnabel, G. 2013. Characterization of *Monilinia fructicola* strains resistant to both propiconazole and boscalid. Plant Dis. 97:645–651.

Chen, W., Wei, L., Zhao, W., Wang, B., Zheng, H., Zhang, P., et al. 2020. Resistance risk assessment for a novel succinate dehydrogenase inhibitor pydiflumetofen in *Fusarium asiaticum*. Pest Manag. Sci. Available at: https://doi.org/10.1002/ps.6053.

De Miccolis Angelini, R. M., Habib, W., Rotolo, C., Pollastro, S., and Faretra, F. 2010. Selection, characterization and genetic analysis of laboratory mutants of *Botryotinia fuckeliana* (*Botrytis cinerea*) resistant to the fungicide boscalid. Eur. J. Plant Pathol. 128:185–199.

Dooley, H., Shaw, M. W., Mehenni-Ciz, J., Spink, J., and Kildea, S. 2016. Detection of *Zymoseptoria tritici* SDHI-insensitive field isolates carrying the *SdhC*-H152R and *SdhD*-R47W substitutions. Pest Manag. Sci. 72:2203–2207.

Duan, Y., Ge, C., Liu, S., Wang, J., and Zhou, M. 2013. A two-component histidine kinase Shk1 controls stress response, sclerotial formation and fungicide resistance in *Sclerotinia sclerotiorum*. Mol. Plant Pathol. 14:708–718.

Duan, Y., Xiu, Q., Li, H., Li, T., Wang, J., and Zhou, M. 2018. Pharmacological characteristics and control efficacy of a novel SDHI fungicide pydiflumetofen against *Sclerotinia sclerotiorum*. Plant Dis. 103:77–82.

Fernández-Ortuño, D., Chen, F., and Schnabel, G. 2012. Resistance to pyraclostrobin and boscalid in *Botrytis cinerea* isolates from strawberry fields in the Carolinas. Plant Dis. 96:1198–1203.

Fernández-Ortuño, D., Pérez-García, A., Chamorro, M., de la Peña, E., de Vicente, A., and Torés, J. A. 2017. Resistance to the SDHI fungicides boscalid, fluopyram, fluxapyroxad, and penthiopyrad in *Botrytis cinerea* from commercial strawberry fields in Spain. Plant Dis. 101:1306–1313.

Fraaije, B. A., Bayon, C., Atkins, S., Cools, H. J., Lucas, J. A., and Fraajie, M. W. 2012. Risk assessment studies on succinate dehydrogenase inhibitors, the new weapons in the battle to control Septoria leaf blotch in wheat. Mol. Plant Pathol. 13:263–275.

FRAC. 2020. FRAC code list 2020: Fungal Control agents sorted by cross resistance pattern and mode of action. https://www.frac.info/publications/downloads [Accessed March 24 2020].

FRAC. 2018a. FRAC Recommendations for SDHI fungicides. https://www.frac.info/frac-teams/working-groups/sdhi-fungicides/recommendations-for-sdhi [Accessed March 24 2020].

FRAC. 2015. FRAC Recommendations for SDHI fungicides. https://www.frac.info/frac-teams/working-groups/sdhi-fungicides/recommendations-for-sdhi [Accessed March 24 2020].

FRAC. 2018b. List of plant pathogenic organisms resistant to disease control agents. https://www.frac.info/publications/downloads [Accessed March 24 2020].

Gao, Y., He, L., Zhu, J., Cheng, J., Li, B., Liu, F., et al. 2020. The relationship between features enabling SDHI fungicide binding to the *Sc-Sdh* complex and its inhibitory activity against *Sclerotinia sclerotiorum*. Pest Manag. Sci. 76:2799–2808.

He, L., Cui, K., Song, Y., Li, T., Liu, N., Mu, W., et al. 2020. Activity of the novel succinate dehydrogenase inhibitor fungicide pydiflumetofen against SDHI-sensitive and SDHI-resistant isolates of *Botrytis cinerea* and efficacy against gray mold. Plant Dis. 104:2168–2173.

Hou, Y.-P., Mao, X.-W., Lin, S.-P., Song, X.-S., Duan, Y.-B., Wang, J.-X., et al. 2018. Activity of a novel succinate dehydrogenase inhibitor fungicide pyraziflumid against *Sclerotinia sclerotiorum*. Pestic. Biochem. Phys. 145:22–28.

Huang, X., Luo, J., Li, B., Song, Y., Mu, W., and Liu, F. 2019. Bioactivity, physiological characteristics and efficacy of the SDHI fungicide pydiflumetofen against *Sclerotinia sclerotiorum*. Pestic. Biochem. Phys. 160:70–78.

Lalève, A., Gamet, S., Walker, A.-S., Debieu, D., Toquin, V., and Fillinger, S. 2014. Site-directed mutagenesis of the P225, N230 and H272 residues of succinate dehydrogenase subunit B from *Botrytis cinerea* highlights different roles in enzyme activity and inhibitor binding. Environ. Microbiol. 16:2253–2266.

Lee, J., Elliott, M., Kim, M., Yamada, T., and Jung, G. 2020. A rapid molecular detection system for SdhB and SdhC point mutations conferring differential SDHI resistance in populations of Clarireedia. Plant Dis. Available at: https://doi.org/10.1094/PDIS-04-20-0724-RE [Accessed September 5, 2020].

Leroux, P., Gredt, M., Leroch, M., and Walker, A.-S. 2010. Exploring mechanisms of resistance to Rrespiratory inhibitors in field Strains of *Botrytis cinerea*, the causal agent of gray mold. Appl. Environ. Microbiol. 76:6615–6630.

Li, C., Wen, A., Shen, B., Lu, J., Huang, Y., and Chang, Y. 2011. FastCloning: a highly simplified, purification-free, sequence- and ligation-independent PCR cloning method. BMC Biotechnol. 11:92.

Li, J., Zhang, Yanhua, Zhang, Yucheng, Yu, P.-L., Pan, H., and Rollins, J. A. 2018. Introduction of large sequence inserts by CRISPR-Cas9 to create pathogenicity mutants in the multinucleate filamentous pathogen *Sclerotinia sclerotiorum*. mBio. 9:e00567-18.

Liang, X., and Rollins, J. A. 2018. Mechanisms of broad host range necrotrophic pathogenesis in *Sclerotinia sclerotiorum*. Phytopathol. 108:1128–1140.

Mallik, I., Arabiat, S., Pasche, J. S., Bolton, M. D., Patel, J. S., and Gudmestad, N. C. 2013. Molecular characterization and detection of mutations associated with resistance to succinate dehydrogenase-inhibiting fungicides in *Alternaria solani*. Phytopathol. 104:40–49.

Mao, X., Wu, Z., Bi, C., Wang, J., Zhao, F., Gao, J., et al. 2020. Molecular and biochemical characterization of pydiflumetofen-resistant mutants of *Didymella bryoniae*. J. Agric. Food Chem. 68:9120–9130.

Miyamoto, T., Hayashi, K., Okada, R., Wari, D., and Ogawara, T. 2020. Resistance to succinate dehydrogenase inhibitors in field isolates of *Podosphaera xanthii* on cucumber: monitoring, cross-resistance patterns and molecular characterization. Pestic. Biochem. Phys. 169:104646.

Oda, M., Furuya, T., Morishita, Y., Matsuzaki, Y., Hasebe, M., and Kuroki, N. 2017. Synthesis and biological activity of a novel fungicide, pyraziflumid. J. Pestic. Sci. 42 4:151–157.

Outwater, C. A., Proffer, T. J., Rothwell, N. L., Peng, J., and Sundin, G. W. 2019. Boscalid resistance in *Blumeriella jaapii* : distribution, effect on field efficacy, and molecular characterization. Plant Dis. 103:1112–1118.

Popko, J. T., Sang, H., Lee, J., Yamada, T., Hoshino, Y., and Jung, G. 2018. Resistance of *Sclerotinia homoeocarpa* field isolates to succinate dehydrogenase inhibitor fungicides. Plant Dis. 102:2625–2631.

Price, D. 1979. W.R. Jarvis, Botryotinia and Botrytis species: taxonomy, physiology and pathogenicity. Monograph No. 15, Research Branch, Canadian Department of Agriculture.

Rehfus, A., Miessner, S., Achenbach, J., Strobel, D., Bryson, R., and Stammler, G. 2016. Emergence of succinate dehydrogenase inhibitor resistance of *Pyrenophora teres* in Europe. Pest Manag. Sci. 72:1977–1988.

Rollins, J. A. 2003. The *Sclerotinia sclerotiorum pac1* gene is required for sclerotial development and virulence. Mol. Plant Microbe Interact. 16:785–795.

Sang, H., Chang, H.-X., and Chilvers, M. I. 2019. A *Sclerotinia sclerotiorum* transcription factor involved in sclerotial development and virulence on pea. mSphere. 4:e00615-18.

Sang, H., Hulvey, J. P., Green, R., Xu, H., Im, J., Chang, T., et al. 2018. A xenobiotic detoxification pathway through transcriptional regulation in filamentous fungi. mBio. 9:e00457-18.

Sang, H., and Lee, H. B. 2020. Molecular nechanisms of succinate dehydrogenase inhibitor resistance in phytopathogenic fungi. Res. Plant Dis. 26:1-7.

Sang, H., Popko, J. T., Chang, T., and Jung, G. 2016. Molecular mechanisms involved in qualitative and quantitative resistance to the dicarboximide fungicide iprodione in *Sclerotinia homoeocarpa* field isolates. Phytopathol. 107:198–207.

Sang, H., Popko, J. T., and Jung, G. 2019. Evaluation of a *Sclerotinia homoeocarpa* population with multiple fungicide resistance phenotypes under differing selection pressures. Plant Dis. 103:685–690.

Scalliet, G., Bowler, J., Luksch, T., Kirchhofer-Allan, L., Steinhauer, D., Ward, K., et al. 2012. Mutagenesis and functional studies with succinate dehydrogenase inhibitors in the wheat pathogen *Mycosphaerella graminicola*. PLoS One. 7:e35429.

Shima, Y., Ito, Y., Kaneko, S., Hatabayashi, H., Watanabe, Y., Adachi, Y., et al. 2009. Identification of three mutant loci conferring carboxin-resistance and development of a novel transformation system in *Aspergillus oryzae*. Fungal Genet. Biol. 46:67–76.

Sierotzki, H., and Scalliet, G. 2013. A review of current knowledge of resistance aspects for the next-generation succinate dehydrogenase inhibitor fungicides. Phytopathol. 103:880–887.

Skinner, W., Bailey, A., Renwick, A., Keon, J., Gurr, S., and Hargreaves, J. 1998. A single amino-acid substitution in the iron-sulphur protein subunit of succinate dehydrogenase determines resistance to carboxin in *Mycosphaerella graminicola*. Curr. Genet. 34:393–398.

Stammler, G., Rehfus, A., Prochnow, A., and Bryson, J. 2014. New findings on the development of insensitive isolates of *Pyrenophora teres* towards SDHI fungicides. Julius-Kühn-Archiv. 447:568.

Steinhauer, D., Salat, M., Frey, R., Mosbach, A., Luksch, T., Balmer, D., et al. 2019. A dispensable paralog of succinate dehydrogenase subunit C mediates standing resistance towards a subclass of SDHI fungicides in *Zymoseptoria tritici*. PLoS Pathog. 15:e1007780.

Sun, H.-Y., Cui, J., Tian, B., Cao, S., Zhang, X., and Chen, H.-G. 2020. Resistance risk assessment for *Fusarium graminearum* to pydiflumetofen, a new succinate dehydrogenase inhibitor. Pest Manag. Sci. 76:1549–1559.

Veloukas, T., Leroch, M., Hahn, M., and Karaoglanidis, G. S. 2011. Detection and molecular characterization of boscalid-resistant *Botrytis cinerea* isolates from strawberry. Plant Dis. 95:1302–1307.

Wang, Yong, Duan, Y., Wang, J., and Zhou, M. 2015. A new point mutation in the iron–sulfur subunit of succinate dehydrogenase confers resistance to boscalid in *Sclerotinia sclerotiorum*. Mol. Plant Pathol. 16:653–661.

Wang, Y., Duan, Y.-B., and Zhou, M.-G. 2015. Molecular and biochemical characterization of boscalid resistance in laboratory mutants of *Sclerotinia sclerotiorum*. Plant Pathol. 64:101–108.

Weld, R. J., Eady, C. C., and Ridgway, H. J. 2006. Agrobacterium-mediated transformation of *Sclerotinia sclerotiorum*. J. Microbiol. Methods. 65:202–207.

Wyand, R. A., and Brown, J. K. M. 2005. Sequence variation in the CYP51 gene of *Blumeria graminis* associated with resistance to sterol demethylase inhibiting fungicides. Fungal Genet. Biol. 42:726–735.

Yin, Y. N., Kim, Y. K., and Xiao, C. L. 2011. Molecular characterization of boscalid resistance in field isolates of *Botrytis cinerea* from apple. Phytopathol. 101:986–995.